Study of Very High-Pressure Fuel-Injection for High-BMEP DI-Diesel Engine

K. T. Rhee
Department of Mechanical and Aerospace Engineering
Rutgers, The State University of New Jersey
Piscataway, New Jersey 08855-0909
ktrhee@jove.rutgers.edu

Executive Summary

In order to help designing a high-power-density (HPD) low-heat-rejection (LHR) high-injection-fuel (HIP) direct-injection compression-ignition engine (DI-CI), two main methods were employed according to the work scope: (1) engine performance analysis; and (2) in-cylinder imaging.

In the performance analysis, a Cummins 903 engine mated with an HIP designed-fabricated at Rutgers equipped with a new high-temperature intake air supply system was used. A new use of a UEGO sensor was introduced in order to rapidly determine the overall air/fuel ratio.

The range of air/fuel ratio studied was from 18-1 to over 35-1, the injection pressure investigated was as high as 30,625 psi (210 Mpa) under varied intake air temperature over 150°C. Over one thousand engine operation conditions were evaluated by averaging digitized pressure-time data accumulated over eight (8) successive cycles to determine the indicated mean effective pressure (IMEP).

In the in-cylinder imaging, a separate optical single-cylinder Cummins 903 engine was used. A high-speed four-color IR digital imaging system (called Super Imaging System, SIS for short) was greatly improved during this contract period. New spectrometric methods were developed to simultaneously determine the distributions of temperature, water vapor and soot concentrations (which have not bee applied in the work yet due to the time limitation). In addition, a new data analysis and presentation method has developed, which permits simultaneous display of as many as twenty-eight (28) movies over a single PC-screen on a controlled manner. This enables us closer analysis and efficient presentation of raw data as well as processed results.

The performance analysis results are reported in two parts: a preliminary report as included in Appendix-I and an additional set of results (Appendix-III).

Some of the in-cylinder imaging results, which are now being captured by the improved SIS after incorporating with new (designed and fabricated in our laboratory) electronic packages, are included (in the text) with brief discussions.

Table of Contents

Study of Very High-Pressure Fuel-Injection for High-BMEP DI-Diesel Engine

K. T. Rhee
Department of Mechanical and Aerospace Engineering
Rutgers, The State University of New Jersey
Piscataway, New Jersey 08855-0909
ktrhee@jove.rutgers.edu

1. INTRODUCTION

Among recent development strategies being taken for achieving a high-power-density (HPD, horsepower per displacement or weight) low-emission direct-injection (DI) Diesel or compression-ignition (CI) engine is the use of an electronically controlled high-injection-pressure (HIP) fuel system. This is basically because an HIP system permits better utilization of the intake air by using overall rich smoke-limited fuel/air mixtures at high engine speeds [1]*, and because it facilitates the injection rate shaping [2].

Since the injection pressure considered in the HIP ranges as high as near 200 MPa (over 30,000psi), the in-cylinder fuel-air mixture preparation by an HIP is expected to be different from that expected in the conventional DI-CI engines. For example, the fuel delivery processes with an HIP is expected to result in even more cavitation in its flow stream within the nozzle hole and sac volume [3], and the high-speed fuel stream leaving the nozzle hole may reach a near sonic speed. Such severe processes are not expected to occur in the low-pressure conventional fuel injection systems.

In addition, the use of ceramic components is considered to be a viable approach for achieving an HPD engine. For example, their use would help eliminate or reduce many parasitic engine components found in the conventional cooling system, producing a compact and tidy engine design. In such a low-heat-rejection (LHR) engine, the compressed air (also very probably the fuel trapped in the injector body) will attain higher temperatures than those in the existing CI engines. This is expected to produce new regimes of physical and thermal preflame processes during the ignition delay period.

When the changes by the LHR design strategy are compounded with the new physical effects stemming from the HIP, the spray formation and subsequent reactions would be further altered from those in the conventional CI systems.

The present analysis of HPD engine development strategies, therefore, considers high-temperature in-cylinder reactions in the environment of an LHR DI-CI engine equipped with an HIP system. Since the study was directed also towards assessment of the cases with room-temperature intake-air for a wide range of injection pressures, as base-line information, a better insight into the engine responses to the HPD engine design strategies was expected to be attained.

Analyzing the engine response to those new changes, at first an initial engine performance evaluation was conducted [1] to find that a DI-CI engine with an HIP permits operation in an air-fuel ratio as rich as 18-1 with exhaust smoke emissions not worse than in the same with a mechanical PT-type injector operated lean, i.e., over 30 to 1. In this

*Numbers in parentheses designate references at end of report.

earlier performance evaluation, it was also discovered that since the ignition delay shifts (with injection pressure and intake air temperature) there was some need for adjusting the injection time for obtaining the best torque for individual speeds (A copy of this paper is included in Appendix-I). The study was directed towards an additional analysis of engine performance and visualization of in-cylinder reactions under matching reaction conditions.

Preflame Reactions and Onset of Combustion. As briefly mentioned earlier, the changes in injection pressure and charge temperature are expected to affect the (invisible) preflame processes during the ignition delay period, which would dictate the subsequent heat release reactions: As a conventional understanding, the longer the ignition delay period the more the mixing of fuel with air to produce less soot emission. When the intake charge temperature is high, the ignition delay will be shortened by reducing the preflame reactions, which would also reduce the amount of heat released during the premixed combustion stage to leave the balance to take place during the slow reacting diffusion combustion stage. Such undesirable impacts by high temperature intake charge may be offset by the use of an HIP, which would increase the amount of heat release during the premixed combustion period, and is an issue to be studied in the present investigation.

Recall that invisible preflame processes include the disintegration of fuel and spray formation concurrent with chemical reactions, which seems to require an additional explanation: Contrary to the conventional expectation that physical delay, involving droplet formation and vaporization combined with mixing precedes the chemical delay commencing endo- and exothermic reactions, it was found that when fuel is delivered into the cylinder by an HIP, the injected fuel immediately starts some significant chemical reactions [4,5]. The finding seems to be reasonable in view that the fuel exposed in the compressed charge whose temperature is well over the self-ignition point would start to decompose, thereby, producing radicals as soon as the injection starts. In order words, there is no clear division in time between the physical and chemical delay periods. Both processes appear to be concurrent.

2. OBJECTIVE OF WORK

The objective of the present work was twofold: It was to evaluate the engine response to the use of HIP and LHR engine design methods (*performance analysis*), and to investigate the in-cylinder reactions (*visualization of in-cylinder processes*) under mutually matching engine conditions.

The present work was conducted according to the scope of work set forth in consultation with the project manager, which is included in Appendix-II for reference. Without altering the basic goal of the study, the work tasks were somewhat modified during the course of the study as discussed later.

3. EXPERIMENTAL APPARATUSES AND METHODS

The method of the study was experimental by applying new research methods on two units of single-cylinder Cummins 903 engines. The research devices and methods employed in the study include: (1) an electronically controlled high-pressure injection system; (2) a high-speed spectrometric IR digital imaging system; (3) spectrometric methods to process the raw data captured by using the IR system; and (4) a data analysis and presentation method.

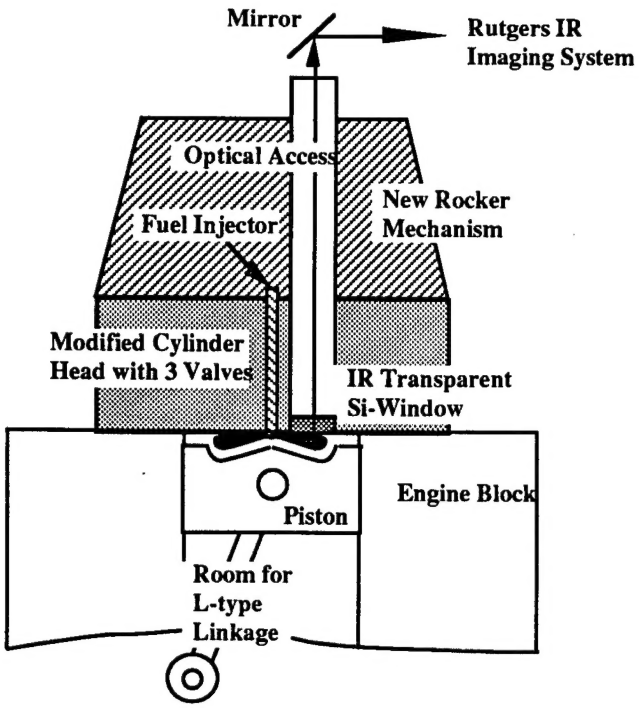

Fig. 1. Single Cylinder Engine Mounted by a Cummins with 903 Cylinder Head with Optical Access for the SIS or Rutgers IR System.

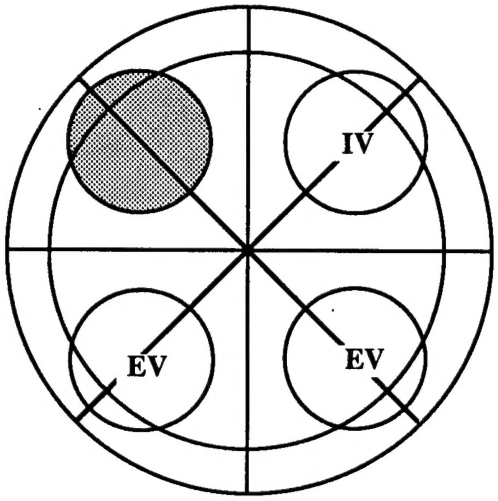

Fig. 2. Optical Access (shaded area) with respect to Spray Plume Axes.

Engines. Two separate engine apparatuses were employed: A V-2 type Cummins 903 single cylinder engine and an optical engine equipped with the same engine-family cylinder head and components. The former was used for the performance analysis and the latter was operated for in-cylinder imaging.

The single-cylinder engine with optical access is basically a Cummins-903 engine having a bore-stroke of 140-121 mm (displacement of 1.85 liters) and compression ratio of 13.5 to 1. In order to obtain images of in-cylinder reactions of the engine, one of two intake vales was converted to an optical access, which is barely big enough to investigate one of eight (8) spray plumes [4,5]. Since the same family of 903 engine has been widely used in the past, no additional discussion on the engine dimensions is made here.

This single-cylinder engine was installed with a new intake-air (electric) heating unit which can increase the air temperature as high as 205°C (400°F) at high speeds, because such a high intake air temperature was expected in an LHR engine whose combustion reactions were to be investigated in the present work. The air was supplied from the building via a pressure controller (maintained at 30.9 KPa or 4.5 psi and higher depending upon the intake air temperature as explained later) and a flow metering unit.

The engine cooling was done by using a closed-flow unit (with glycol as coolant) connected to a water-cooled heat exchanger for temperature control. The unit was designed to accommodate a coolant temperature as high as 149°C or 300°F. The engine was sufficiently instrumented for conducting the present study including a pressure transducer in the cylinder head, many thermocouples at critical places of the engine, and a smoke meter.

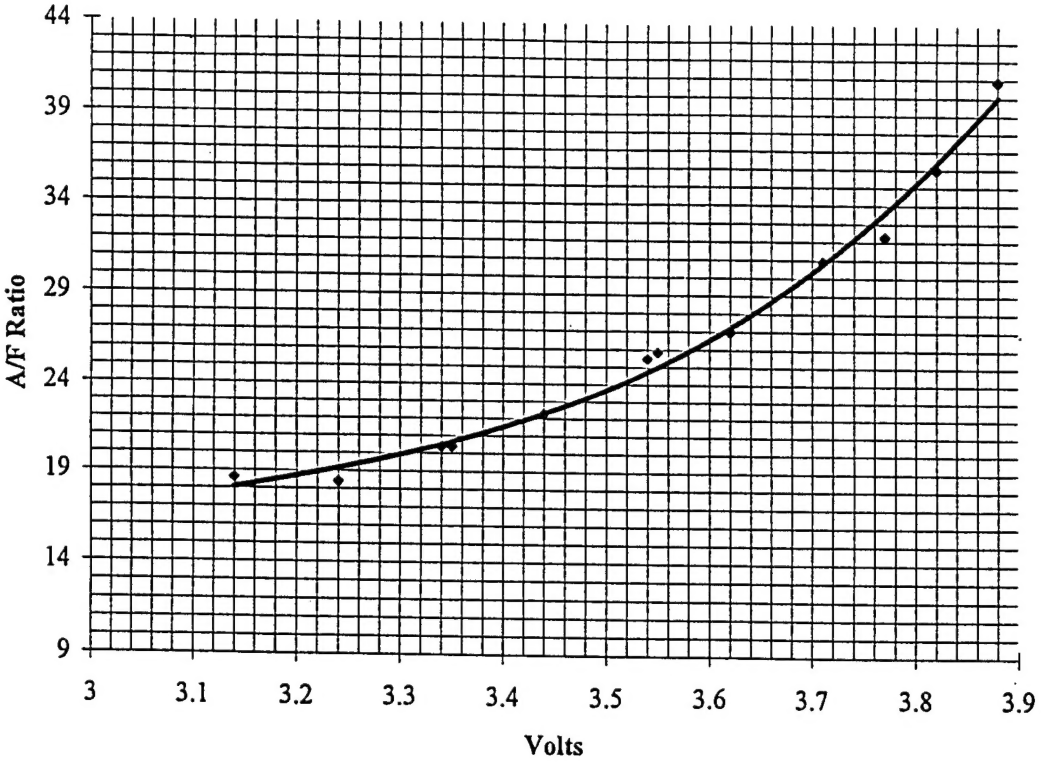

Fig. 3. Calibration of UEGO Sensor to Determine Instantaneous Air/Fuel Ratios.

Determination of Air/Fuel Ratio. In order to expedite the measurement of the overall air/fuel ratio (without running the engine for a long periods of time) in particular when the in-cylinder imaging was performed, an universal exhaust gas oxygen sensor (UEGO) was employed. The unit was calibrated using a bench-top apparatus. Since the response of the UEGO sensor was found to be relatively prompt and consistent in this bench-top test, the tedious and often erroneous flow measurement of fuel and air was replaced by this method. Figure 3 shows the calibration curve of the UEGO sensor, which was employed throughout the present experiment. It is noted that if this UEGO sensor were used in the range of very lean air/fuel ratios the accuracy of calibration would have been somewhat uncertain.

High Injection Pressure (HIP) Fuel System. The electronically controlled HIP used in the present study was basically the same design as BKM's Servo-jet type [6]. It is a pressure intensifier type whose functional details were described elsewhere [1]. Since the factory delivered unit was not compatible to the engine explained above, an entirely new unit was fabricated to deliver injection pressure of up to 165 MPa (24,000 psi) for earlier studies [4,5], which offered the basic expertise towards the new design-construction of an improved HIP employed in a recent study [1], which was also used in the present investigation.

The distinctive difference of the Rutgers-built unit from the original Servo-jet is that it uses the existing Cummins nozzle tips (0.15mm nozzle hole diameter) for technical and economical flexibility and that the fuel intake and return ports in the Cummins engine were directly interfaced with the new unit. That is, the new assembly directly replaces the Cummins PT-type injector. Figure 2 shows the spray axis with respect to the imaging IR window indicated by a shaded circular portion.

A schematic drawing of the new HIP units built at Rutgers may be found in Appendix-I (Fig. 1). The low-pressure fuel supply was made as high as 12 MPa (1,750 psi) through the fuel gallery in the cylinder head, which intensified to an injection pressure of 210 MPa (30,625 psi) by the new unit. According to an extensive bench-top and engine experiment, performance of this new HIP was measurably affected by the temperature of the injection nozzle, as discussed later.

After completing construction of the new unit, an extensive system characterization was performed using a bench-top test device. The injection time was determined by placing a pressure transducer at a location approximately 10 mm away from the nozzle hole while the period of energizing the three-way valve was varied. This determines the period of connection between the rail pressure and the primary piston. The timing of the pressure transducer signal was compared with the end of the energizer period when the needle was expected to rapidly lift up. The performance of this injector evaluated in the bench-top experiment is shown in Figs. 2 and 3 in Appendix-I, which include the relationship of the amount of fuel delivery to the engine speed for varied rail pressure.

The result exhibits a predictable performance of the new unit, a trend which was the same for all spacer thickness employed in the experiment. Note that the rail pressure represents the injection pressure determined by the intensifier (area) ratio, that is 17.5. For example, the rail pressure of 12 MPa corresponds to an injection pressure of 210 MPa (30,625 psi) at the nozzle opening.

Results obtained using all of the spacers were combined to plot Fig. 3 in Appendix-I, which facilitated determination of the amount of fuel delivery during the experiment. As expected, for a given spacer thickness, the higher the rail pressure the greater the amount of fuel delivered. The results shown in the figure for variation of spacer thickness and rail pressure were employed for the range of the present parametric study of the HPD CI-DI engine with HPI. For example, the mass of air flow into the engine was compared with the fuel delivery from this plot in order to determine the overall air-fuel ratio for each engine running condition. At the same time, the reading from UEGO sensor was monitored.

High-speed Four-band IR Digital Imaging System. The fingerprint of (both low and high temperature) thermo-chemical molecular characteristics (such as distributions of temperature, reaction fronts and species population) can be found more in the IR domain than the visible range. This fact motivated us to develop a new high-speed spectral IR digital imaging system several years ago. The development of our IR system at Rutgers has been a progressive course of work.

The first generation of this research tool captured successive flame images at high rates using only a single camera head [7]. The next system employed two camera heads in order to capture two geometrically (pixel-to-pixel) identical IR images in respective spectral bands, i.e., a two-color system [8], which permitted determination of temperature and water vapor distributions in flames. Its prototype electronic systems were all fabricated via hand-wiring directly using many transistor-transistor-logic (TTL) components. One of the main functions of the camera circuits was to generate the timing signals required to operate the charge-coupled-device (CCD). This two-color system was redesigned (using Protel and Orcad design systems) and constructed in printed boards, which included several programmable logic gate arrays (using Max-Plus, Altera Corp.) that replaced most TTL components helping to minimize noise in the IR images.

In the new SIS, four separate high-speed IR cameras are lined up to a single optical unit, and are simultaneously triggered at successive instants of time by using signals generated from the engine being investigated. This permits capturing a set of four

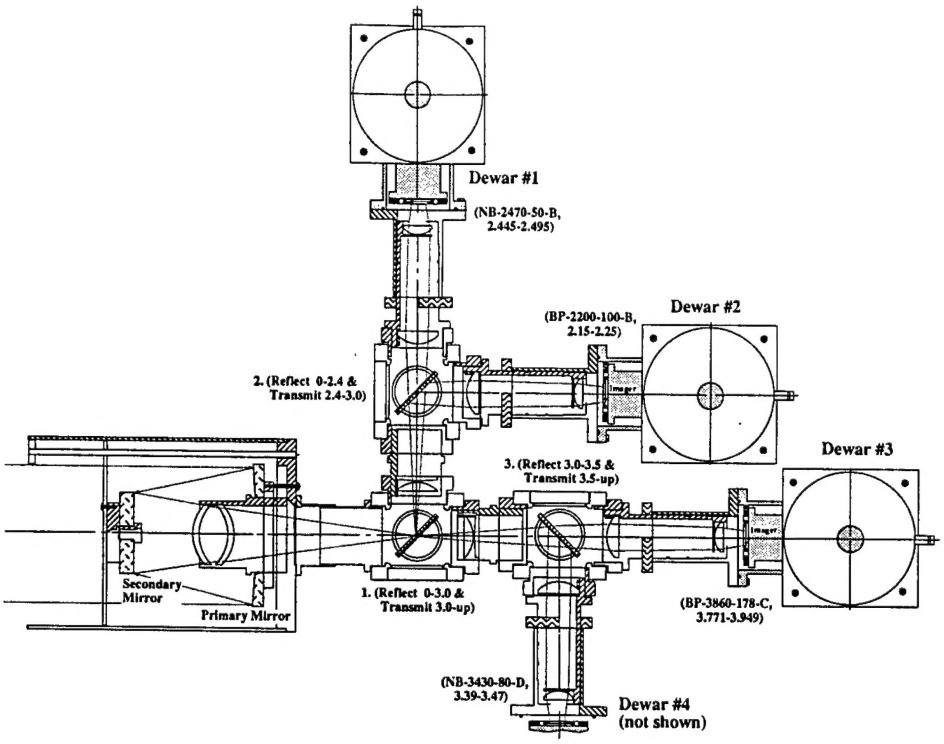

Fig. 4. Schematic Presentation of an Optical Setup Lined up with Four IR Cameras having Respective Filter Bands in Front.

geometrically identical images at each moment [8]. In order to maximize the radiation energy incident on the imagers housed in the liquid-nitrogen cooled Dewars, a large reflective optical head (152mm diameter) was employed which was followed by three new spectral beam splitters. This divides the IR domain into four ranges for respective imagers. Narrow band filters were installed in front of the respective cameras.

Among the filters with central wavelengths employed to date are 2.2μm, 2.47μm, 3.42μm, and 3.8μm. In spite of the small amount of radiation passing through those band filters, cryogenically cooled PtSi imagers have sufficiently high sensitivity. Unlike most high-speed visible-range imaging, no separate (IR) light source was needed. The digital data obtained in respective spectral bands were processed to determined simultaneous distributions of temperature, water vapor, and soot [8].

A schematic presentation of the optical head, which contains four high-speed IR camera, is included in Fig. 4. At present the system can be operated at a rate of over 2,000 frames/sec/camera, that is, the total 8,000 pieces of 64x64 data matrices per second in 12-bid dynamic resolution.

Data Analysis and Presentation Method. The amount of data accumulated by using the SIS is far more than one can possibly handle manually, such as printing the sets of images (in colors) and placing them side by side even in order to perform the initial screening work. An absolute need was realized for developing something efficient to replace such manual data analysis method. For this, the development of a new PC-based computer software was initiated several years ago, and improvement has become reality

and proven useful, which is referred to as Rutgers Animation Program and called RAP for short (Copyright application is pending).

Briefly, using the RAP, the raw data transferred into a PC from the SIS can be individually displayed over the PC screen, and at the same time the sets of images can animated side by side, which help understand the dynamics of in-cylinder reactions. Several choices of animation are among the functions of the program, namely simultaneous display of: (1) one movie; (2) two movies; (3) four movies; (4) six movies and (5) eight movies. Mentioning other advantages of these features, when the six-movie animation is employed, three sets of spectral (raw) data can be simultaneously animated along with three sets of quantitative results obtained by the corresponding raw data and spectral methods (i.e., three band iterative method) on the same screen. For more utility and versatility, the RAP is being further developed. For example, an additional feature is being added to the RAP at present, which is to simultaneously display as many as twenty-eight (28) sets of high-speed movies over a single PC screen in a controlled manner. This feature would be particularly useful in analyzing a large amount of in-cylinder images, because a typical engine study accumulates typically over a thousand sets of movie.

4. RESULTS AND DISCUSSION - PERFORMANCE MEASUREMENT

The results are presented in two parts: The engine performance measurements are explained first, and the in-cylinder imaging results are discussed later.

Some amount of initial engine measurements was accumulated [1] towards meeting the original work task requirements. The analysis of the engine measurements in this experiment, however, suggested that the fixed injection timing for a wide range of engine variation was improper due to the change of ignition delay period.

Consequently, the same engine experiment was performed at varied injection times identifying the best-torque under the respective operating conditions, a new step of the experiment which was not planned in the original work scope. This finding led us to accumulate a considerably larger amount of engine data, which appears to be yet insufficient, however. While this adjustment was made, due to the time limit (contractual), the extent of the work was inevitably modified from the original scope.

The entirely new sets of experimental results were obtained based on the preliminary engine evaluation [1], which are summarized in Figs. 5 (A) and (B). The numbers (from 1 to 34) in the circle and square represent the individual graphs obtained with engine speeds of 600 rpm and 1,200 rpm, respectively. The figures designated by those numbers are all included in Appendix-III. They were constructed to accommodate many measurements obtained under varied injection times ranging anywhere from 20 to 50 data points. They, therefore, represent the engine measurements from over 1,000 individual engine operation conditions.

The range of measurements include variations in air/fuel ratio of 19-26, intake air temperature of 100-300° F (37-149° C), and the (expected) injection pressure of 17,000-29,000psi (117-199MPa). Basically the results were obtained in order to evaluate parametric impacts on the indicated mean effective pressure (IMEP). It is noted that, unless otherwise noted, each point of IMEP over those graphs was the averaged value of digitized pressure-time over eight (8) consecutive cycles.

(A)

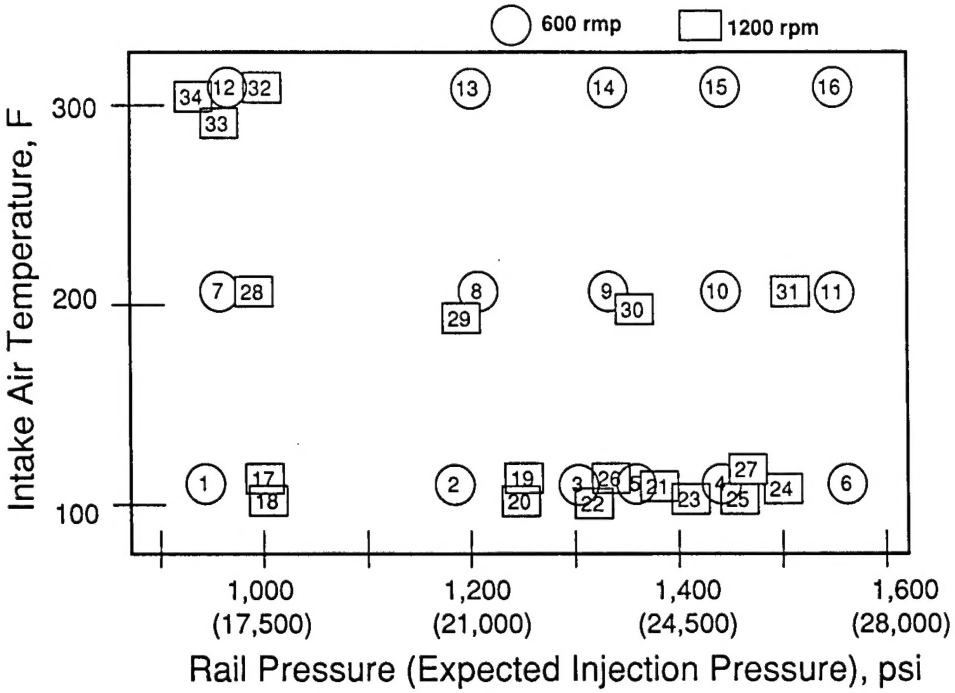

(B)

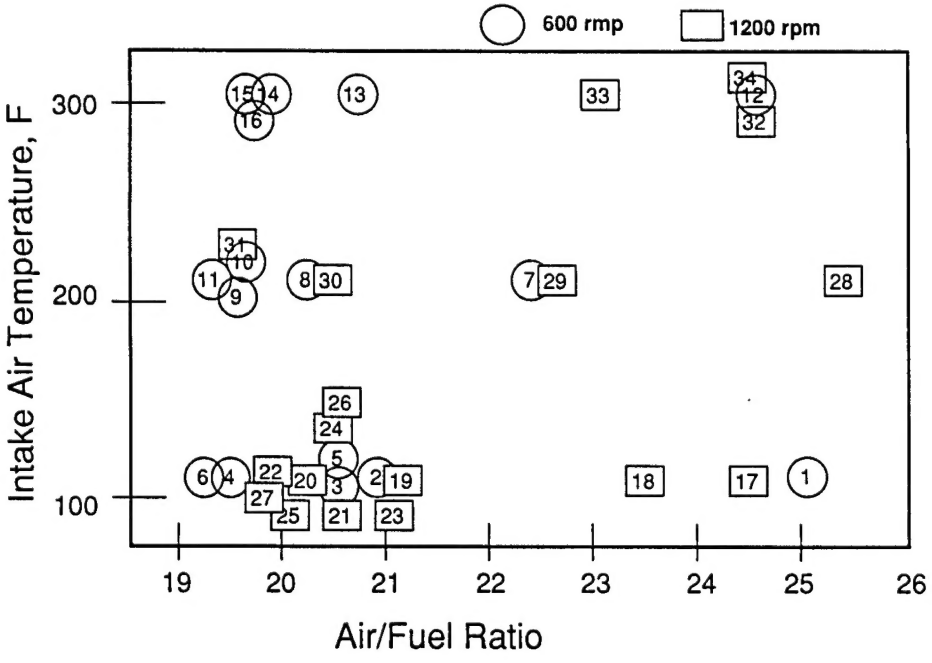

Fig. 5. Summary of LHR HIP DI-CI Engine Performance Analysis:
(A) IMEP in Varied Intake-air Temperature vs. Injection Pressures;
(B) IMEP in Varied Intake-air Temperature vs. Air/Fuel Ratios.

Intake Air Temperature. It is especially noted that when the intake air temperature was varied throughout the experiment, the inlet pressure was accordingly changed in order to introduce the same amount of air. This method was chosen because the effect of temperature on the volumetric efficiency is well known, and was not to be investigated in the present study. Rather, the focus was to evaluate the combustion phenomena under the same volumetric efficiency.

Referring to Figs. 5-(A) and -(B), under the same injection pressures, the same engine speed, and also the same (or similar) air/fuel ratios, the following groups of figures are compared to each other (Fig. A-**2**, for example, represents that marked by **2** in one of figures included in Appendix-III):

(A) 600 rpm for the comparable injection pressure approximately,

17,500 psi: Figs. A-1 & A-12;
21,000 psi: Figs. A-2 & 13;
24,500 psi: Figs. A-4, A-10 & A-15;
28,000 psi: Figs. A-6, A-11 & A-16.

(B) 1,200 rpm for the comparable injection pressure approximately,

21,000 psi: Figs. A-21 & 30;
24,500 psi: Figs. A-27; A-31

Reviewing the individual sets of data listed above, the results exhibit *a highly consistent observation*: As long as the air/fuel ratio is comparable and the injection time is adjusted for obtaining the maximum torque, *the temperature variation of the intake air did not appear to affect the IMEP*. This observation is quite different from deteriorated engine performance with increased intake air when results from LHR (or uncooled) DI-CI engines equipped with ceramic components were reported by others. (This finding is also highly encouraging for developing a high-power-density HIP CI engine with ceramic engine components.)

This observation is rather unexpected because when the intake charge temperature is elevated, as briefly mentioned earlier the onset of the self-ignition would be prematurely advanced so that a greater amount of heat release was expected to occur during the relatively sluggish diffusion flame stage resulting in a deteriorated thermal efficiency.

Among the possible reasons for this encouraging result regarding the temperature effect (because the power output would not deteriorate in an LHR engine due to any observable combustion abnormality) is the use of and HIP system. That is, while the fuel spray by low-pressure conventional injectors may suffer (by an increase in the intake air temperature) via prematurely advanced onset of premixed combustion, the enhanced atomization of the HIP seems to result in a rapid heat release during the premixed combustion stage.

Injection Pressure Effects. Looking at Figs. 5 (A) and (B), a list similar to above can be made in order to find the effects of injection pressure change on the IMEP:

(A) 600 rpm for the intake temperature of (under a comparable air/fuel ratio)

100 deg F: Figs. A-2, A-3 & A-5; Figs. A-4 & A-6.
200 deg F: Figs. (A-8) A-9, A-10 & A-11.
300 deg F: Figs. A-14, A-15 & A-16.

(B) 1200 rpm for intake air temperature of

100 deg F: Figs. A-20 & A-25; Figs. A-22 & A-27; Figs. A-24 & A-26.
200 deg F: (Figs. A-30 & A-31)
300 deg F:

When the intake air temperatures were relatively low (100 deg F), the effects of injection pressure on the IMEP seemed to be insignificant. On the other hand, they were found to be measurable when they were high (200 deg F). That is, the higher the injection pressure, the greater the IMEP. This trend, however, was not found when they became very high (300 deg F). This may be due to an excessively early onset of self-ignition, which the roles of HIP probably were not able to offset. This issue certainly needs an additional study.

According to the review of these results, while the effects of increased injection pressure are not significant in enhancing the IMEP, they were found to be quite remarkable in reducing the soot emissions [1].

Air Utilization. After finding some significant advantages of producing smaller amounts of soot emission when the fuel was introduced at high pressures using an HIP, the present measurement were made with the air/fuel ratio varied from 19-1 to 26-1. Recall that the present engine was operable at the overall air/fuel ratio of 18-1 having soot emissions no worse than those with 30-1 by the conventional low-pressure PT-type injector [1]. A similar list is made below in order to assess the effects of air utilization on the IMEP.

(A) 600 rpm for the intake temperature of (under the comparable intake air temperature and pressure)

100 deg F: Unavailable
200 deg F:
300 deg F:

(B) 1200 rpm for intake air temperature of

100 deg F: Figs. A-19 & A-20; Figs. A-22 & A-26
200 deg F:
300 deg F: Figs. A-33 & A-34; Figs. A-32 & A-33.

Since this attempt of comparison is rather restricted, that is, to find the engine running conditions under the same intake air temperature and at the same time with the comparable fuel injection pressure, the list became incomplete by selecting those from the present pool of data.

As expected, however, according to what is available in the list, the effects of air utilization on the IMEP was the most significant of all parameters investigated. That is, the lower the air/fuel ratio the higher the IMEP.

Injection Time. As briefly mentioned earlier, unlike the relatively fixed injection time employed in the conventional DI-CI engine with a low-pressure injection unit, according to the preliminary performance analysis, there seems to be an optimum time for the best output under a given engine condition of varied intake air and injection pressure

[1]. That is, a high-power-density LHR DI-CI engine (equipped with an HIP and ceramic components) may have to vary the start of injection in order to maximize the engine output.

The need seems to be reasonable in view that the higher the intake air temperature, the shorter the ignition delay. In addition, it is also expected that the higher the injection pressure, the shorter the ignition delay. When these effects are compounded with variations of air/fuel ratio which affects the engine temperature (so does the intake air temperature), the need for variable injection time in the new LHR engine seems to be reasonable.

When the need for adjusting the injection time in an LHR HIP DI-CI engine is considered, the engine operating speed is expected to be an important variable because the change of ignition delay mentioned above is a measure in time while the adjustment will have to be made in engine crank angle which however is subjected to change with the engine speed.

Due to limitations of the present work (in time and instrumentation), the present data pool obtained two different (relatively low) speeds may be insufficient for a meaningful analysis of the need for the injection time in an LHR HIP CI engine. (Note that there was a need for operating the engine at a relatively low engine speed, that is 600 rpm, in order to determine the engine response to the abovementioned parametric variation to be studied in the low-speed optical engine.)

Even if the results obtained at the engine speed of 600 rpm are excluded (because it is not a typical engine speed at which an engine is normally operated), some of the results accumulated at 1,200 rpm as included in the present data pool show some trend exhibiting the need for the timing adjustment. That is, the higher the injection pressure, the later the injection time for the best IMEP. At the same time, the higher the intake air temperature, similarly the later the injection time in order to obtain a high IMEP.

5. PRESENTATION OF IN-CYLINDER HIGH-SPEED IR IMAGES

In order to facilitate the discussion of the present spectral IR images, Fig. 6 is included, which indicates the spectral bands employed for the imaging with respect to spectrodiagrams of several species expected to be present during the reaction period.

Ideally, the individual spectral images would indicate four distinctively different signatures of species according to the reaction condition of the combustion chamber. This did not happen, however, due to the mutual interference by radiations from many different species which are present in the DI-CI engine combustion environment, in particular since the real-world D-2 fuel oil was used in the experiment.

Spectral Images of DI-CI Combustion. In selecting the spectral bands in the study, images via bands of 2.47μm and 3.42μm were expected to reveal the radiation mainly from water vapor. The latter was later found to exhibit chemiluminescent radiation emitted by some unknown intermediate species formed during the ignition delay period. It became an interesting discovery that chemical reactions commenced as soon as the fuel is introduced into the cylinder. Spectral bands, 3.80 μm and 2.20 μm were employed in the imaging in the expectation that the captured radiation would be mostly from soot radiations in absence of those from other species. The latter, however, was found to include some measurable amount of radiation from water vapor [9], which was compensated for in the quantitative imaging.

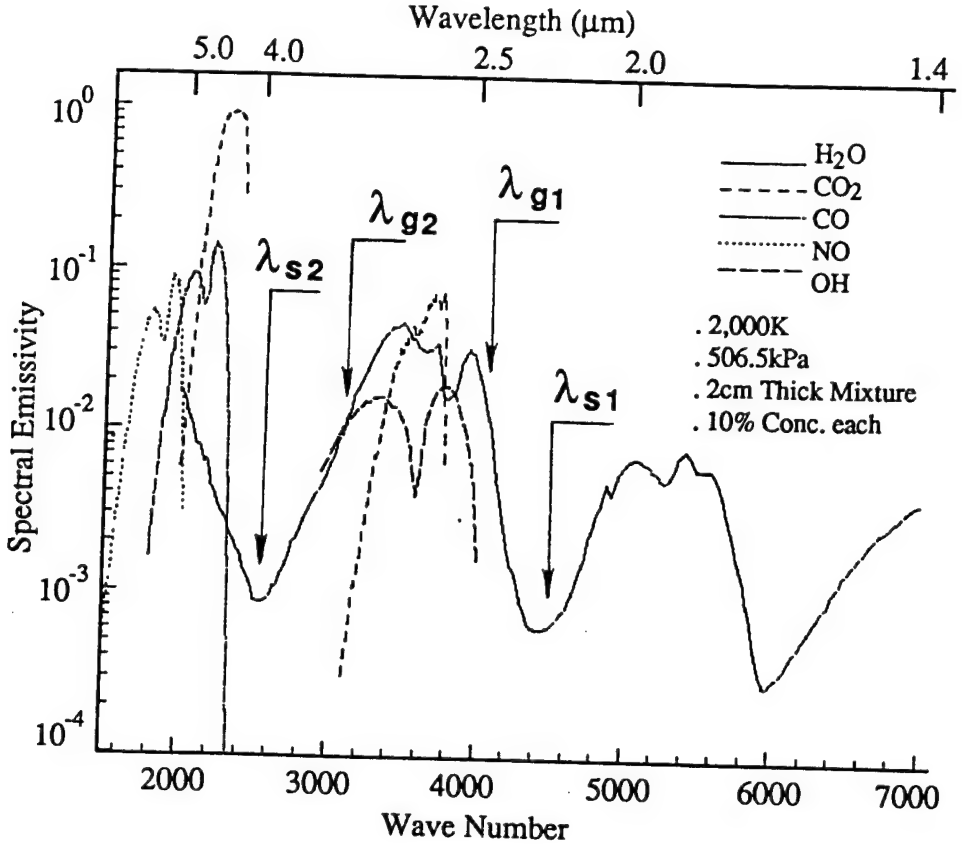

Fig. 6. Spectrodiagram of a Mixture and Spectral Bands Employed in the Imaging.

A set of typical high-speed spectral IR images taken from the optical engine is explained first by presenting Fig. 7 (A)-(D). It is noted that the entire image results included here were taken at the engine speed of 600 rpm and the imaging rate of 1,887 frames/sec with the start of imaging, which resulted in approximately a 2-CA imaging interval. The direction of spray growth is from the lower right corner to the upper left end, which may be referred to Fig. 2 where the axis of spray is located in the imaging area marked by a shaded circle.

Even though the digital images were captured in 12-bit dynamic resolution, that is 4,096 to 1 ratio between the highest number to the lowest one in scale, the presentation here is a gray-scale, which severely limits the representation of overall variations. In order to help exhibit the local variation, in particular, a modified gray-scale was employed in plotting those images. Therefore, the brightness does not directly relate to the corresponding radiation strength.

Explaining the results in Fig. 7, the engine was operated at the overall air/fuel ratio of 22.7 and injection pressure of 25,375 psi (175 Mpa) with the room-temperature intake air. The first frame started at 21 bTDC and the imaging thereafter continued in a 2-CA interval as explained above. Since the first image taken via 3.42μm band (Fig. 7-(C)) almost immediately reflects the presence of the fuel in the combustion chamber, the injection started at around 12 bTDC, which compares with the bench-top evaluation. While the radiation in this band exhibits the growth of spray structure indicating some remarkable chemical reactions thereby producing such radiating species, according to the images obtained via 2.74 μm (Fig. 7-(D)), there is no signature of radiation from water vapor formation, the onset of the premixed combustion stage. (According to this observation the ignition delay in this reaction was approximately a period of 10CA.)

(A)

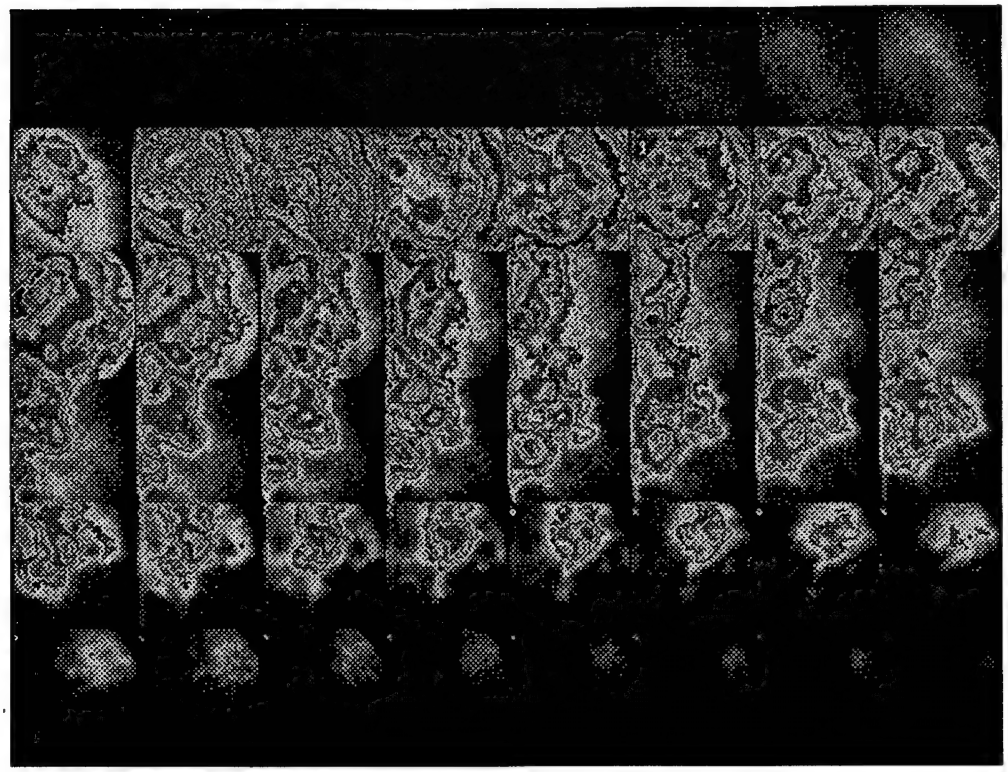

(B)

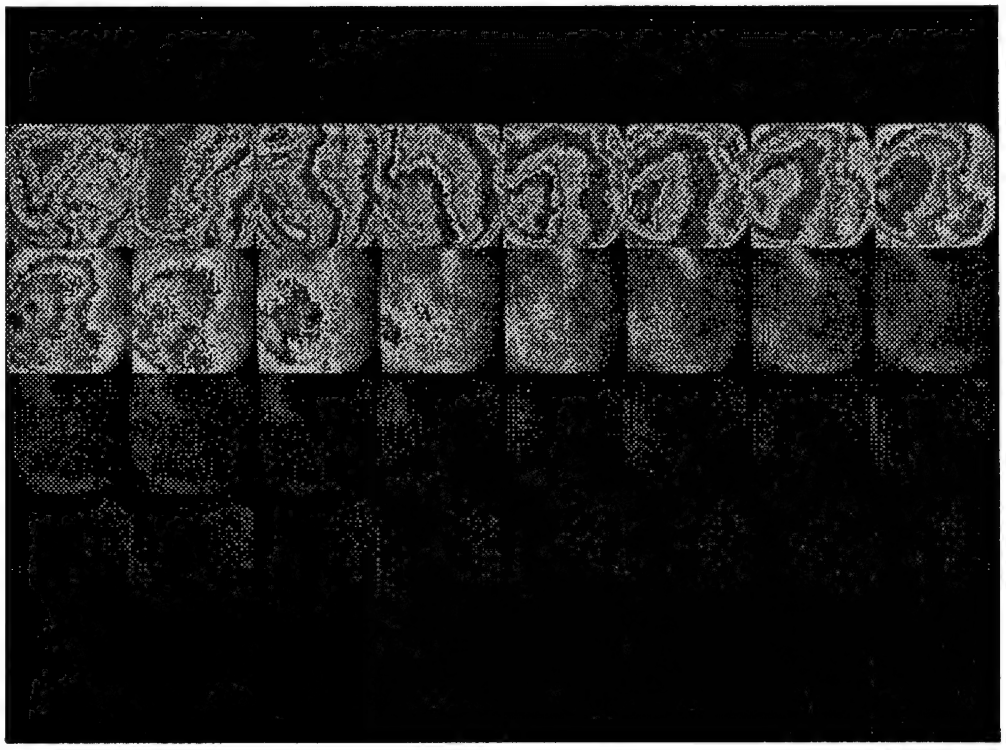

Fig. 7. High-speed Spectral Images from DI-CI engine with an overall air/fuel ratio of 22.7 and injection pressure of 25,375 psi (175 Mpa): (A) 3.8μm and (B) 2.2μm.

(C)

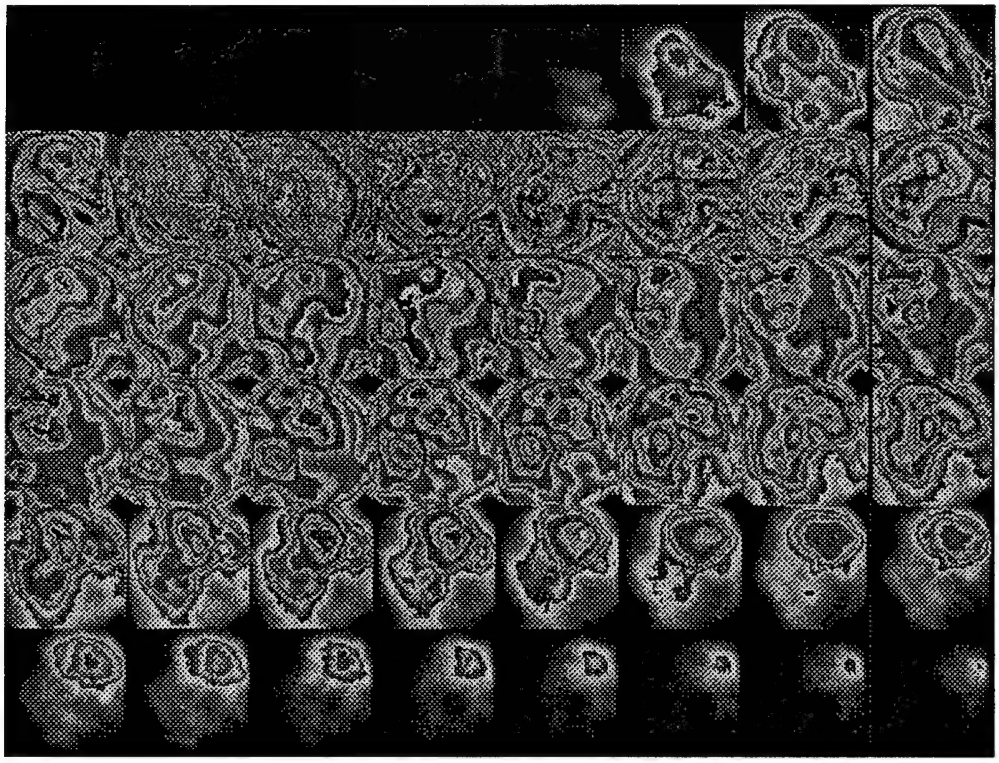

(D)

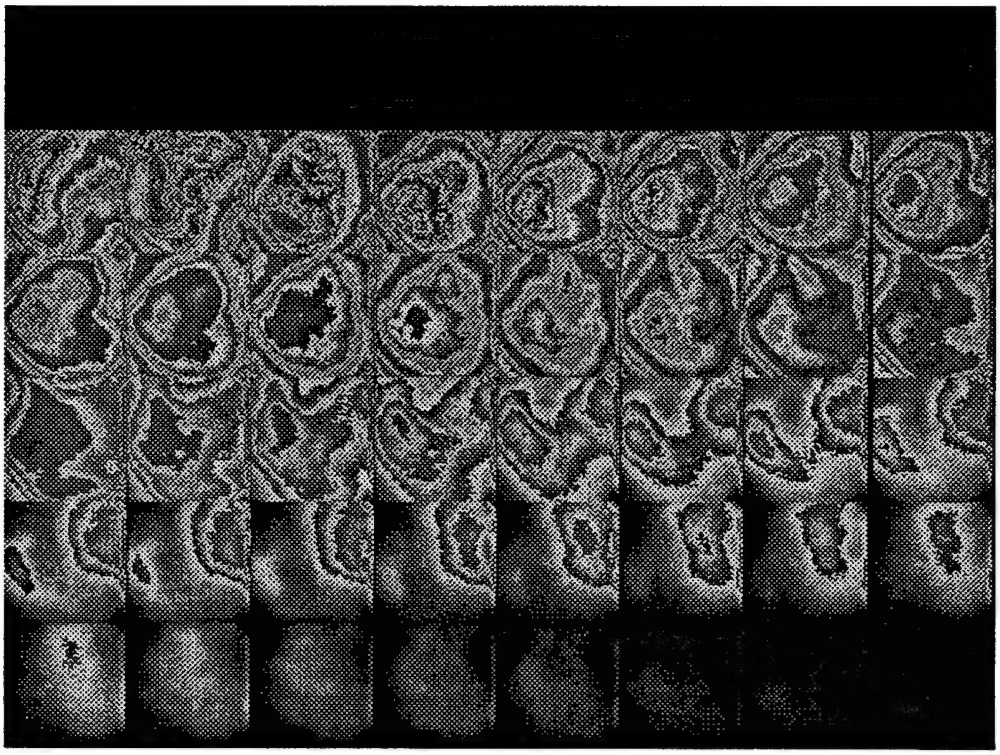

Fig. 7. High-speed Spectral Images from DI-CI engine with an overall air/fuel ratio of 22.7 and injection pressure of 25,375 psi (175 Mpa): (C) 3.42μm and (D) 2.27μm.

(A)

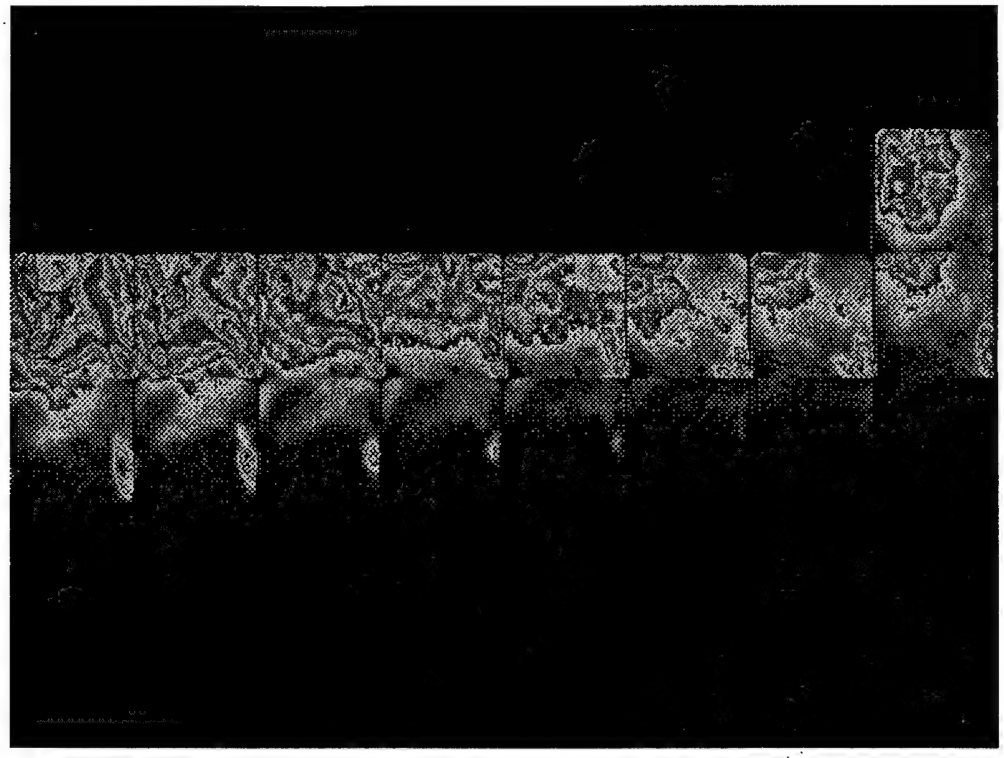

(B)

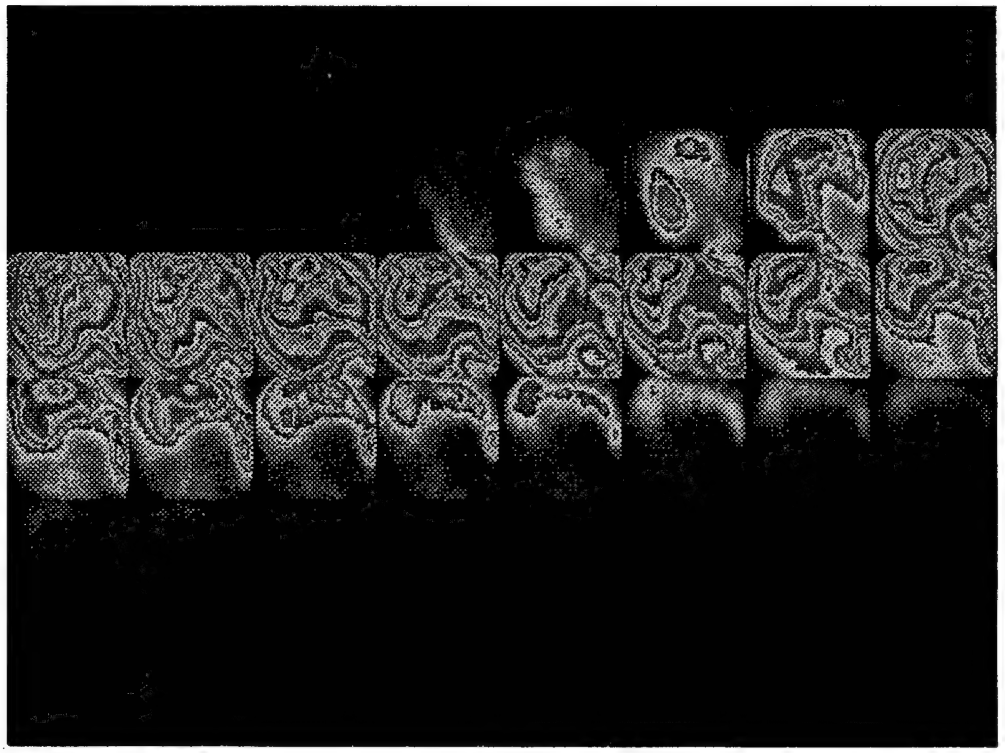

Fig. 8. High-speed Spectral Images with intake air at 38°C, an overall air/fuel ratio of 30-1 and injection pressure of 16,625 psi (114 Mpa): (A) 2.47μm and (B) 3.42μm.

(A)

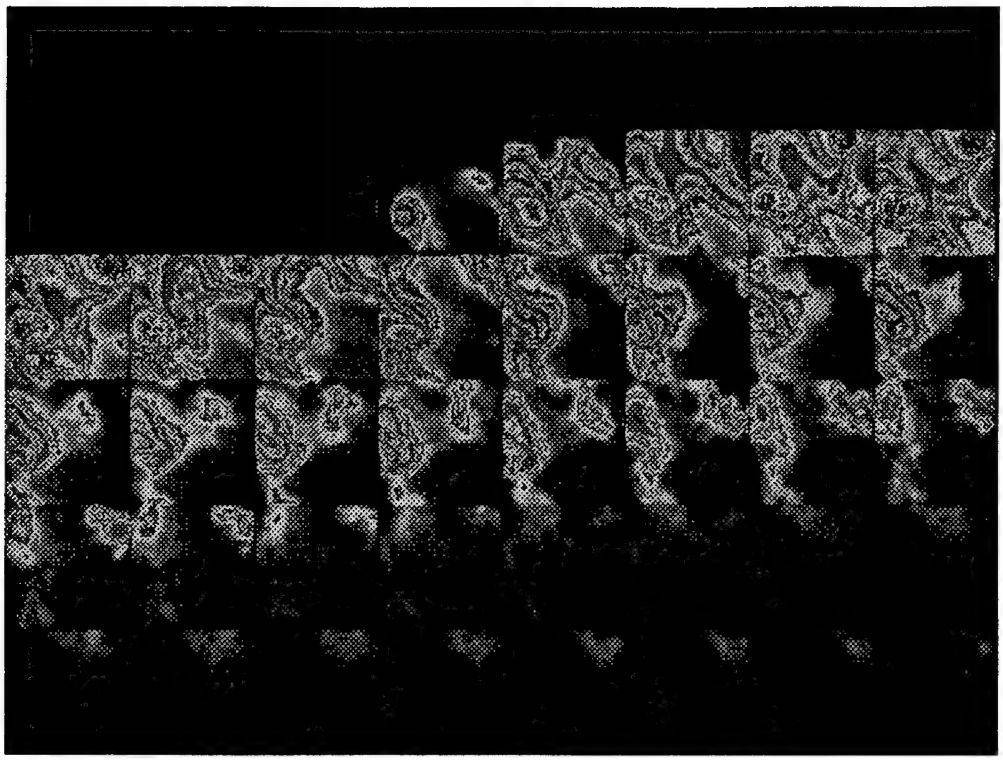

(B)

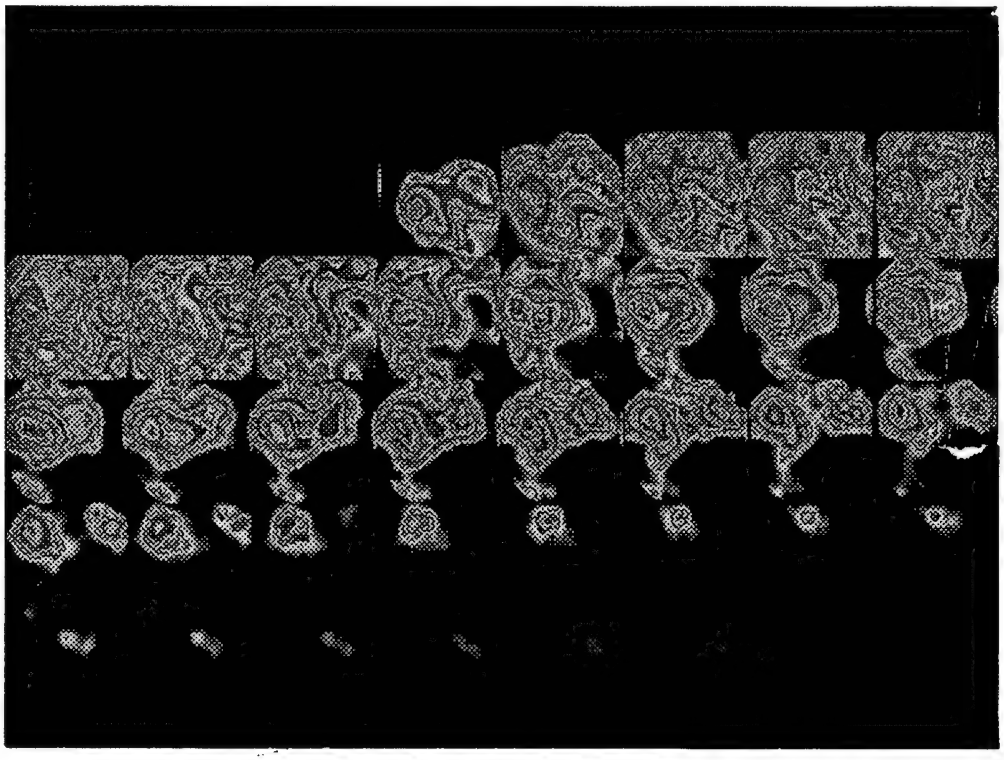

Fig. 9. High-speed Spectral Images with intake air at 150°C, an overall air/fuel ratio of 30-1 and injection pressure of 16,625 psi (114 Mpa): (A) 2.47μm and (B) 3.42μm.

(A)

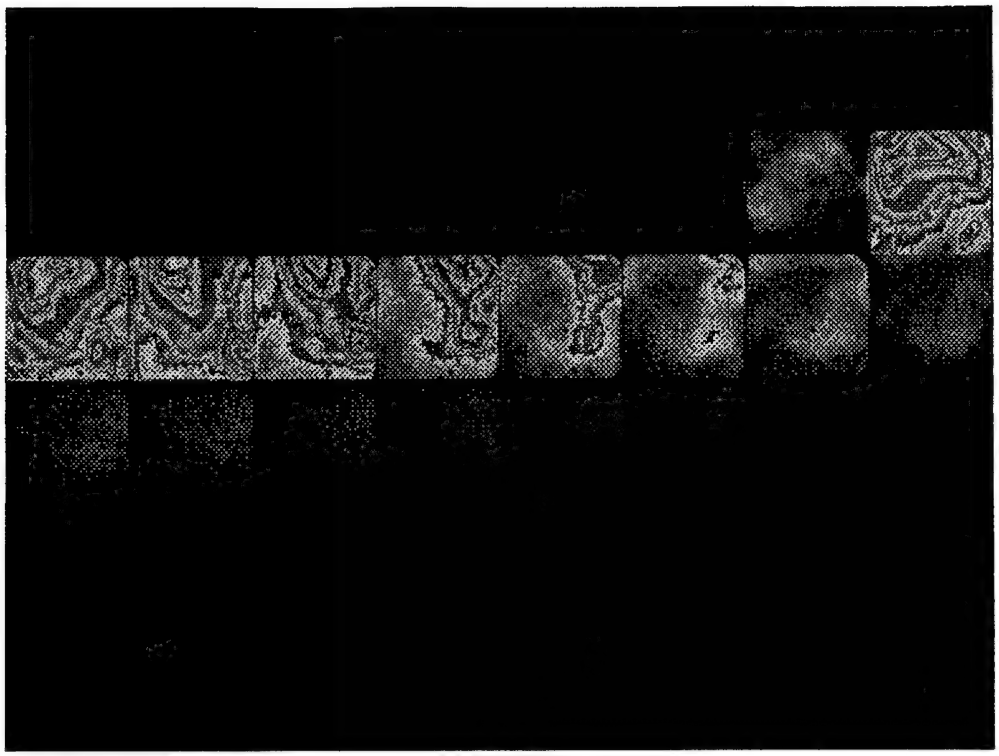

(B)

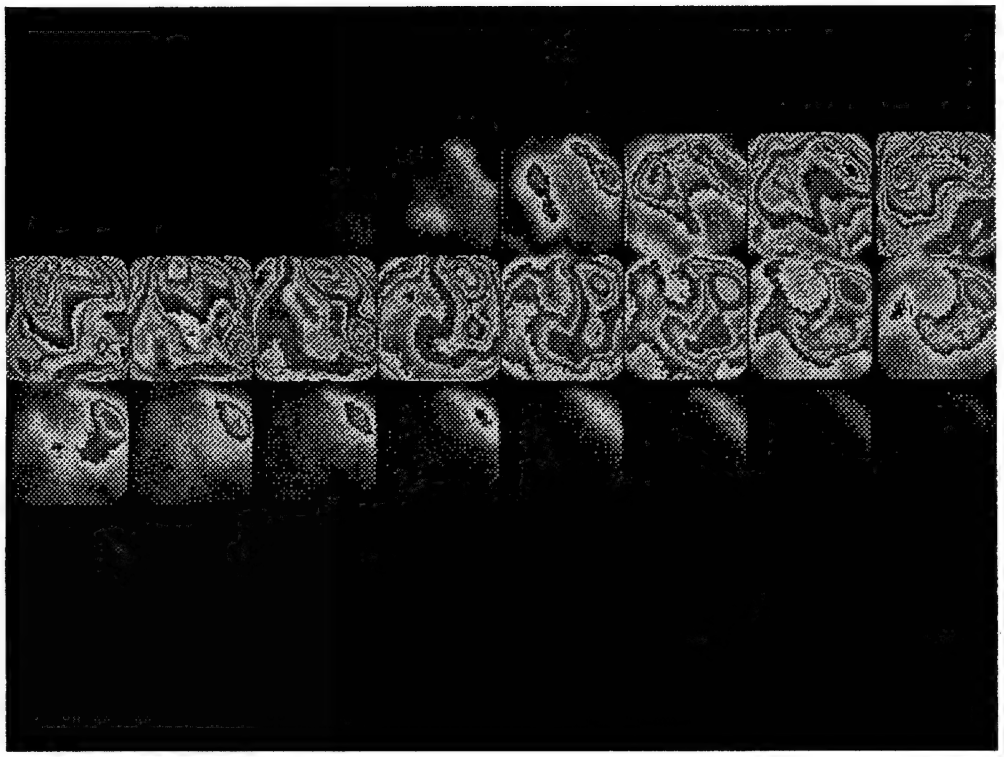

Fig. 10. High-speed Spectral Images with intake air at 38°C, an overall air/fuel ratio of 30-1 and injection pressure of 30,625 psi (210 Mpa): (A) 2.47μm and (B) 3.42μm.

(A)

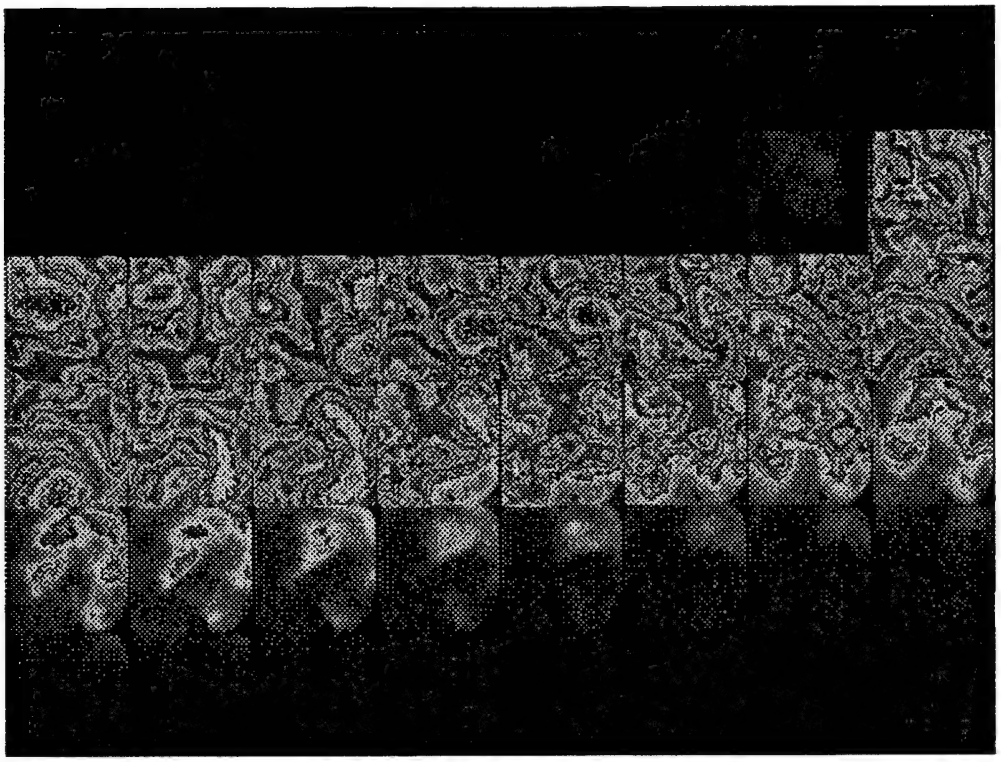

(B)

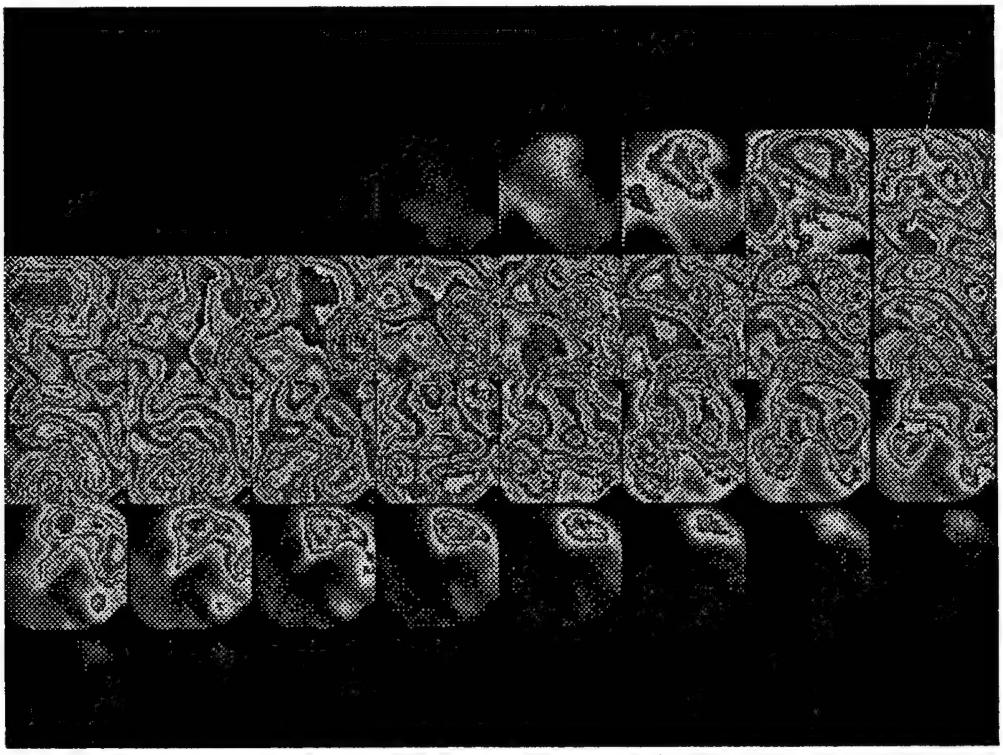

Fig. 11. High-speed Spectral Images with intake air at 38°C, an overall air/fuel ratio of 20-1 and injection pressure of 30,625 psi (210 Mpa): (A) 2.47μm and (B) 3.42μm.

Note that at about the same time when the first abovementioned chemiluminescent image was captured, there was a similar trace of radiating image is realized via the 3.8μm band (Fig. 7-(A)). The source of the radiation for this signature is not known at present, however. Without taking rigorous steps of determining quantitative imaging, one could qualitatively expect is that images in the 3.8μm band are likely dominated by radiation from soot because it is relatively free from those of other species. Since there would not be any soot formation to occurring during the ignition delay period, the signature of radiation via this band at that time offers a new question to be studied.

Since the reaction processes in the DI-CI engine are heterogeneous and stratified, and since the respective band filters are expected to capture signatures of different species and the temperature variations, it may not be surprising to find that the corresponding images in those bands do not necessarily match each other throughout the reaction period. Of course, in some periods of the reaction, they appear to be mutually comparable each other. Among the remaining tasks of the work, therefore, would be to identify and also to quantify the reasons why they are different from each other.

What is to be studied from this digital information includes determination of distributions of temperature, water vapor concentration and soot over the spray, which is being carried out by using our three band iterative method. (In addition, a new spectrometric method employing four band results, four-band reference method is being developed at present.)

There is no doubt that much can be discussed about these results, in particular when they are animated using the RAP, the data analysis and presentation method mentioned earlier. The dynamics of in-cylinder reactions under varied parameters, when they are displayed by the RAP, is better understood, which can not be conveyed in a report.

Intake-air Temperature Effects on In-cylinder Reactions. Two sets of high-speed spectral images taken (in 2.47μm and 3.42μm bands) with intake air temperatures of 38°C and 150°C are shown in Figs. 8 and 9, respectively. The engine was operated with the injection pressure of 16,625 psi (114 MPa) and air/fuel ratio of 30-1. (It is pointed out that Figs. 8-11 were taken with the identical imaging system sensitivity, which is somewhat different from the setting employed when Fig. 7 was taken.)

Looking at Fig. 8 for intake air at 38°C, the ignition delay was a period of 10 CA with onset of abrupt and strong premixed combustion relatively free of residual oxidation in the later stage of combustion. The same taken with intake air at 150°C (Fig. 9), on the other hand, reveals that there is basically no ignition delay period. That is, the onset of premixed combustion occurs almost as soon as the fuel entered the combustion chamber. When this happened, the combustion reaction seemed to be rather sluggish having a long combustion period. It is pointed out that the intake temperature of 150°C is rather unusual even in the LHR engine environment. (Note that it was within the range of the work scope.)

It is most likely that the soot formation would be very high under this condition. This expectation was confirmed from an increased amount of soot deposit accumulated over the IR window compared with that under the engine operation with a relatively low air temperature. In spite of such deterioration of combustion in terms of the heavy soot formation, the IMEP was little affected by the intake air temperature as long as the volumetric efficiency is maintained the same.

The intake air effect may be an even more serious problem than the seemingly simple discussion made above. When the LHR engine is operated, the engine intake air temperature is expect to be high, and its effected was briefly discussed above, but the effect would not be confined to the air only. An additional concern is an increased fuel temperature to be encountered in the LHR engine. When this happens, which evidently affected the present measurements, the spray formation would be altered from what is expected in the conventional DI-CI engine. (It is noted that when the intake air temperature was high, the performance of our HIP system was noticeably changed, which is beyond the scope of the present discussion) The effect of the increased intake air temperature will have to be, therefore, reflected on the consideration of its impacts on the (fuel and) injector.

Injection Pressure Effects on In-cylinder Reactions. In order to discuss the effect of the injection pressure on the in-cylinder reactions in an HIP DI-CI engine, Figs. 8 and 10 are compared to each other. Fig. 10 included the results obtained from the same engine but at a high injection pressure, which was (expected to be) 30,265 psi (210 Mpa).

A noticeable difference between the two sets of results is that the radiation intensity with the higher injection pressure (30,625psi) was remarkable lower than that with the low injection pressure (16,625 psi). The combustion period was also noticeably shorter with the high injection pressure. Although the gray-modified scale presentation of the result may not reveal it, the higher injection pressure resulted in a greater uniformity of combustion reaction over the reaction volume, which may explain the reasons for low soot formation as explained in the earlier report [1] included in Appendix-I.

Although the noise measurements were not conducted in the present experiment, the noise increased quite significantly with the injection pressure, which may be of concern in designing the production LHR HIP DI-CI engine.

Air/Fuel Effects on In-cylinder Reactions. Since the main avenue to achieve a high-power-density DI-CI engine is the greater intake air utilization, the reaction processes of such an engine is of great concern. For this, Figs. 10 and 11 are reviewed together. Note that the results in Fig. 11 were obtained under the same condition for those in Fig. 10 but with a lower air/fuel ratio, which was 20-1.

The occurrence of preflame reactions appeared to be mutually comparable. Flame developments of the early stage in both cases are also quite similar to each other. An extended combustion is realized with the richer overall combustion. It is reminded, however, that the smoke emission with such a rich mixture produced no worse than that of operation by using the conventional mechanical injector with an overall air/fuel ratio of over 35-1.

Note. It was recently discovered that the in-cylinder observation made during the very first several cycles do not appear to represent what is happening in a warm engine. It is noted that most photographic studies of in-cylinder reactions are made in such a manner as to minimize the deposit formation over the optical window. Nevertheless, when such a method is employed, again, the observation would be different from the reaction in the typically warm engines.

Figures 8-11 were obtained earlier in a similar manner as mentioned above. Those in Fig. 7, were obtained after discovering this finding. However, the basic trends, all discussed in this report, appear to be the same even under warm engine conditions, which will be reported in the future.

SUMMARY

In order to provide some basic knowledge for designing a high-power-density (HPD) low-heat-rejection (LHR) high-injection-fuel (HIP) direct-injection compression-ignition engine (DI-CI), two main methods were employed according to the work scope: (1) engine performance analysis; and (2) in-cylinder imaging. This work was performed with the support of two graduate students over a period of two years.

In the performance analysis, a Cummins 903 engine mated with an HIP designed-fabricated at Rutgers equipped with a new high-temperature intake air supply system (which can provide the intake air as high as 204°C) was used. A new use of a UEGO sensor was introduced (by calibrating using a bench-top apparatus) in order to rapidly determine the overall air/fuel ratio.

The range of air/fuel ratio studied was from 18-1 to over 35-1, the injection pressure investigated was as high as 30,625 psi (210 Mpa) under varied intake air temperature over 150°C. Over one thousand engine operation conditions were evaluated by averaging digitized pressure-time data accumulated over eight (8) successive cycles to determine the indicated mean effective pressure (IMEP).

For the in-cylinder imaging, a separate optical single-cylinder Cummins 903 engine was used. A high-speed four-color IR digital imaging system (called Super Imaging System, SIS for short) was greatly improved during this contract period. New spectrometric methods were developed to simultaneously determine the distributions of temperature, water vapor and soot concentrations (which have not been applied in the work yet due to the time limitation). In addition, a new data analysis and presentation method has developed, which permits simultaneous display of as many as twenty-eight (28) movies over a single PC-screen on a controlled manner. This enables us closer analysis and efficient presentation of raw data as well as processed results.

The performance analysis results are reported in two parts: a preliminary report as included in Appendix-I and an additional set of results (Appendix-III).

Some of the in-cylinder imaging results, which are now being captured by the improved SIS after incorporating with new (designed and fabricated in our laboratory) electronic packages, are included (in the text) with brief discussions.

7. REFERENCES

1. Themel, T., Jansons, M., Campbell, S. and Rhee, K.T.," Diesel Engine Response to High Fuel-Injection Pressures," SAE Paper 982683, 1998.

2. Han, Z., Hampson, G., Reiz, R., and Uludongan, A., "Mechanism of Soot and NOx Emission Reduction using Multiple-injection in a Diesel Engine," SAE Paper-960633, 1996.

3. Arcoumanis, C., Flora, H., Gavaise, M., Kampais, N., "Investigation of Hole Cavitation in a Vertical Multi-hole Diesel Injector," SAE Paper 2999-01-0524.

4. Clasen, E., Campbell, S., and Rhee, K.T., "Spectral IR Images of Direct Injection Diesel Engine Combustion with High Pressure Fuel Injection," SAE Paper-950605, 1995.

5. Clasen, E., Song, K., Campbell, S., and Rhee, K.T., "Fuel Effects on Diesel Combustion Processes," SAE Paper-962066, 1996.

6. Abata, D., Stroia, B.J., Beck, N.J., and Roach, A.R., "Diesel Engine Flame Photographs with High Pressure Injection," SAE Paper-880298, 1988.

7. McComiskey, T., Jiang, H., Qian, Y., Rhee, K.T., and Kent, J.C., "High-Speed Spectral Infrared Imaging of SI Engine Combustion," SAE Paper- 930865, 1993.

8. Jiang, H., Qian, Y. and Rhee, K.T., "High-Speed Dual- Spectra Infrared Imaging," Optical Engineering, 32 (6), pp. 1281-1289, 1993.

9. Chang, C., Clasen, E., Song, K., Campbell, S., Jiang, H., Rhee, K.T., "Quantitative Imaging of In-cylinder Processes by Multispectral Methods," SAE Paper-970872, 1997.

982683

Diesel Engine Response to High Fuel-Injection Pressures

T. Themel, M. Jansons, S. Campbell, and KT Rhee
Rutgers, The State University of New Jersey
Piscataway, New Jersey

ABSTRACT

A single-cylinder direct-injection (DI) Diesel engine (Cummins 903) equipped with a new laboratory-built electronically controlled high injection pressure fuel unit (HIP) was studied in order to evaluate design strategies for achieving a high power density (HPD) compression ignition (CI) engine.

In performing the present parametric study of engine response to design changes, the HIP was designed to deliver injection pressures variable to over 210 MPa (30,625psi).

Among other parameters investigated for the analysis of the HPD DI-CI engine with an HIP were the air/fuel ratio ranging from 18 to 36, and intake air temperature as high as 205°C (400°F). The high temperatures in the latter were considered in order to evaluate combustion reactions expected in an uncooled (or low-heat-rejection) engine for a HPD, which operates without cooling the cylinder.

Engine measurements from the study include: indicated mean effective pressure, fuel consumption, and smoke emissions.

It was found that a Diesel engine incorporated with an HIP under varied operational conditions, including those encountered in uncooled engine design needs variation of injection parameters, namely the start of injection and the rate shape.

When the engine operating condition shifts, the rapid variation of those parameters are needed in order to optimize the engine power delivery and fuel consumption as well as to minimize smoke emissions.

Other engine responses to the varied parameters in the high-pressure Diesel engine are also reported in the paper.

INTRODUCTION

The Diesel engine, or compression ignition (CI) engine has several advantages over the spark-ignition (SI) engine. It is more efficient, reliable, fire-safe, and environmentally-friendly than the SI engine, and therefore is almost exclusively employed in long-haul heavy-duty trucks and buses, basically the entire US military fleet (safer fuel and less vulnerable), and merchant marine (lower insurance premium). The engines being used in mining galleries are all CI systems.

A great portion of passenger cars in countries which are trading with the US (in particular Europe and Japan) are powered by CI engines. Since the CI engine is more efficient, it emits less greenhouse gas (CO_2) than a comparable SI engine, a contribution towards the world-wide efforts of minimizing global warming.

The CI engine will be more widely used if it achieves a higher power-density (HPD, horsepower per displacement or weight), cleaner emissions, and quieter operation, goals which have become more sought after and attainable in recent years. For example, consider the two former goals: Better air utilization for a HPD will increase the exhaust gas temperature, which facilitates development of an efficient catalytic converter. Also high air utilization, which has been limited by the smoke emission, has become more feasible through the use of modern electronically-controlled high injection pressure fuel systems (HIP). In addition, the HIP offers a potential for increasing the engine speed, another approach to an HPD.

In developing an HPD CI engine mated with an HIP, however, many design problems will have to be overcome, including a greatly increased engine block temperature (therefore temperatures of intake air, fuel and lubricating oil). The increase will undoubtedly affect processes of CI combustion, notably the preflame reactions and onset of self-ignition, as well as the subsequent heat release and pollutant formation. The impacts on the processes would be more unpredictable when operated at high speeds.

When the methodology of the uncooled CI engine is incorporated in a HPD, which eliminates parasitic components (e.g. the water pump and radiator) as well as the water jacket, the engine power density will further increase. However, the many problems including those mentioned above will undoubtedly become more difficult to solve. In spite of such difficulties, development of an uncooled HPD CI with an HIP operated at high speeds is a great challenge worthy to strive for because it offers a new dimension of opportunity for engine technology advancements and usefulness.

Realizing the need for analysis of the engine response to an HIP, which is expected to alter various in-cylinder reactions as mentioned above, a new study was initiated towards a goal of HPD by the uncooled direct injection (DI) CI engine methodology. Since no such HPD engine is widely used at present, a more reasonable approach was to employ an experimental apparatus representing a real-world DI-CI mated with an HIP operated under varied thermal conditions. This was because the existing DI-CI reciprocating engine is considered to be the system basis employed for the goal of the new HPD engine. Results from the study, thus, were expected to help construct a more useful road-map to the development of an HPD CI engine. The study was also directed to assessing the new engine concept and whether it would satisfy regulatory as well as user requirements.

EXPERIMENTAL

When a DI-CI engine with an HIP is operated at high speeds in order to achieve a HPD, the heat release per displacement will become closer to that in a typical SI engine. This will greatly increase the overall engine temperature, which will affect the in-cylinder reactions to become presumably very different from those in the conventional DI-CI engine. In order to closely investigate the processes, the engine apparatus was constructed to offer engine combustion environments representing as closely as possible those in an HPD DI-CI engine, which is discussed next.

Engine. A Cummins 903 engine (V-8) was utilized to make a unit of V-2 apparatus, a saw-off of a quarter of the original engine, which then was modified to operate only one cylinder and to have the remaining cylinder-piston reciprocate without compression in order to help achieve dynamic balancing. The engine has a bore-stroke of 140-121 mm (displacement of 1.85 liters) and compression ratio of 13.5 to 1. Since the same family of 903 engine has been widely used in the past, no additional discussion on the engine dimensions is made here.

This single-cylinder engine was installed with a new intake-air (electric) heating unit which can increase the air temperature as high as 205°C (400°F) at high speeds, because such a high intake air temperature was expected in an uncooled engine whose combustion reactions were to be also studied. The air was supplied from the building via a pressure controller (maintained at 30.9 KPa or 4.5 psi and higher depending upon the intake air temperature as explained later) and a flow metering unit. The engine cooling was done by using a closed-flow unit (with glycol as coolant) connected to a water-cooled heat exchanger for temperature control. The unit was designed to accommodate a coolant temperature as high as 149°C or 300°F.

The apparatus lined up with an electric dynamometer was sufficiently instrumented in order to implement the objective of the study, including an in-cylinder pressure transducer, temperature probes, and a smoke meter.

High Injection Pressure Fuel System (HIP). Since high utilization of the intake air is an important precondition for achieving an HPD DI-CI engine, which is facilitated by an HIP, a considerable amount of design and development work on a new HIP was a logical step taken in the present study. Note that for earlier studies, a laboratory-built HIP which delivered an injection pressure of up to 165 MPa (24,000psi) was employed [1-3]*, which offered the basic expertise toward the new design-construction of an improved HIP, which is explained in the following.

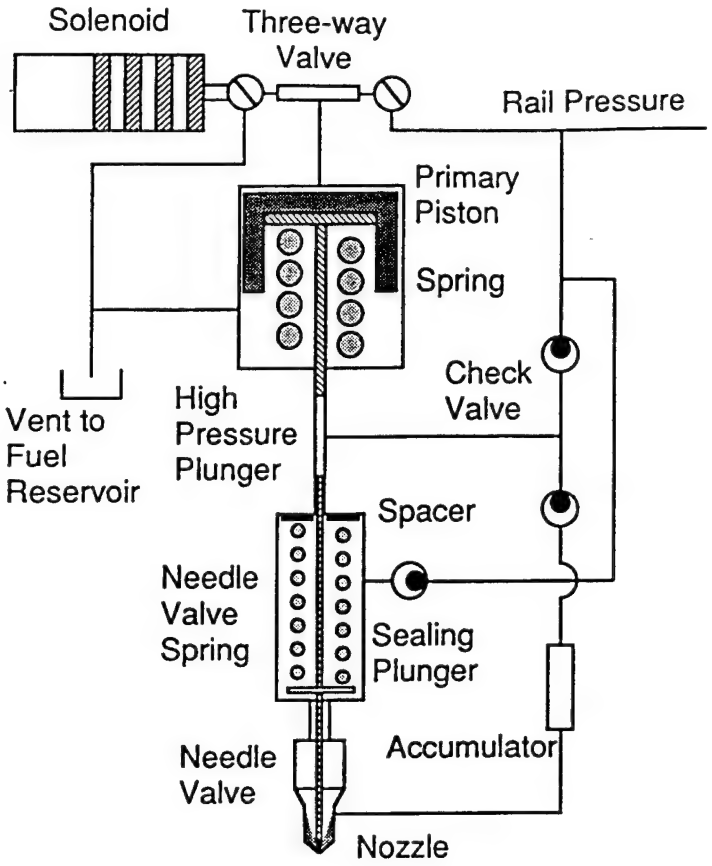

Fig. 1. Laboratory-built Electronically Controlled High Injection Pressure (HIP) Fuel Unit.

In developing and characterizing an HIP unit, one of the more uncertain issues associated with the system performance is the actual injection pressure that a unit can deliver. For example, in a common-rail type HIP, the pressure at the accumulator does not represent the injection pressure at the nozzle tip due to pressure drop expected to occur between the two locations. The pressure intensifier type HIP to be discussed next, however, is considered to be more apprehensive on the issue, that is it generates the injection pressure closer to the nominal value.

A schematic drawing of our new HIP is shown in Fig. 1, and was basically the same design as BKM's Servo-jet type [4]. It is a "pressure intensifier type" having a primary piston where a variable low pressure fuel (as high as 12 MPa or 1,750 psi in this) is connected via a three-way

*Numbers in parentheses designate references at end of paper.

valve at a position as shown in the drawing. The fuel trapped in the lower side of the primary piston and accumulator is compressed by the factor of the area ratio (17.5 for the present design) between the piston and plunger. Since the needle valve is under the same high pressure, no fuel escapes through the nozzle at this time. When the injection is to be made, the three-way valve is switched to a valve position 90 degrees clock-wise from that shown in the figure. This will abruptly relieve the pressure on the upper portion of the primary piston by draining the fluid to the vent reservoir. The subsequent pressure imbalance across the sealing plunger, then, lifts the needle to spill the fuel at a high pressure into the combustion chamber.

The present unit was designed/fabricated in such a way as to directly engage it with the low-pressure fuel supply port in the Cummins 908 engine cylinder head, which was not possible in the factory-delivered Servo-jet unit. That is, the original stock PT-type injector in the engine was simply replaced by the newly designed unit with no additional modification of the head. This resulted in a unit with the same external dimensions as the PT injector. This consideration suggested a direct use of, in the new unit, both a nozzle tip holder and the nozzle tip as well as the o-ring from the PT injector.

By taking the high pressure fuel injection into consideration, which will produce high injection rates, a stock nozzle tip having the smallest nozzle hole diameter (0.15mm) available to us was incorporated in the new unit. (This measure was also meaningful for flexibility and economic reasons.) In designing the new unit, however, a computational analysis indicated that the nozzle tip holder in the existing PT-nozzle was not made sufficiently strong to withstand the high-pressure generated by the present intensifier. Consequently, all of the components in the unit were newly fabricated in our laboratory except for the three-way solenoid valve and the abovementioned nozzle-tip.

Regarding the pressure at the nozzle tip before the injection, recall the dead-weight type calibration-device for testing pressure gages, which utilizes a similar concept as the present unit does. Except for the dynamic and transient nature of the performance in the present unit, the injection pressure at the opening of the nozzle, thus, is considered to closely represent the nominal pressure determined by the (low) rail pressure and the area ratio mentioned above. Although the physical concept of the dead-weight device employed in the unit is perceptive, it would be desirable if the pressure-time history at the tip would have been determined for backing up this expectation, however.

The control of the injection pressure, therefore, was made by adjusting the fuel rail pressure from a gear-pump. On the other hand, the amount of fuel injected by the new unit was controlled by the thickness of a spacer placed at the upper end of the needle valve spring. The purpose of using the spacer was to vary the cut-off pressure of fuel injection. That is, the thicker the spacer, the stronger the preload of the spring and the earlier closing of the needle valve. Note that the cut-off pressure without any spacer was adjusted at approximately 61 MPa (10,000 psi). For varied amounts of fuel injection, the unit opens the needle valve at the same time, but closes it sooner for a smaller amount of fuel injected but at a higher cut-off pressure.

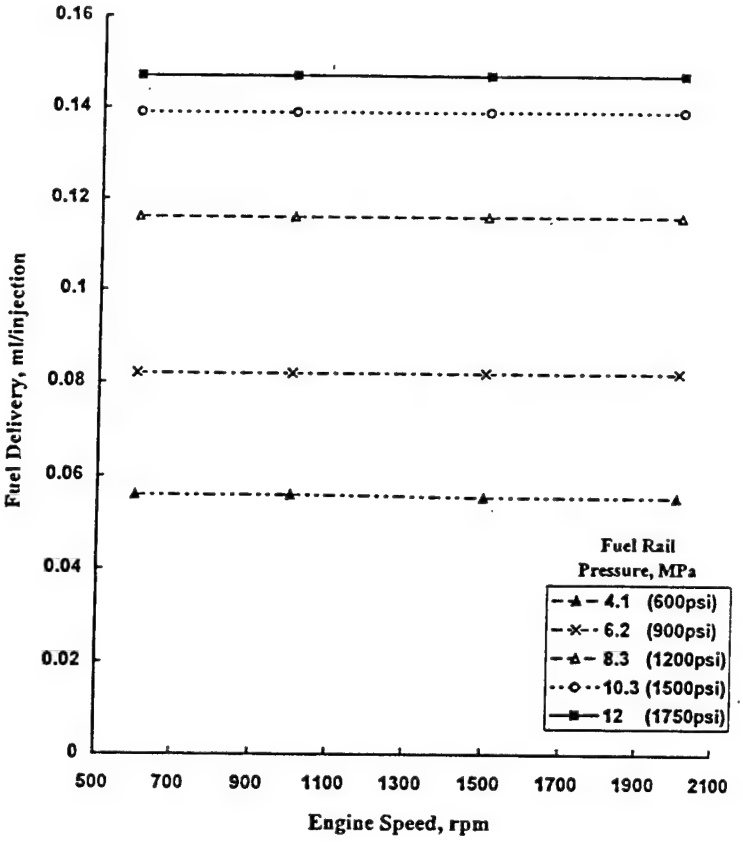

Fig. 2. Relationship of Fuel Delivery to Engine Speed and Fuel Rail Pressure (Spacer thickness, 0.76 mm).

Characterization of HIP. After completing construction of the new unit, an extensive system characterization was performed using a bench-top test device. The injection time was determined by placing a pressure transducer at a location approximately 10 mm away from the nozzle hole while the period of energizing the three-way valve was varied. This determines the period of connection between the rail pressure and the primary piston. The timing of the pressure transducer signal was compared with the end of the energizer period when the needle was expected to rapidly lift up.

Figure 2 shows the relationship of the amount of fuel delivery to the engine speed for varied rail pressure. The result exhibits a predictable performance of the new unit, a trend which was the same for all spacer thicknesses employed in the experiment. Note that the rail pressure represents the injection pressure determined by the intensifier (area) ratio, that is 17.5. For example, the rail pressure of 12 MPa corresponds to an injection pressure of 210 MPa (30,625 psi) at the nozzle opening.

Results obtained using all of the spacers were combined to plot Fig. 3, which facilitated determination of the amount of fuel delivery. As expected for a given spacer thickness, the higher the rail pressure the greater the amount of fuel delivered. The results shown in the figure for variation of spacer thickness and rail pressure were employed for the range of the present parametric study of the

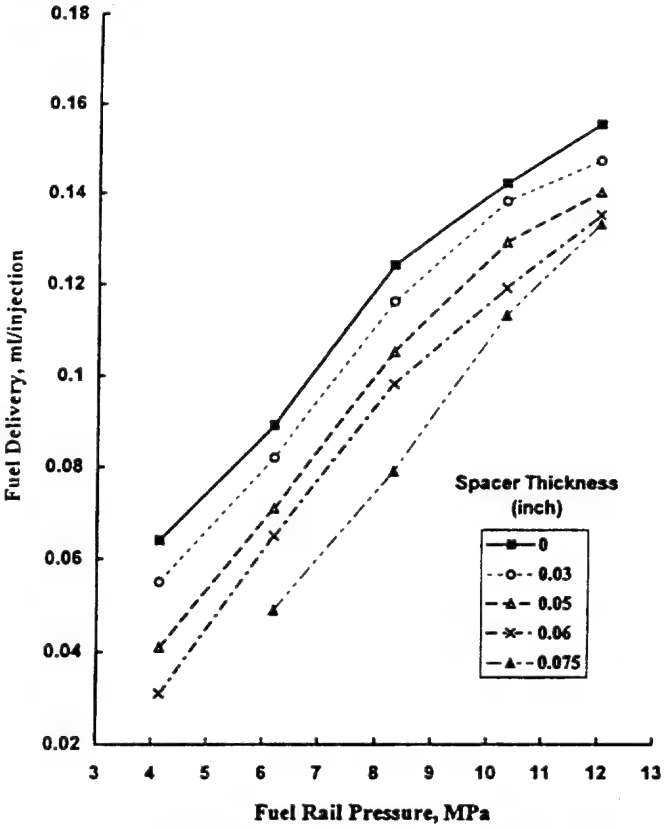

Fig. 3. Fuel Delivery Affected by Rail Pressure and Spacer Thickness.

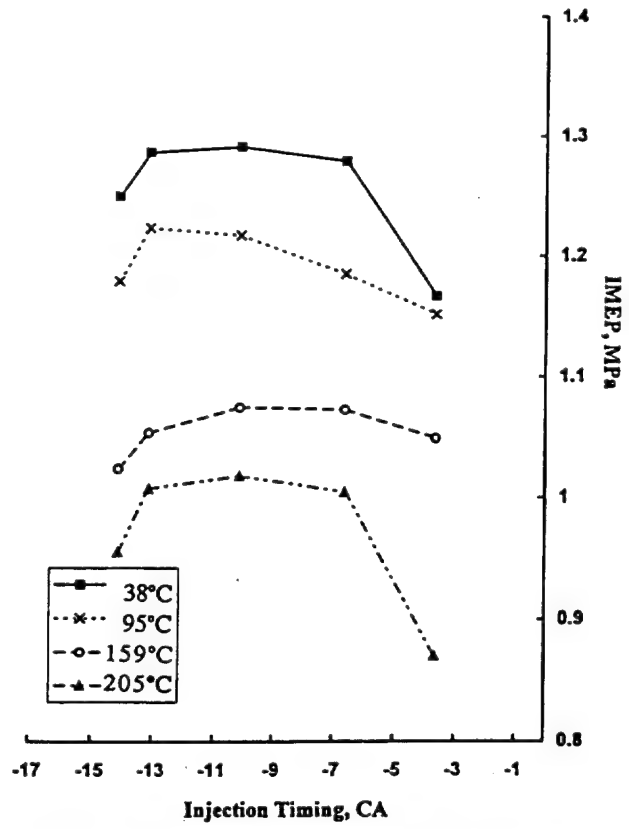

Fig. 4. IMEP for Varied Injection Timing and Intake Air Temperature (1000rpm, Rail Pressure 12Mpa).

HPD CI-DI engine with HPI. For example, the mass of air flow into the engine was compared with the fuel delivery from this plot in order to determine the overall air-fuel ratio for each engine running condition.

RESULTS AND DISCUSSION

The experiment was conducted in two steps. At first, the engine equipped with the new HIP was operated by varying injection time for different intake air temperatures as listed in Fig. 4. This was done at 1,000 rpm speed and 210 MPa injection pressure (by having rail pressure of 12 MPa). Measurements shown in Fig. 4 suggested that the start of injection at 10 degrees of crank angle (CA) before the top-dead-center (bTDC) was proper for the experiment. Therefore, the first part of the experiment was performed at this fixed injection time.

The analysis of the large amount of engine measurements accumulated in the above experiment, however, indicated that the fixed injection timing for a wide range of engine variation was improper as explained later. Consequently, the same engine experiment was performed at varied injection times producing the best-torque under the respective operating conditions, the second step of the experiment which was not planned in the beginning.

Explaining the results, the indicated mean effective pressure (IMEP) determined from the pressure-time data are shown in Fig. 5 for varied engine conditions as noted by individual symbols. The family of curves obtained for fuel injection pressures in MPa of 210 (30,625 psi), 180 (26,250 psi), and 144 (21,000 psi) is included, respectively. The overall results exhibit a trend as expected, which is the lower the air/fuel ratio, the higher the IMEP. The engine speed did not appear to significantly affect the results for the range of investigation in the study, which is further discussed below. Most notably, it was possible to run the engine as rich as 18 to 1 air/fuel ratio while the smoke emission was no worse than that observed with the conventional PT injector operated at leaner overall ratios of 35 to 1.

The increase of IMEP achieved in the present CI-HIP engine by better utilization of the trapped air, which increased by a factor of almost two compared with the conventional engine, is highly promising in paving the way to designing an HPD engine. It is pointed out that the generation of high injection pressures requires an increased consumption of the power from the host engine, which will deteriorate the specific fuel consumption, as further discussed later. Nevertheless, the present results by the use of an HIP seemed to shed some strong light into a possibility of operating a CI engine at richer air/fuel ratios, which are more closer to the stoichiometric.

Although no attempt was made to measure engine noise in the study, it is pointed out that noise became higher when the engine was operated overall rich, i.e., as it came closer to the stoichiometric. Expecting that the elimination

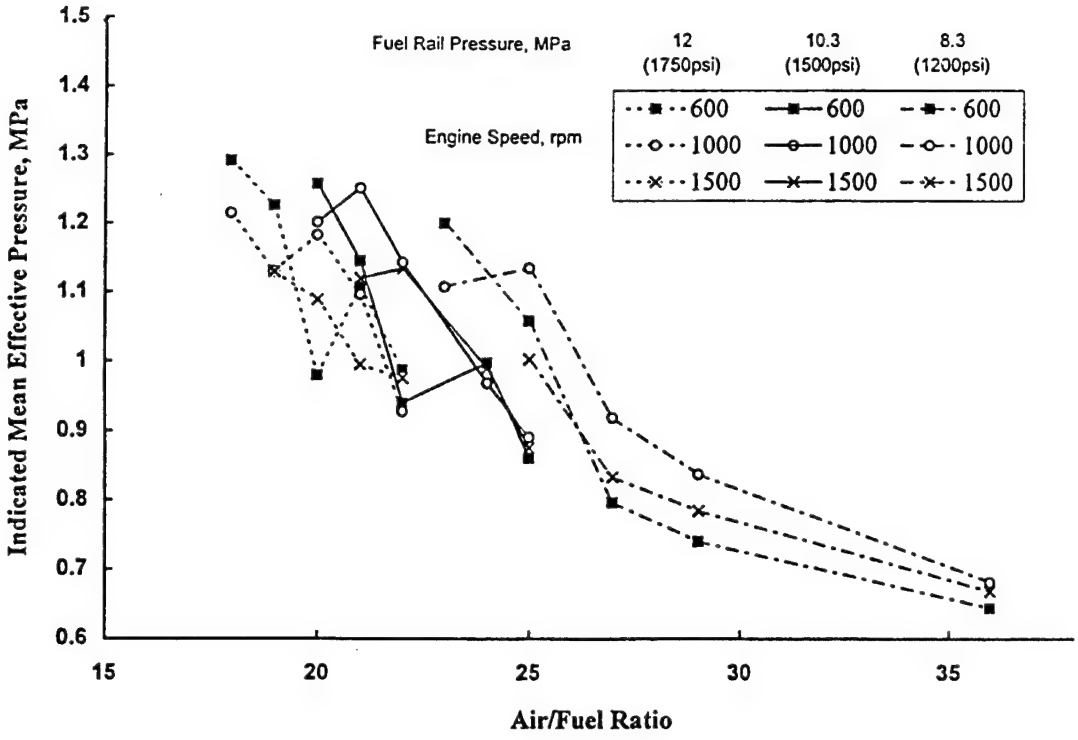

Fig. 5. Indicated Mean Effective Pressure (IMEP) as a Function of Air/fuel Ratio (all engine speeds at Intake Air Temperature 38°C and Injection Timing of 10 BTDC.

of exhaust NOx emission by a catalytic converter would be facilitated when the exhaust gas temperature greatly increases via a high air utilization, no attempt was made to measure its emissions. To support this consideration, it is noted that the exhaust temperature ranged between 360-416° C (680-780° F) when the engine ran at air/fuel ratios of 30-20 to 1.

Recalling Fig. 3, since for a given thickness of the spacer, the higher the rail pressure (thus the injection pressure) the greater the amount of fuel flow through the nozzle, the IMEP increased with the rail pressure (Fig. 6). This trend was similarly found for other intake air temperatures. As briefly mentioned above, the speed effect on the measurement was small except that it appeared to peak at 1000 rpm, the same speed employed for determining the (optimum) injection time (Fig. 4). An additional discussion is made later on the need for varied injection time as related to this observation.

Intake Air Temperature. The measurements explained above were obtained for intake air temperatures (°C) at 38, 95, 150, and 205, respectively. Figures 7-10 were plotted for comparison purpose of intake temperature effects on IMEP for varied overall air/fuel ratios and injection pressures. Although the observation of a higher IMEP by a richer air/fuel ratio was expected, its great deterioration at higher intake air temperature was a surprise. Since the fuel system was adjusted to deliver a fixed amount of fuel according to the bench-top calibration (Fig. 3), the intake pressure was increased to compensate the deterioration of volumetric efficiency with increase of the air temperature. It is reminded that the measurements were obtained for high

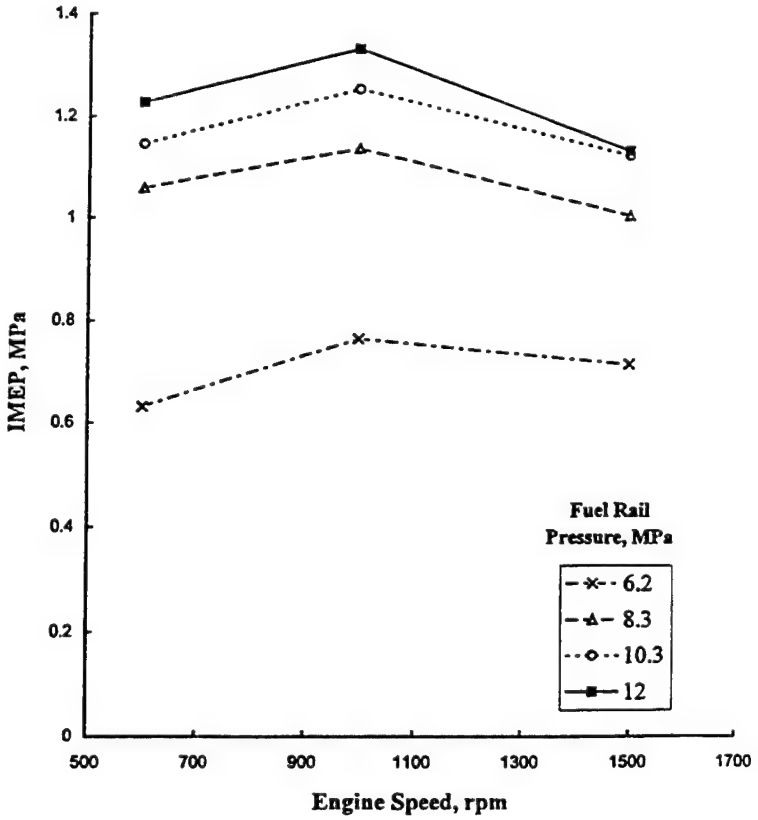

Fig. 6. IMEP as a Function of Injection Pressure (Spacer, 0.76mm). Intake Air Temperature, 38°C.

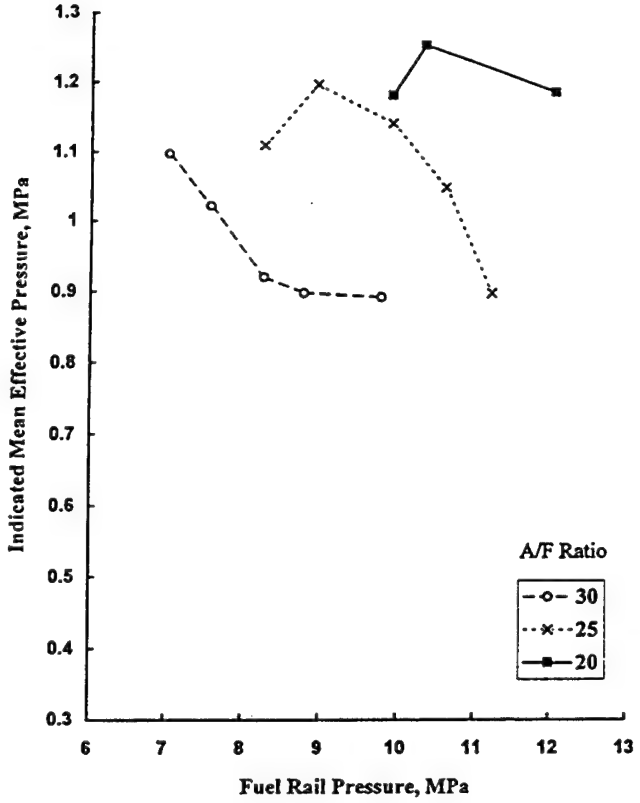

Fig. 7

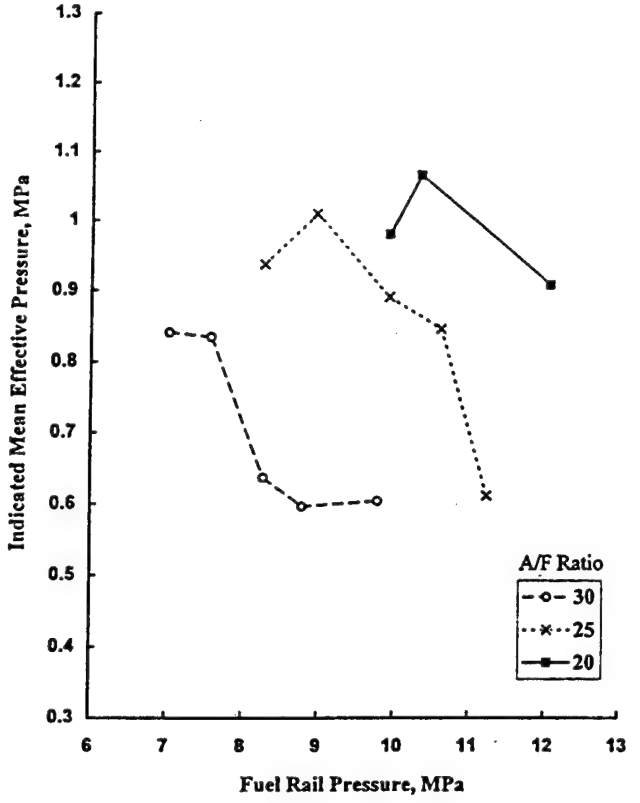

Fig. 9

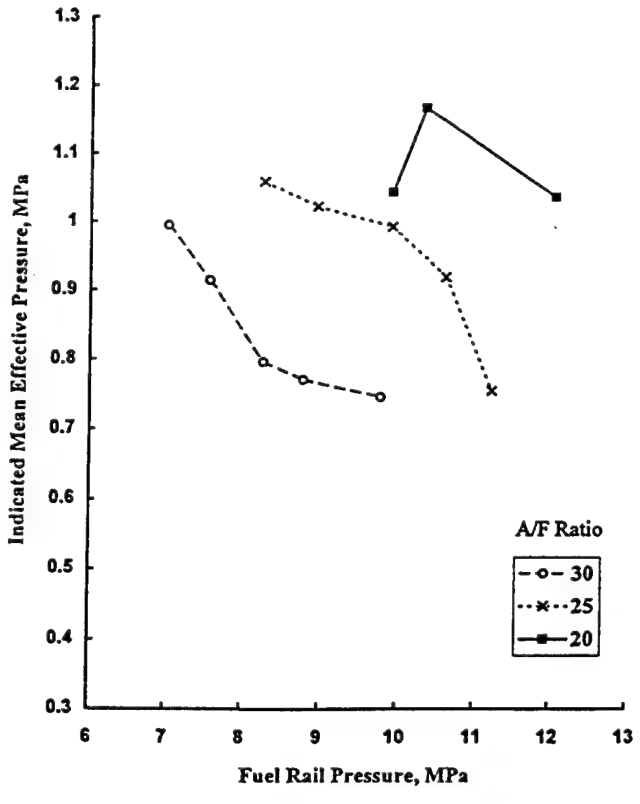

Fig. 8

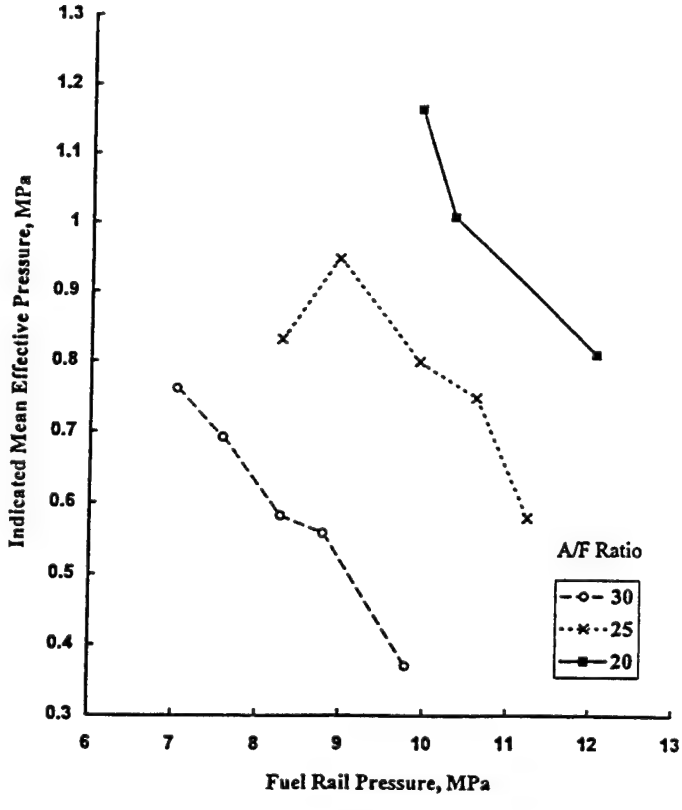

Fig. 10

Figs. 7-10. Indicated Mean Effective Pressure (IMEP) as a Function of Air/fuel Ratio and Rail Pressure for Varied Intake Air Temperatures (T_a): Fig. 7, T_a =38°C; Fig. 8, T_a =95°C; Fig. 9, T_a =150°C; Fig. 10, T_a =205°C.

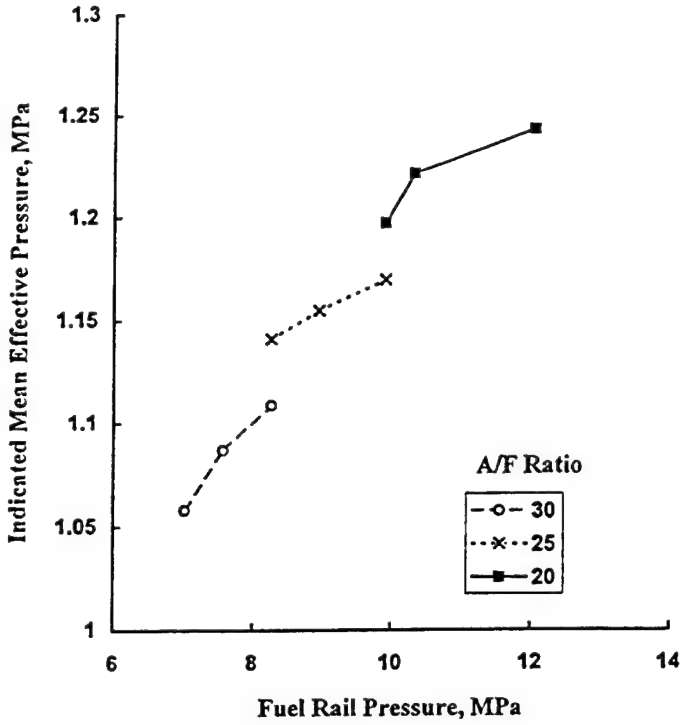

Fig. 11. Indicated Mean Effective Pressure as a Function of Fuel Rail Pressure (1000rpm, 38°C Intake Air Temperature) for Variable Injection Timing.

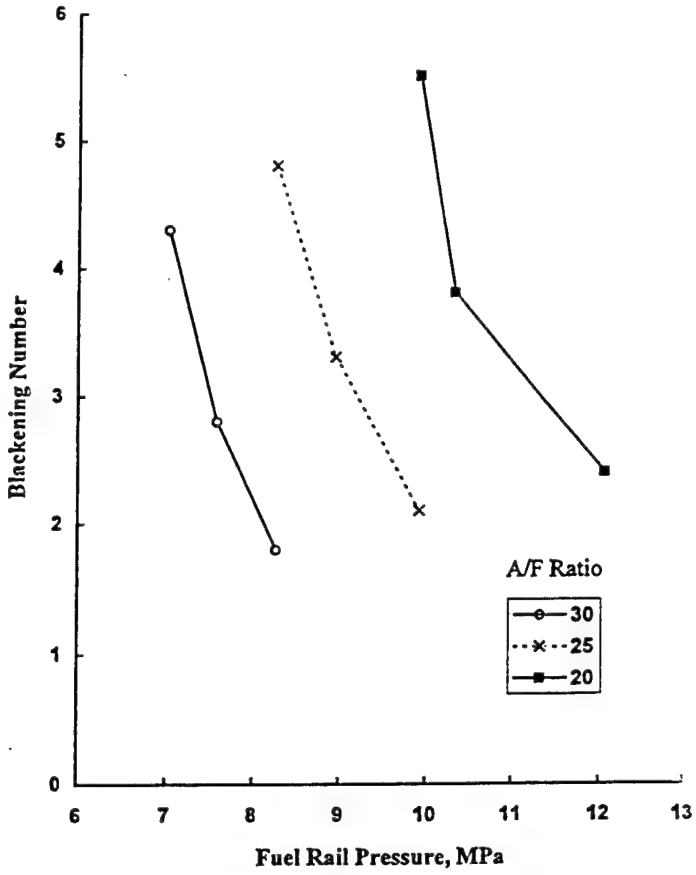

Fig. 12. Smoke Emission, Bosch Blakening Number as Function of Fuel Rail Pressure and Air/fuel Ratio.

temperatures of the intake air in order to assess the engine response when the uncooled (low heat-rejection) design is incorporated, which would have a high engine-block temperature resulting in the intake air heating.

Several reasons for the significantly decreased IMEP with increased intake air temperature may be considered. First of all, since the ignition delay (ID) would decrease with the temperature, a fixed injection time (and even the rate shape) should have been shifted for an optimum power torque output. Next, a decreased ID will result in a smaller amount of heat release from the premixed combustion stage (and thus an increased amount of heat release via the diffusion-controlled combustion) to cause a deteriorated cycle efficiency. Note that when these happen, the formation of soot, in general, is expected to increase, which in fact was the exact observation in the experiment. While such a deterioration of combustion and energy conversion efficiency is considered, recall Fig. 3 showing the calibration results determining fuel flow rate obtained at room temperature using a bench-top apparatus. Those measurements, however, may not be repeated when the intake temperature was increased, because of a probable decrease in the flow rate with increase of the temperature. If this is the case, a decreased IMEP is expected to occur, which needs further investigation.

Also, what was most unexpected was the somewhat decreasing trend of IMEP with increase of the rail pressure (thus the injection pressure), which was contrary to an expectation that combustion would improve when a "better" fuel spray is achieved by an HIP. The decreasing trend was found in *all* temperatures of intake air and air/fuel ratios. Reviewing the measurements, it came to examine the effect of the injection time, which was tested in the beginning and set at 10 bTDC for the experiment (Fig. 4). This was because when the injection pressure was varied, the change in ignition delay was considered to be altered enough to affect the energy conversion efficiency. Note that the need for shifting the injection time is unusual in the conventional CI-DI engines equipped with a mechanical injection unit, which mostly maintain the injection time at a fixed CA.

Figure 11 shows the results obtained in a similar measurement performed as above by varying the injection time that produces the best torque for each engine condition especially at respective injection pressures. The overall trend was quite the same at other intake air temperatures, which indicates an obvious need for adjusting the engine fuel system to deliver a new injection time in order to obtain the best IMEP. This observation led us to recall the adjustment of ignition time in the SI engine under different engine conditions.

Since an HPD from a CI engine is meaningful if the exhaust smoke emission is acceptably low, its measurement was conducted (using a Bosch smoke meter) and the results are plotted in Fig. 12. As expected the higher the injection

pressure, the lower the smoke emission. When the injection pressure was at 210 MPa, the measurement with air/fuel ratio of 20 was almost as low as that obtained for air/fuel ratio of 30 (injection pressure of 145 MPa, or 21,000 psi). The result suggests that an additional reduction is possible if the injection pressure is further increased in all air/fuel ratios investigated. It is reminded that these measurements were much lower than those observed in the same engine with the (low-pressure) conventional PT injector.

A HIGH-POWER-DENSITY CI ENGINE

The present study was directed towards investigation of some engine design strategies to achieve an HPD DI-CI engine, in particular when the engine is equipped with ceramic components for uncooled operations. Several issues may be discussed in consideration of achieving the goal.

An increased air utilization appears to be highly promising by the use of an HIP as demonstrated in the present study. It was possible to operate an engine having an injection pressure of 210 MPa by using an HIP at air-fuel ratio as high as 18-1 to produce smoke emissions comparable or lower than those from a DI-CI engine equipped with a conventional low pressure injection unit. The high air utilization, however, resulted in several consequences, including high engine block and exhaust temperatures, and increased noise. Note that the temperatures will become higher when an uncooled engine design approach is employed, whose impacts on the goal of developing an HIP are in need of discussion.

Most of all, the volumetric efficiency will greatly deteriorate, in an uncooled high air-utilization engine, to cause a low mean effective pressure as studied in the present work. The use of a high performance turbocharger or supercharge, therefore, may become a precondition for an HPD uncooled engine, which also may have to use inter-cooling. In addition, the high engine temperature will undoubtedly increase the injector as well as the fuel temperature. The results obtained in the present study suggest it is probable that the fuel flow rate out of the injector may be affected with the injector temperature. When there is no positive remedy for this, the fuel would attain super critical temperatures. This then will modify the spray formation, affect the lubrication of the injector itself and even damage the nozzle holes by cavitation in the fuel stream.

The high exhaust gas temperature, on the other hand, may be a useful ingredient for achieving an HDP engine by facilitating the incorporation of a turbocharger in the engine. Also, the high exhaust temperature may offer an opportunity for using an exhaust catalytic converter to produce a cleaner emission, which then may make it possible to further increase the air utilization.

The development strategies of an uncooled HDP DI-CI engine using ceramic components is certainly a great challenge involving various technical problems as briefly discussed above. There is no question that they would not be easy to surmount, but they offer an exciting opportunity for advancing the engine technology.

ACKNOWLEDGMENT

The present work has been performed under the sponsorship of the U.S. Army Research Office

REFERENCES

1. Clasen, E., Campbell, S., and Rhee, K.T., "Spectral IR Images of Direct Injection Diesel Engine Combustion with High Pressure Fuel Injection," SAE Paper-950605, 1995.

2. Clasen, E., Song, K., Campbell, S., and Rhee, K.T., "Fuel Effects on Diesel Combustion Processes," SAE Paper-962066, 1996.

3. Chang, C., Clasen, E., Song, K., Campbell, S., Jiang, H., Rhee, K.T., "Quantitative Imaging of In-cylinder Processes by Multispectral Methods," SAE Paper-970872, 1997.

4. Abata, D., Stroia, B.J., Beck, N.J., and Roach, A.R., "Diesel Engine Flame Photographs with High Pressure Injection," SAE Paper-880298, 1988.

Appendix-II. Original Scope of Work

The work scope setting forth of the present study is included for reference. The scope was somewhat altered during the course of the study due to several reasons, including: (1) some of the evaluation ranges were found to be excessively wide: (2) the engine apparatus proposed to employ for the work did not deliver the upper limits of some evaluation parameters; and (3) some of work tasks were found to be highly labor-intensive and time-consuming. Consequently, it was decided to achieve an optimum amount of results under the given research condition.

1. Moderate Pressure Injection (25,000psi) vs.High Pressure Injection (30,000psi).

   Evaluation Parameters:

   . Air/Fuel Ratio (30 - 20)
   . Intake Air (200 - 400 deg F)
   . Speed (1200 - 2,800 rpm)
   . Oil Temperature (250 deg F)
   . Coolant Temperature (230 deg F)
      - o. Pressure-time
      - o. BSFC
      - o. Exhaust Temperature, Smoke, etc.

2. The Same is Repeated as #1 with

   . Oil Temperature (300 deg F)
   . Coolant Temperature (300 deg F)

3. In-cylinder Investigation using Rutgers Super Imaging System,
   Evaluation Phenomena:
      - o. Preflame Reactions
      - o. Very First Flame Kernel
      - o. Distribution of Temperature and Soot
      - o. Post Flame Oxidation, and Others

4. Advanced HPI Engine Studies.

Appendix-III. Engine Response to LHR HIP DI-CI Engine Methods (Total 34 Graphs)

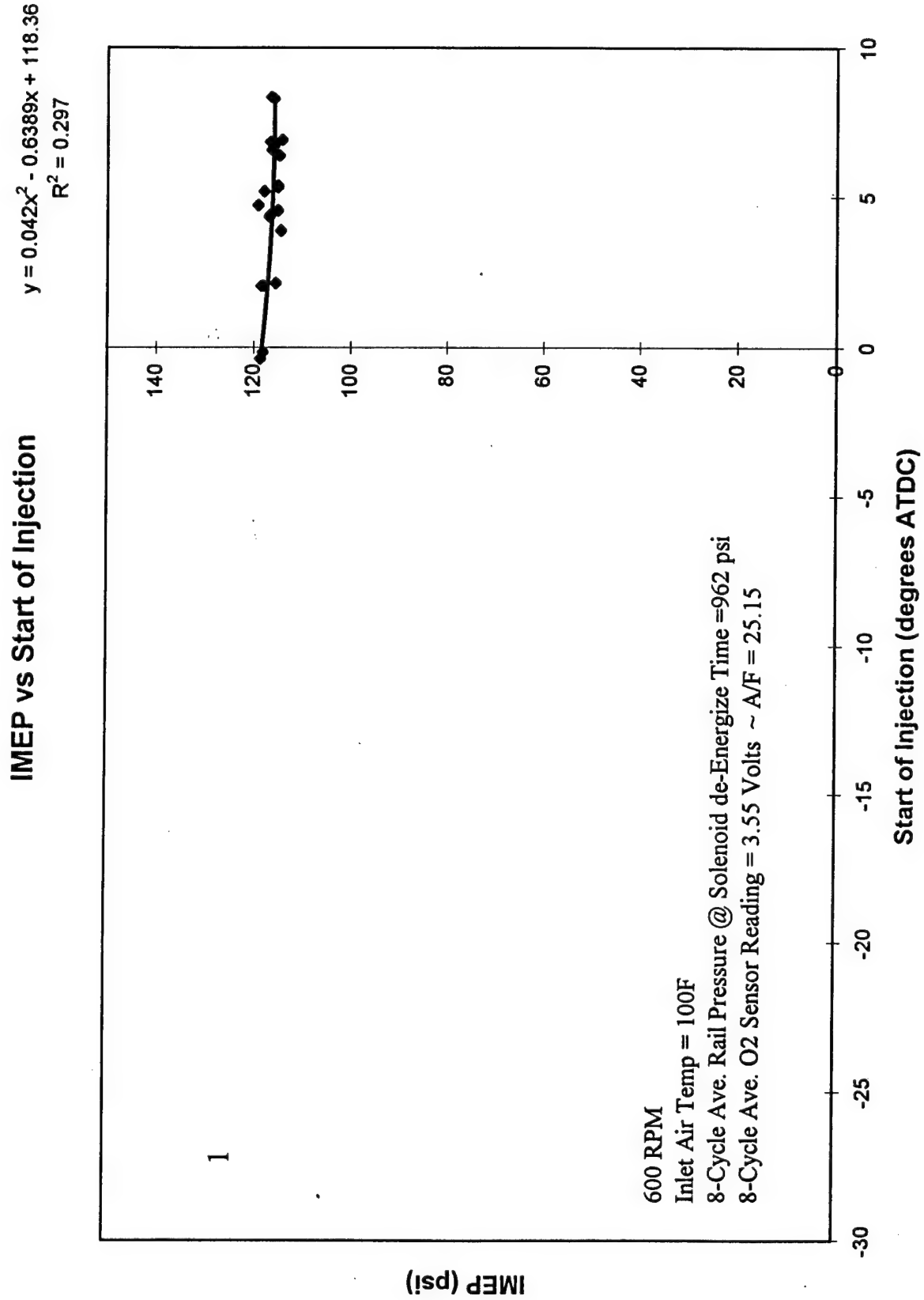

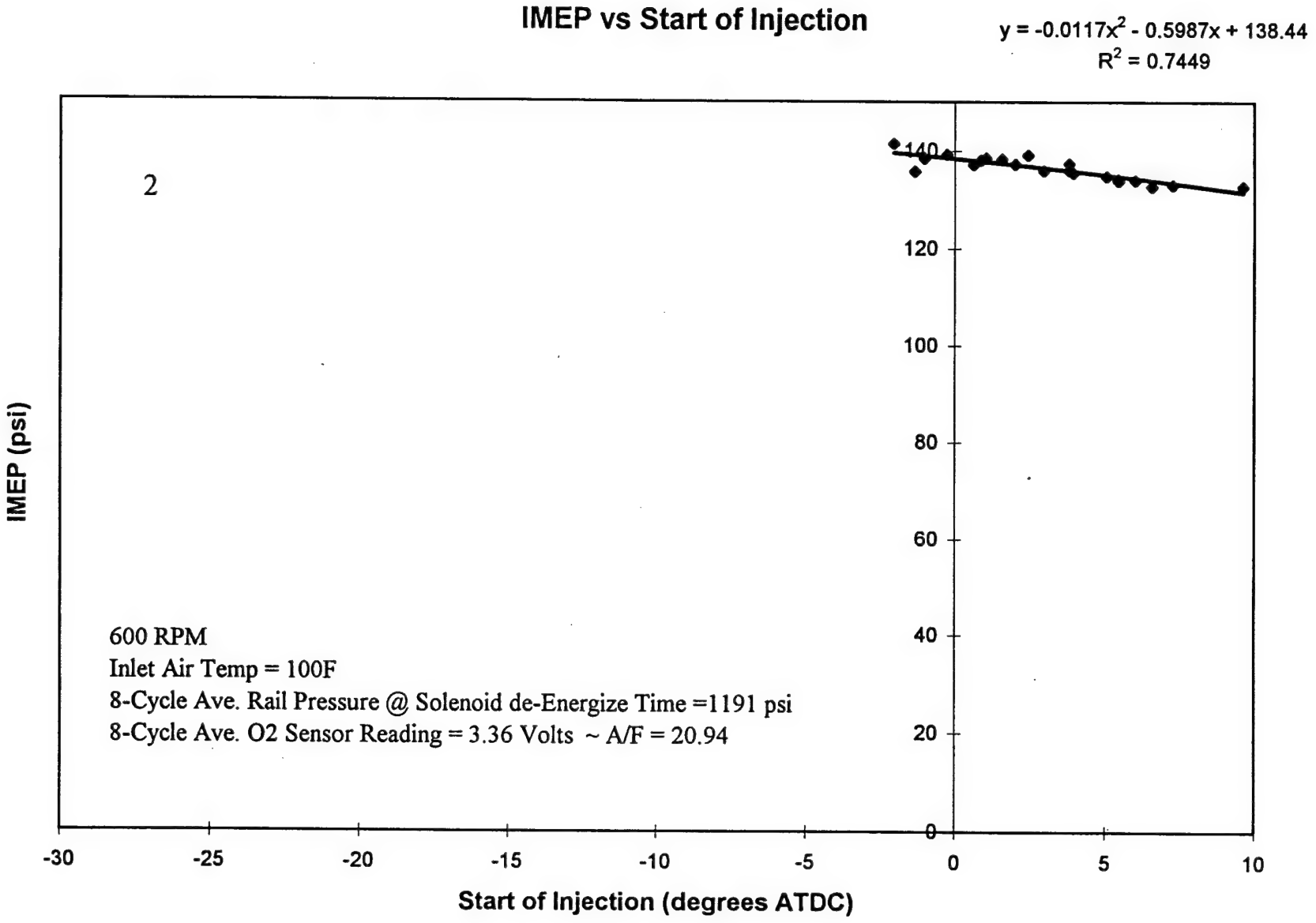
IMEP vs Start of Injection
y = -0.0117x² - 0.5987x + 138.44
R² = 0.7449
2
IMEP (psi)
140
120
100
80
60
40
20
0
-30
-25
-20
-15
-10
-5
0
5
10
Start of Injection (degrees ATDC)
600 RPM
Inlet Air Temp = 100F
8-Cycle Ave. Rail Pressure @ Solenoid de-Energize Time =1191 psi
8-Cycle Ave. O2 Sensor Reading = 3.36 Volts ~ A/F = 20.94

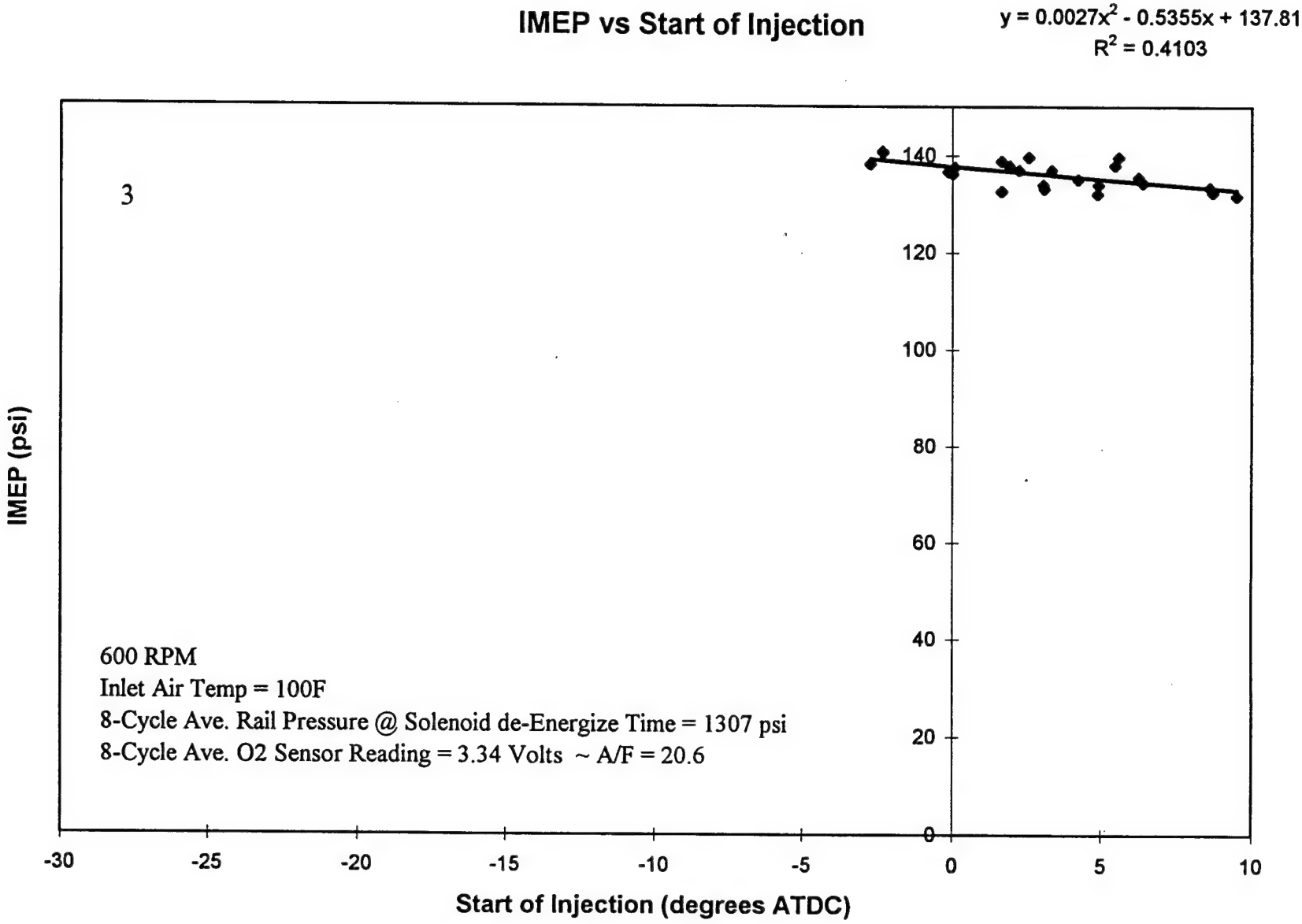
IMEP vs Start of Injection
y = 0.0027x² - 0.5355x + 137.81
R² = 0.4103
3
600 RPM
Inlet Air Temp = 100F
8-Cycle Ave. Rail Pressure @ Solenoid de-Energize Time = 1307 psi
8-Cycle Ave. O2 Sensor Reading = 3.34 Volts ~ A/F = 20.6
IMEP (psi)
140
120
100
80
60
40
20
0
-30
-25
-20
-15
-10
-5
0
5
10
Start of Injection (degrees ATDC)

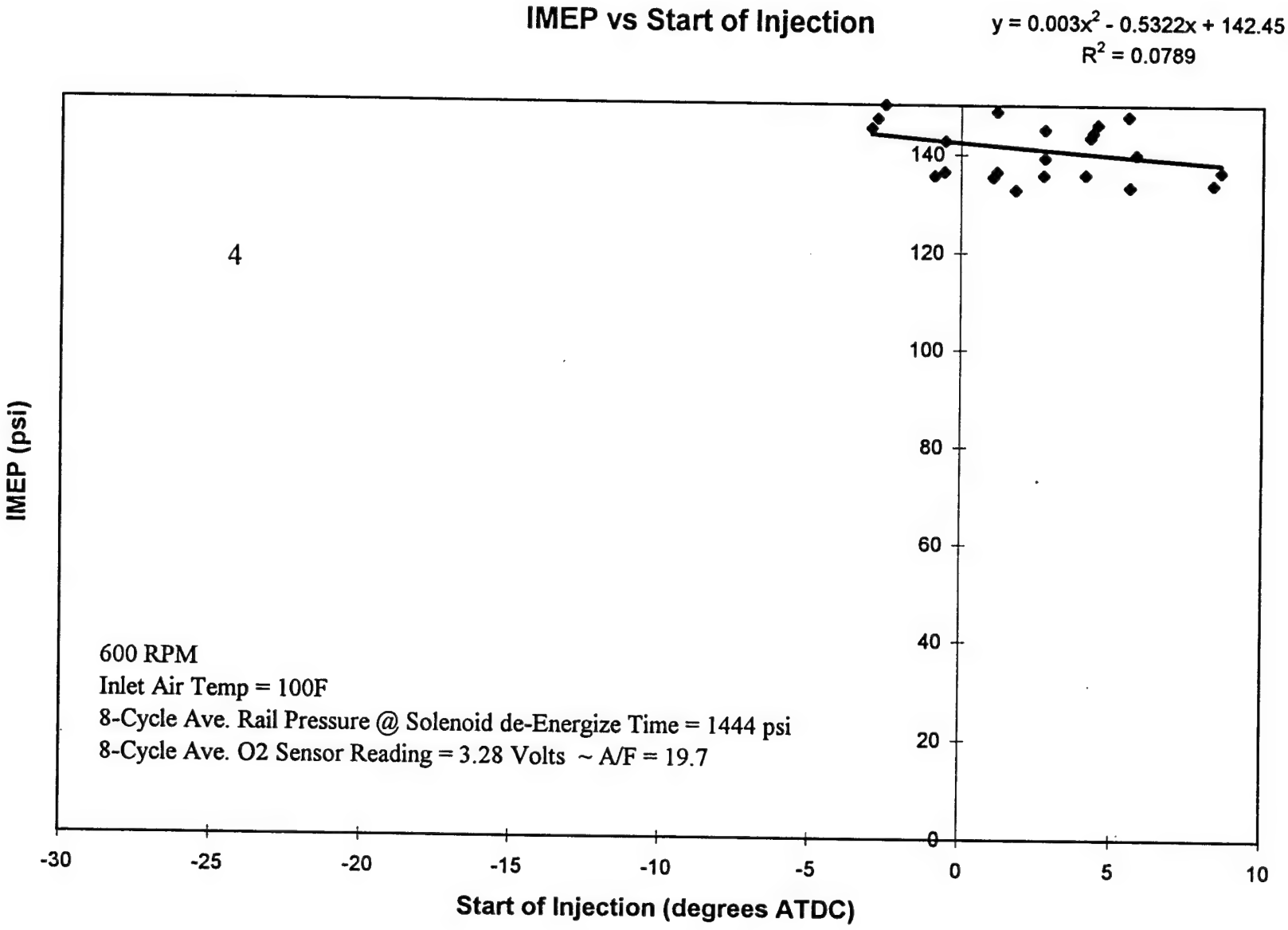
IMEP vs Start of Injection
y = 0.003x² - 0.5322x + 142.45
R² = 0.0789
4
600 RPM
Inlet Air Temp = 100F
8-Cycle Ave. Rail Pressure @ Solenoid de-Energize Time = 1444 psi
8-Cycle Ave. O2 Sensor Reading = 3.28 Volts ~ A/F = 19.7
IMEP (psi)
0
20
40
60
80
100
120
140
-30
-25
-20
-15
-10
-5
0
5
10
Start of Injection (degrees ATDC)

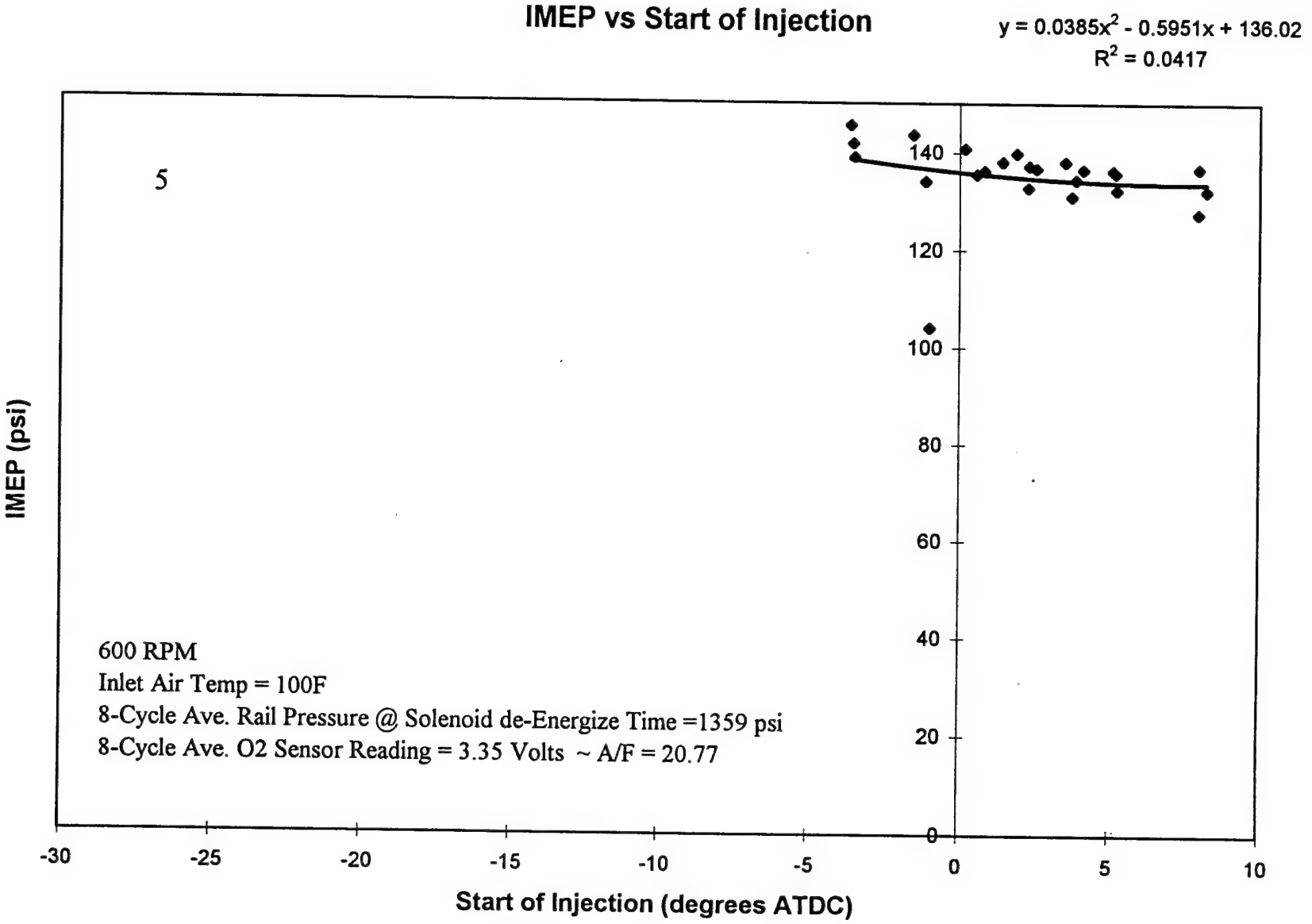
IMEP vs Start of Injection
y = 0.0385x² - 0.5951x + 136.02
R² = 0.0417
5
600 RPM
Inlet Air Temp = 100F
8-Cycle Ave. Rail Pressure @ Solenoid de-Energize Time =1359 psi
8-Cycle Ave. O2 Sensor Reading = 3.35 Volts ~ A/F = 20.77
IMEP (psi)
140
120
100
80
60
40
20
0
-30
-25
-20
-15
-10
-5
0
5
10
Start of Injection (degrees ATDC)

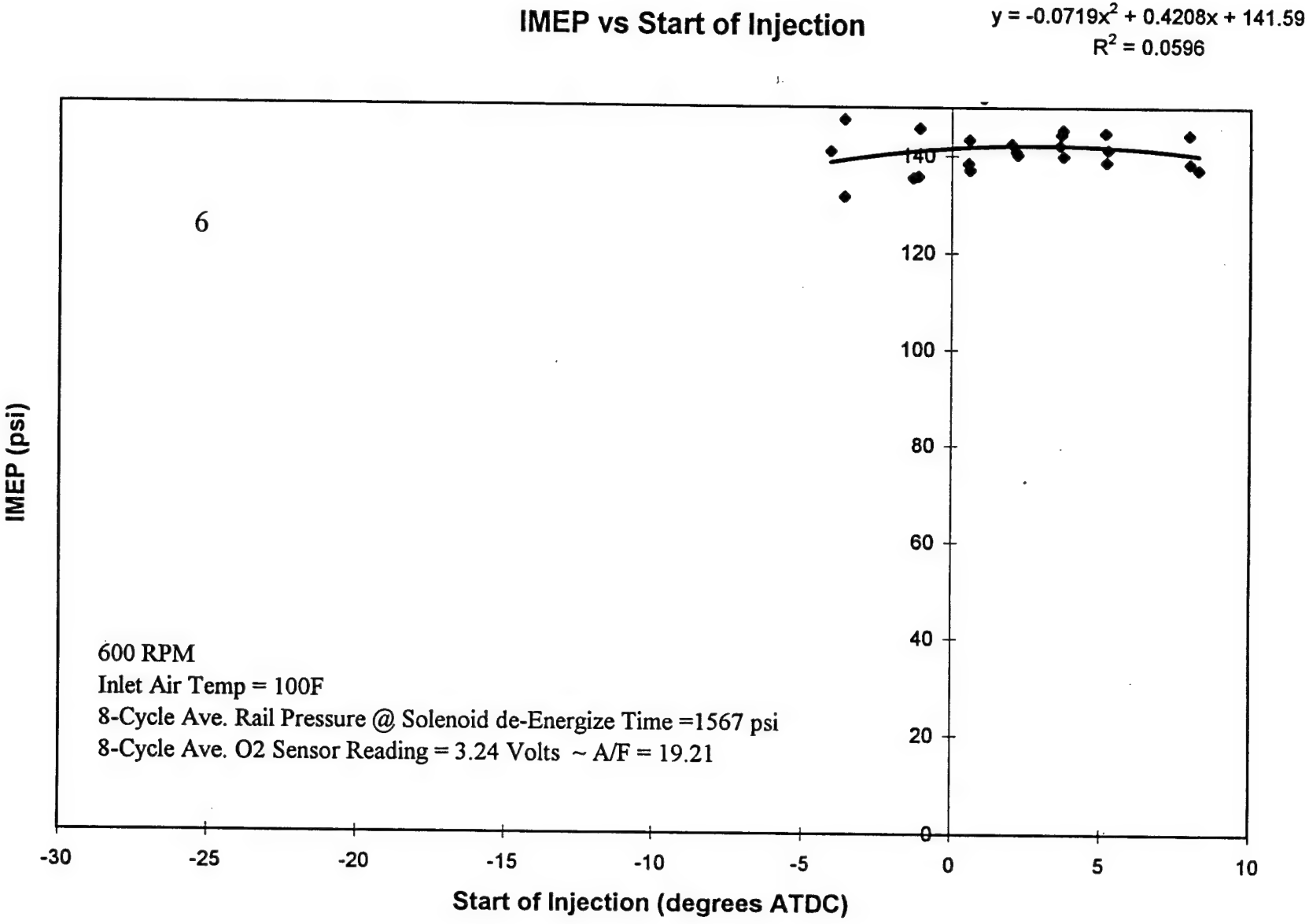
IMEP vs Start of Injection
y = -0.0719x² + 0.4208x + 141.59
R² = 0.0596
6
IMEP (psi)
140
120
100
80
60
40
20
0
-30
-25
-20
-15
-10
-5
0
5
10
Start of Injection (degrees ATDC)
600 RPM
Inlet Air Temp = 100F
8-Cycle Ave. Rail Pressure @ Solenoid de-Energize Time =1567 psi
8-Cycle Ave. O2 Sensor Reading = 3.24 Volts ~ A/F = 19.21

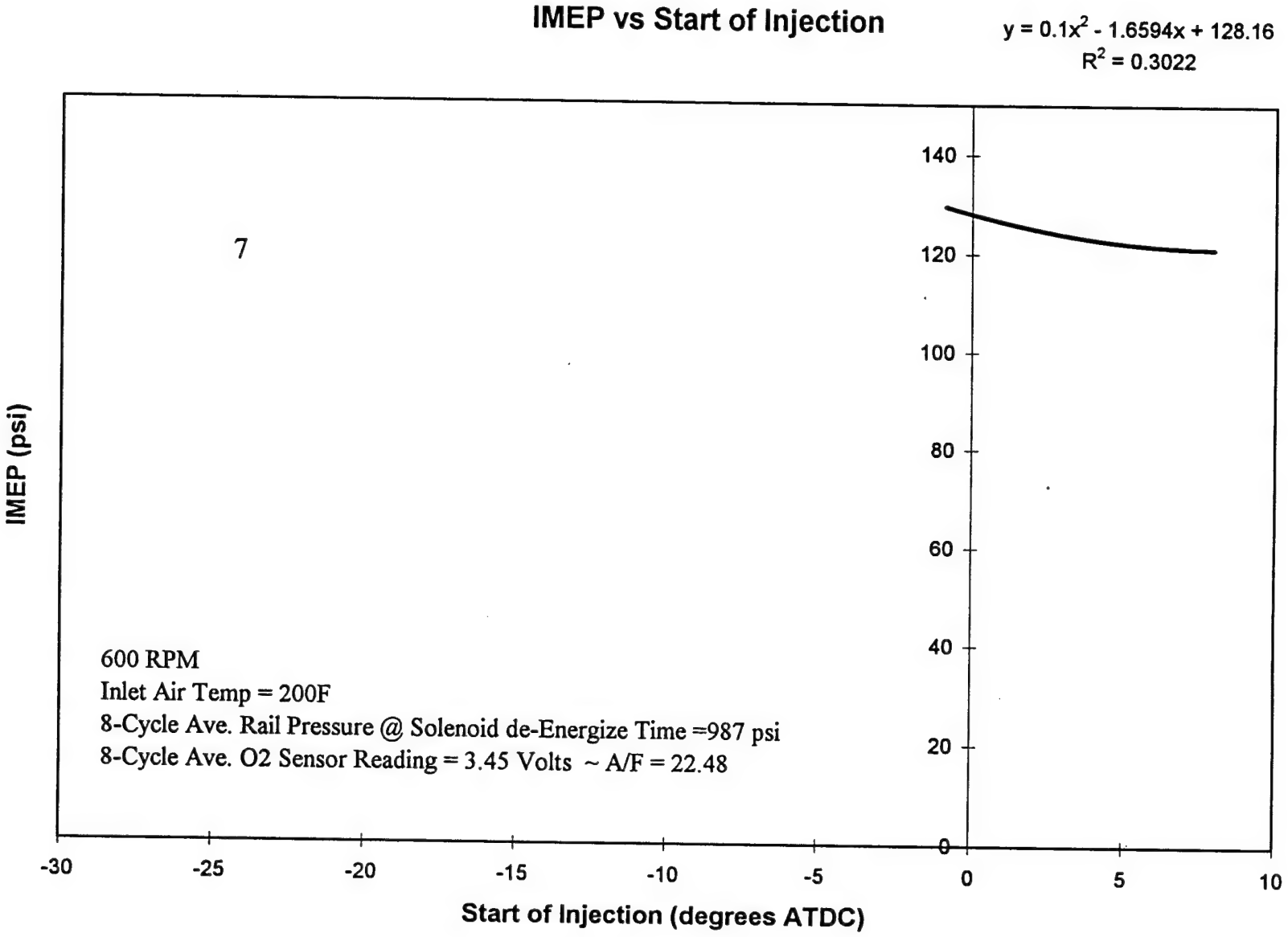
IMEP vs Start of Injection
y = 0.1x² - 1.6594x + 128.16
R² = 0.3022
7
600 RPM
Inlet Air Temp = 200F
8-Cycle Ave. Rail Pressure @ Solenoid de-Energize Time =987 psi
8-Cycle Ave. O2 Sensor Reading = 3.45 Volts ~ A/F = 22.48
IMEP (psi)
140
120
100
80
60
40
20
0
-30
-25
-20
-15
-10
-5
0
5
10
Start of Injection (degrees ATDC)

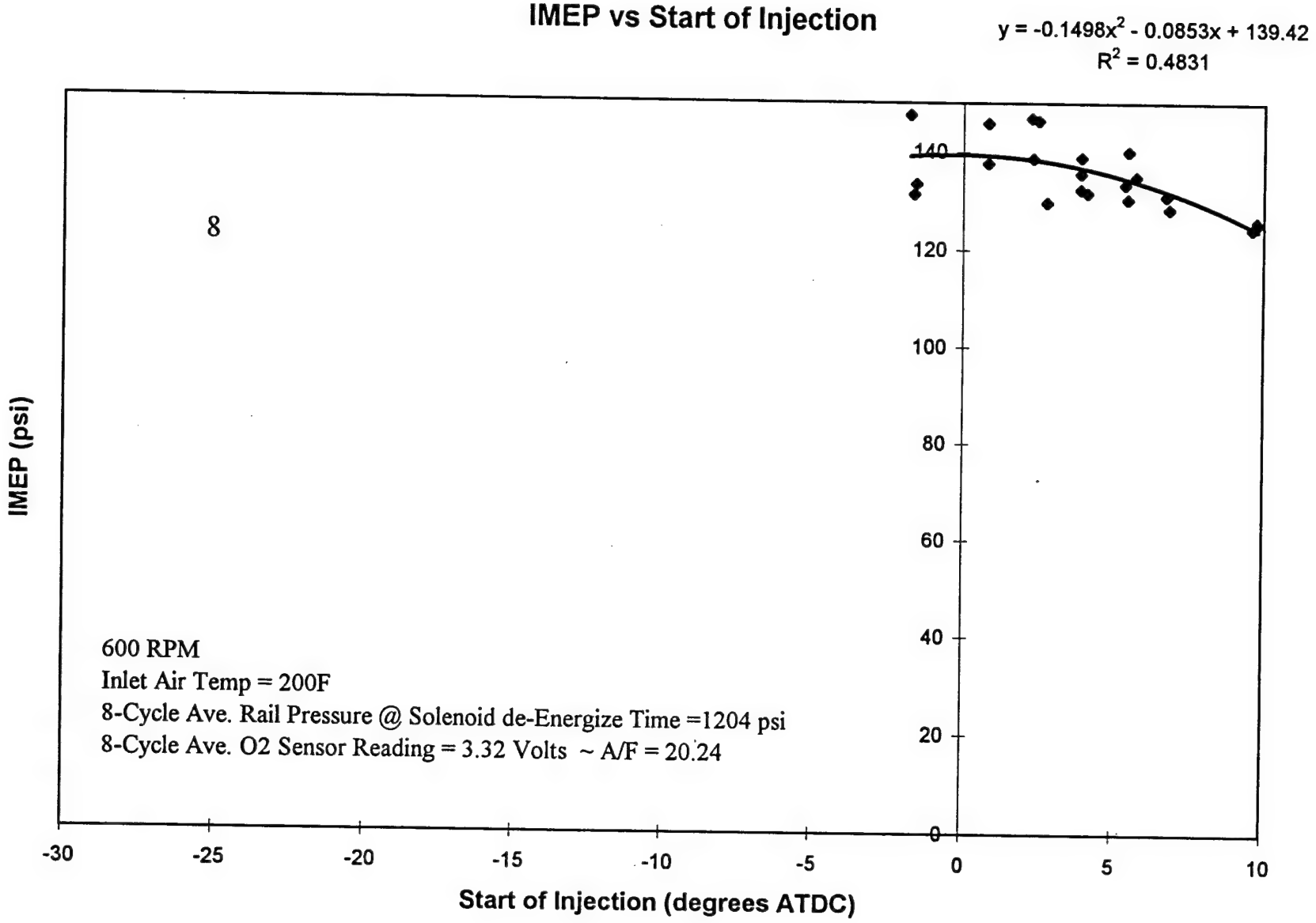
IMEP vs Start of Injection
y = -0.1498x² - 0.0853x + 139.42
R² = 0.4831
8
IMEP (psi)
140
120
100
80
60
40
20
0
-30
-25
-20
-15
-10
-5
0
5
10
Start of Injection (degrees ATDC)
600 RPM
Inlet Air Temp = 200F
8-Cycle Ave. Rail Pressure @ Solenoid de-Energize Time =1204 psi
8-Cycle Ave. O2 Sensor Reading = 3.32 Volts ~ A/F = 20.24

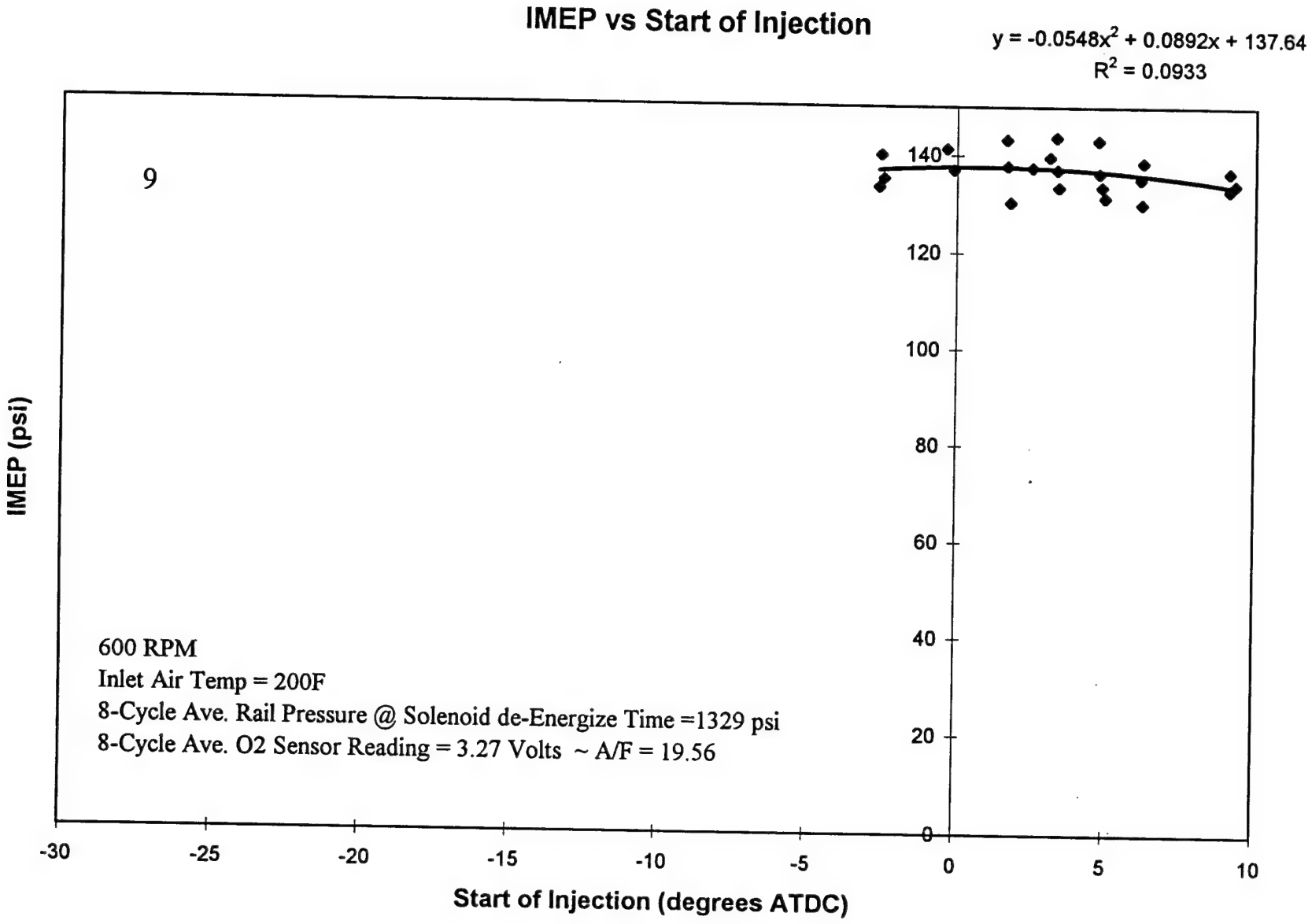
IMEP vs Start of Injection
y = -0.0548x2 + 0.0892x + 137.64
R2 = 0.0933
9
600 RPM
Inlet Air Temp = 200F
8-Cycle Ave. Rail Pressure @ Solenoid de-Energize Time =1329 psi
8-Cycle Ave. O2 Sensor Reading = 3.27 Volts ~ A/F = 19.56
IMEP (psi)
140
120
100
80
60
40
20
0
-30
-25
-20
-15
-10
-5
0
5
10
Start of Injection (degrees ATDC)

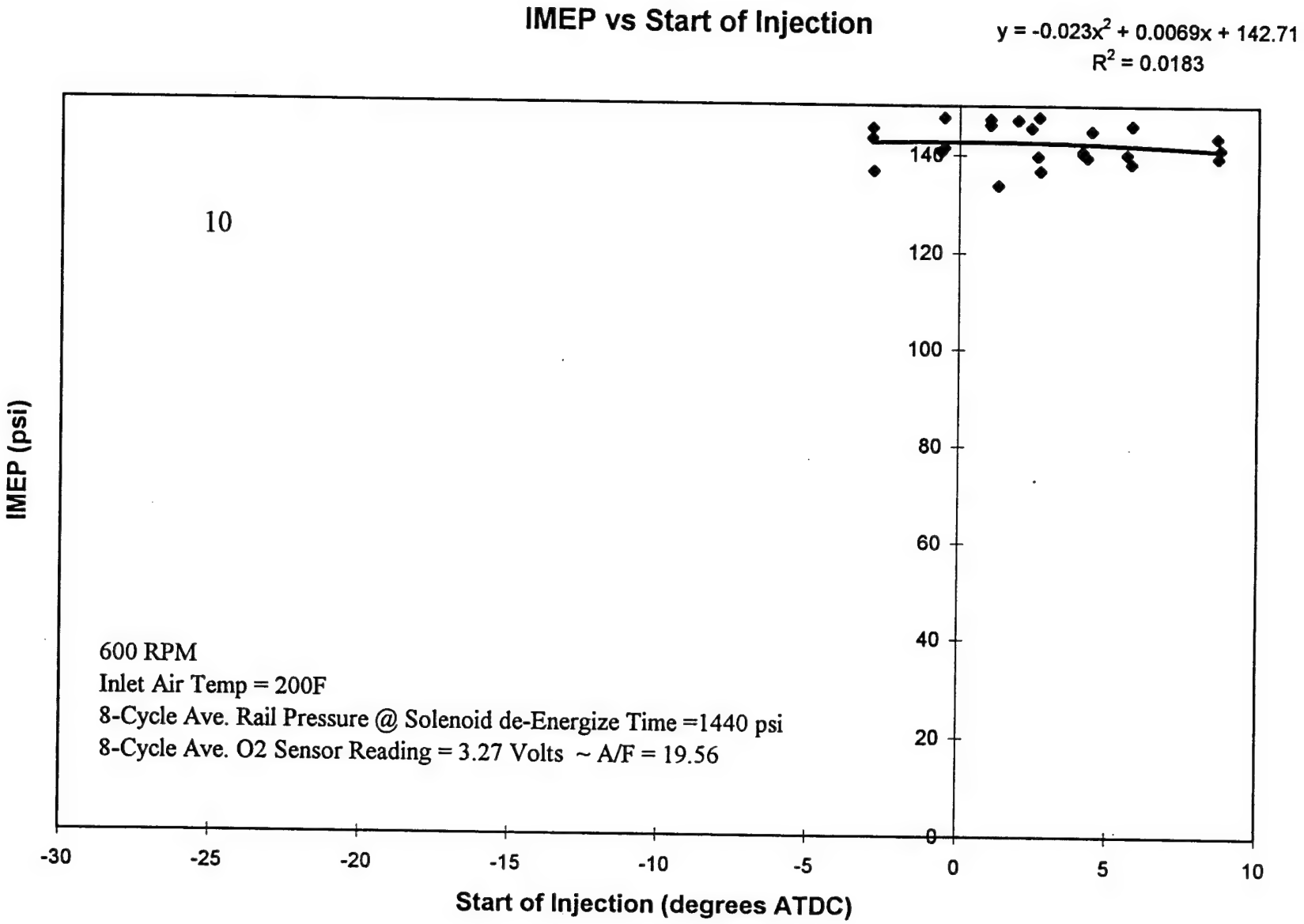
IMEP vs Start of Injection
y = -0.023x² + 0.0069x + 142.71
R² = 0.0183
10
600 RPM
Inlet Air Temp = 200F
8-Cycle Ave. Rail Pressure @ Solenoid de-Energize Time =1440 psi
8-Cycle Ave. O2 Sensor Reading = 3.27 Volts ~ A/F = 19.56
IMEP (psi)
140
120
100
80
60
40
20
0
-30
-25
-20
-15
-10
-5
0
5
10
Start of Injection (degrees ATDC)

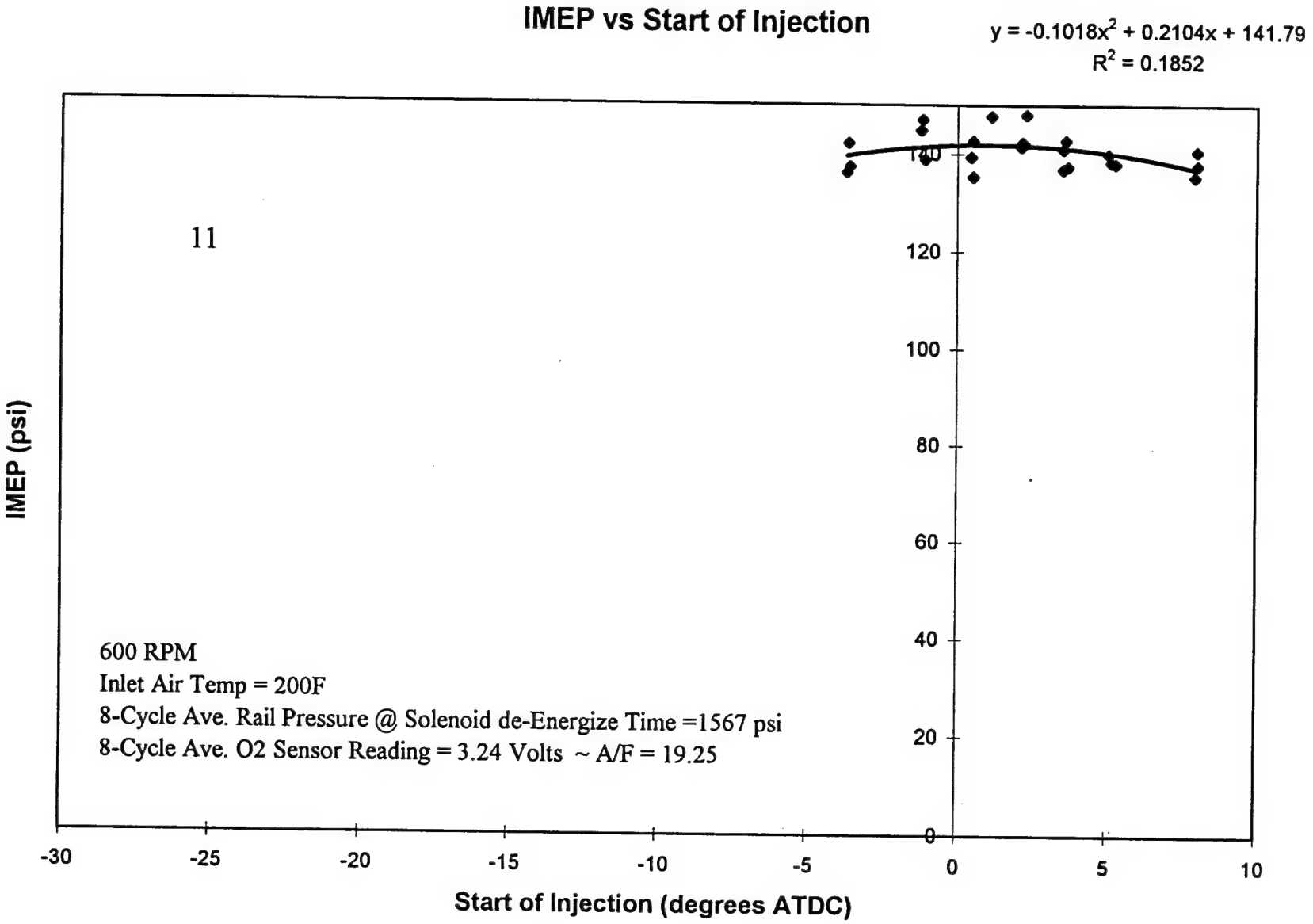
IMEP vs Start of Injection
y = -0.1018x² + 0.2104x + 141.79
R² = 0.1852
11
600 RPM
Inlet Air Temp = 200F
8-Cycle Ave. Rail Pressure @ Solenoid de-Energize Time =1567 psi
8-Cycle Ave. O2 Sensor Reading = 3.24 Volts ~ A/F = 19.25
IMEP (psi)
140
120
100
80
60
40
20
0
-30
-25
-20
-15
-10
-5
0
5
10
Start of Injection (degrees ATDC)

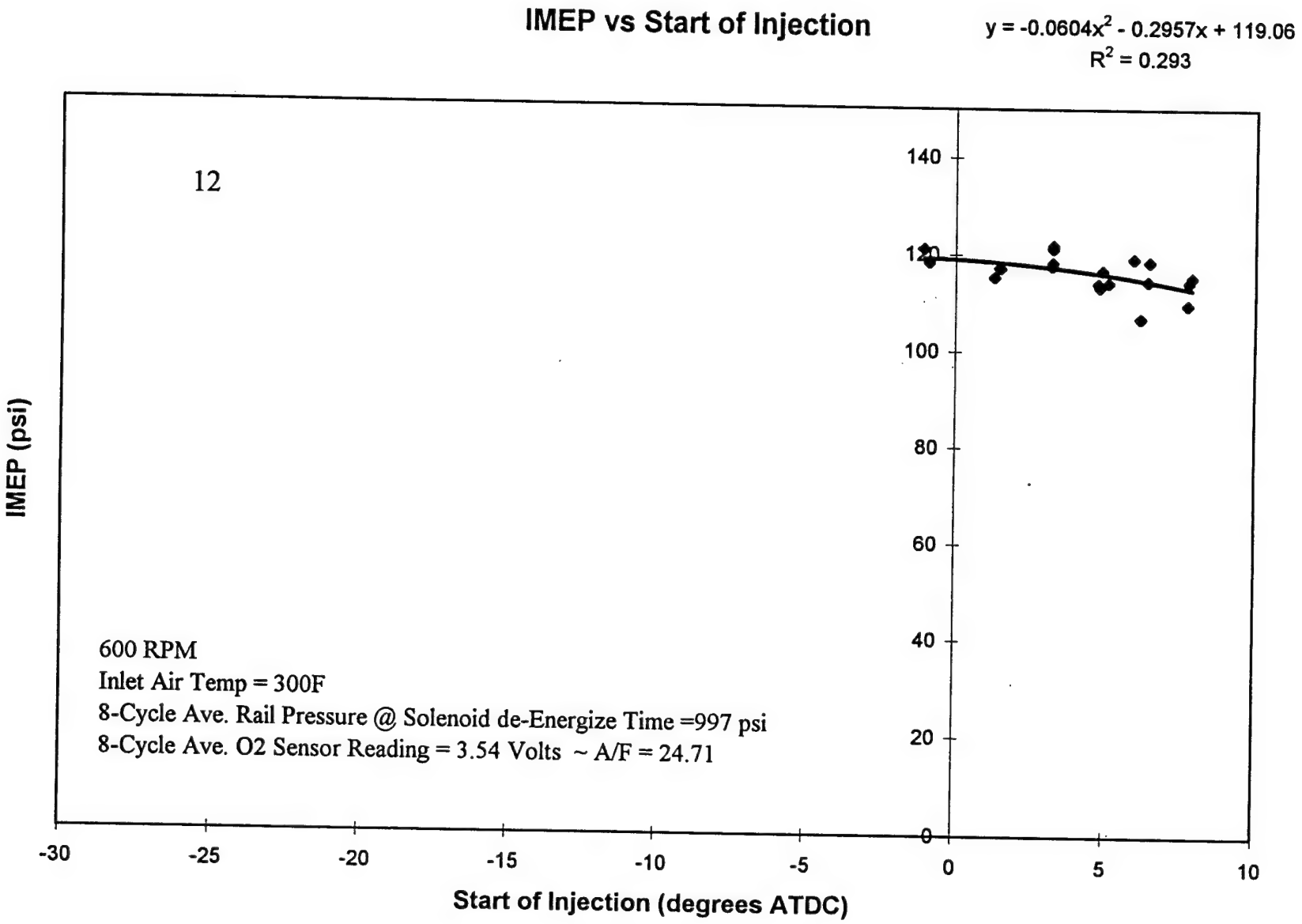
IMEP vs Start of Injection
y = -0.0604x² - 0.2957x + 119.06
R² = 0.293
12
600 RPM
Inlet Air Temp = 300F
8-Cycle Ave. Rail Pressure @ Solenoid de-Energize Time =997 psi
8-Cycle Ave. O2 Sensor Reading = 3.54 Volts ~ A/F = 24.71
IMEP (psi)
140
120
100
80
60
40
20
0
-30
-25
-20
-15
-10
-5
0
5
10
Start of Injection (degrees ATDC)

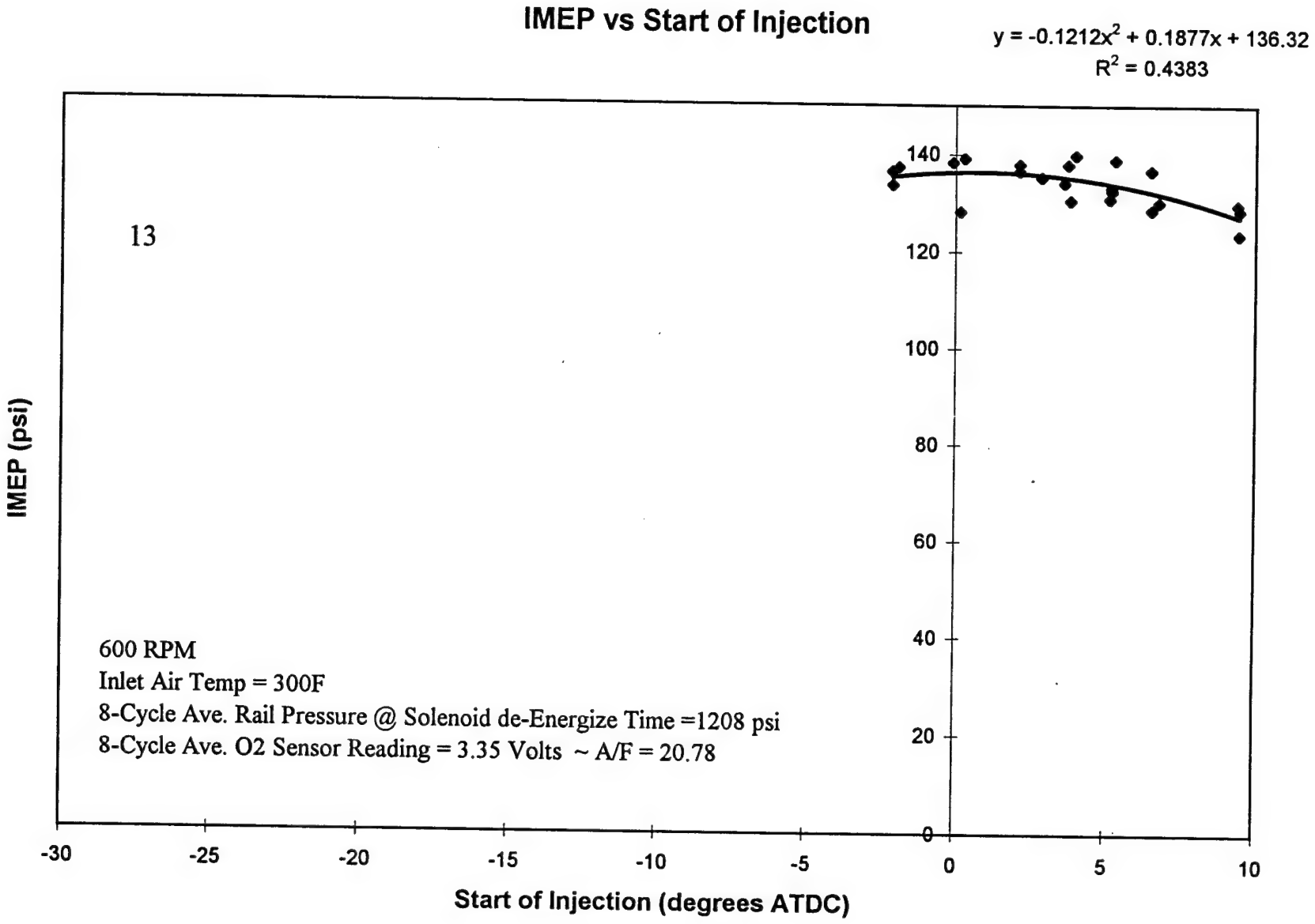
IMEP vs Start of Injection
y = -0.1212x2 + 0.1877x + 136.32
R2 = 0.4383
13
600 RPM
Inlet Air Temp = 300F
8-Cycle Ave. Rail Pressure @ Solenoid de-Energize Time =1208 psi
8-Cycle Ave. O2 Sensor Reading = 3.35 Volts ~ A/F = 20.78
IMEP (psi)
140
120
100
80
60
40
20
0
-30
-25
-20
-15
-10
-5
0
5
10
Start of Injection (degrees ATDC)

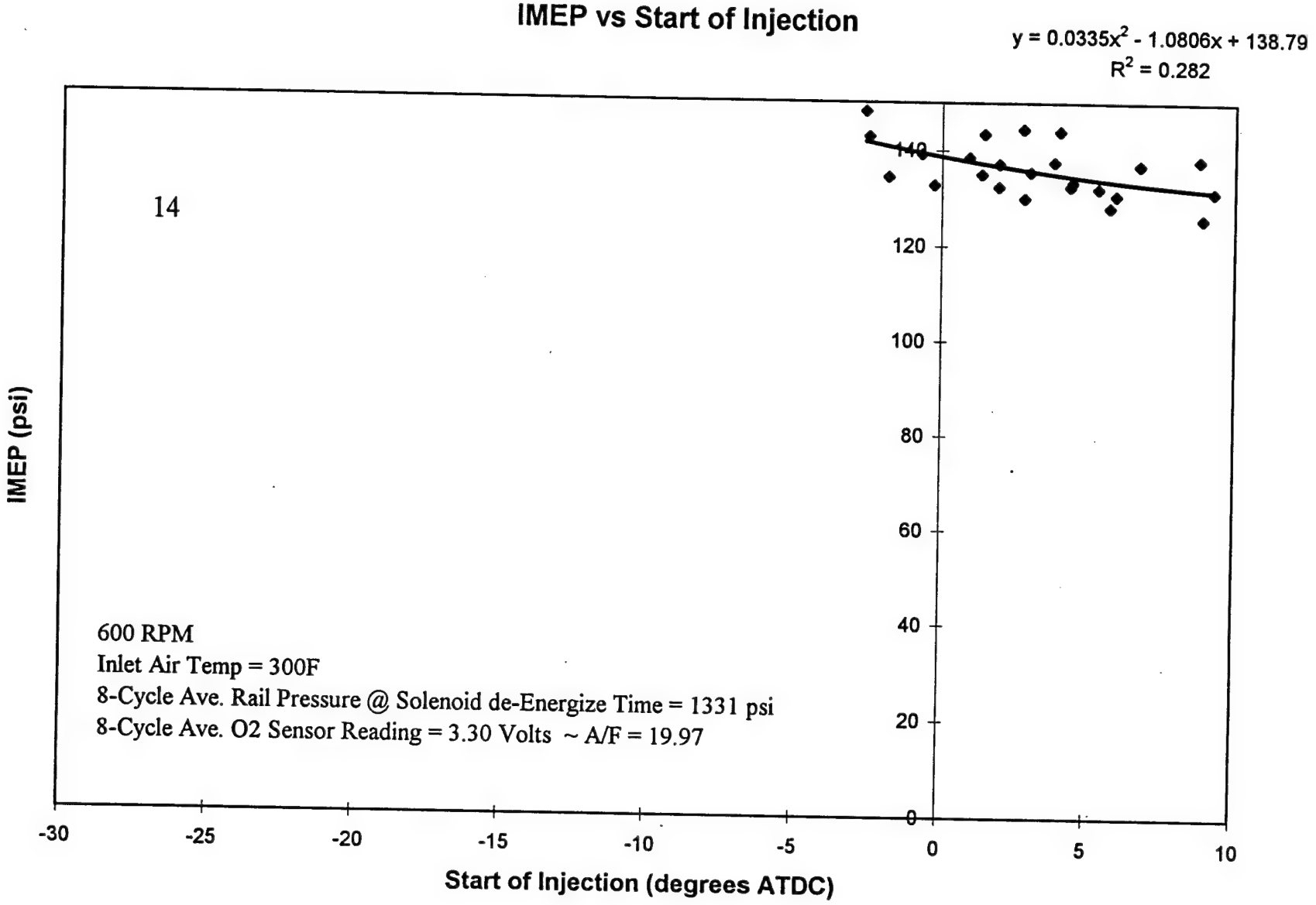
IMEP vs Start of Injection
y = 0.0335x² - 1.0806x + 138.79
R² = 0.282
14
600 RPM
Inlet Air Temp = 300F
8-Cycle Ave. Rail Pressure @ Solenoid de-Energize Time = 1331 psi
8-Cycle Ave. O2 Sensor Reading = 3.30 Volts ~ A/F = 19.97
IMEP (psi)
140
120
100
80
60
40
20
0
-30
-25
-20
-15
-10
-5
0
5
10
Start of Injection (degrees ATDC)

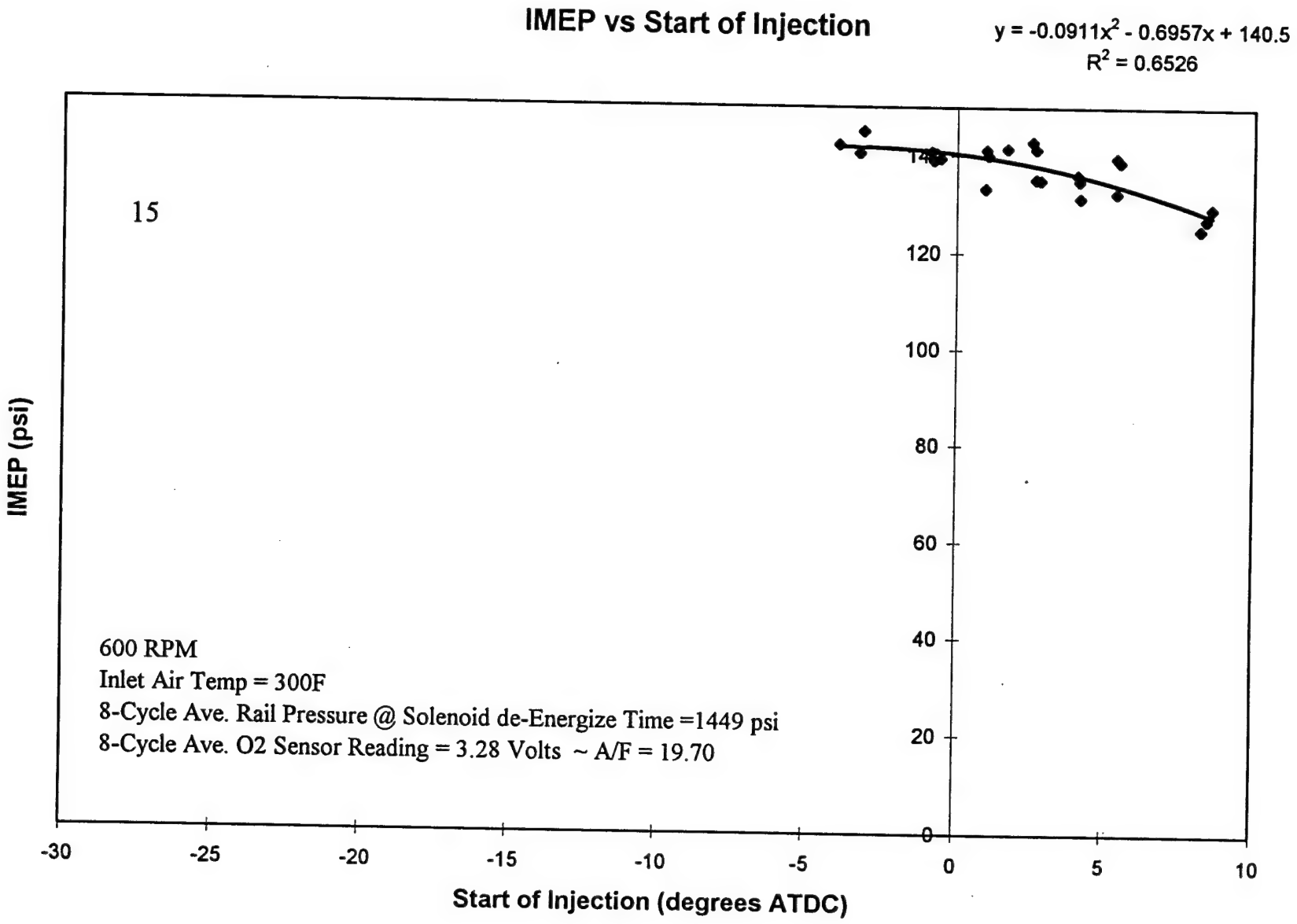
IMEP vs Start of Injection
y = -0.0911x² - 0.6957x + 140.5
R² = 0.6526
15
600 RPM
Inlet Air Temp = 300F
8-Cycle Ave. Rail Pressure @ Solenoid de-Energize Time =1449 psi
8-Cycle Ave. O2 Sensor Reading = 3.28 Volts ~ A/F = 19.70
IMEP (psi)
120
100
80
60
40
20
0
-30
-25
-20
-15
-10
-5
0
5
10
Start of Injection (degrees ATDC)

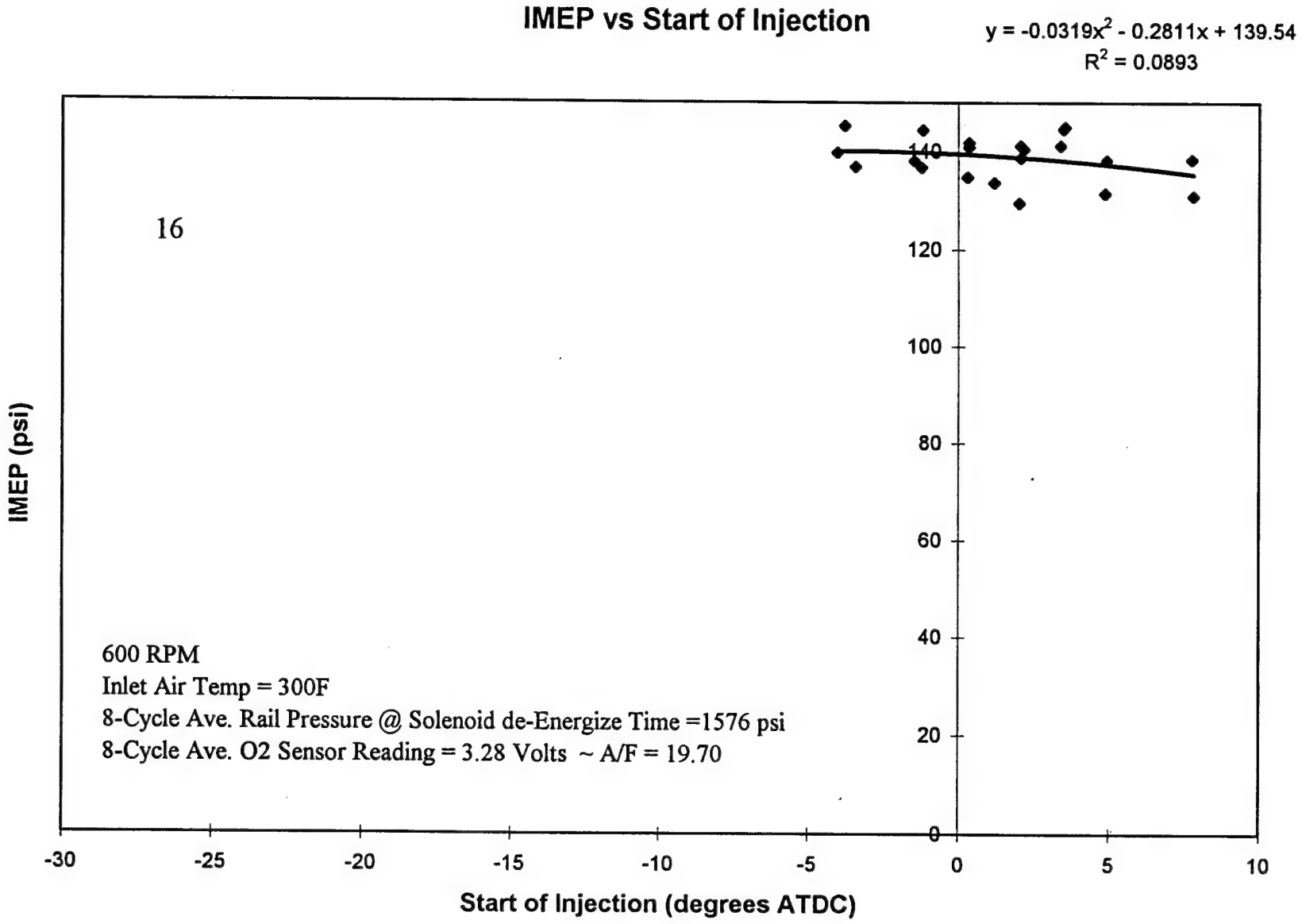
IMEP vs Start of Injection
y = -0.0319x² - 0.2811x + 139.54
R² = 0.0893
16
600 RPM
Inlet Air Temp = 300F
8-Cycle Ave. Rail Pressure @ Solenoid de-Energize Time =1576 psi
8-Cycle Ave. O2 Sensor Reading = 3.28 Volts ~ A/F = 19.70
IMEP (psi)
140
120
100
80
60
40
20
0
-30
-25
-20
-15
-10
-5
0
5
10
Start of Injection (degrees ATDC)

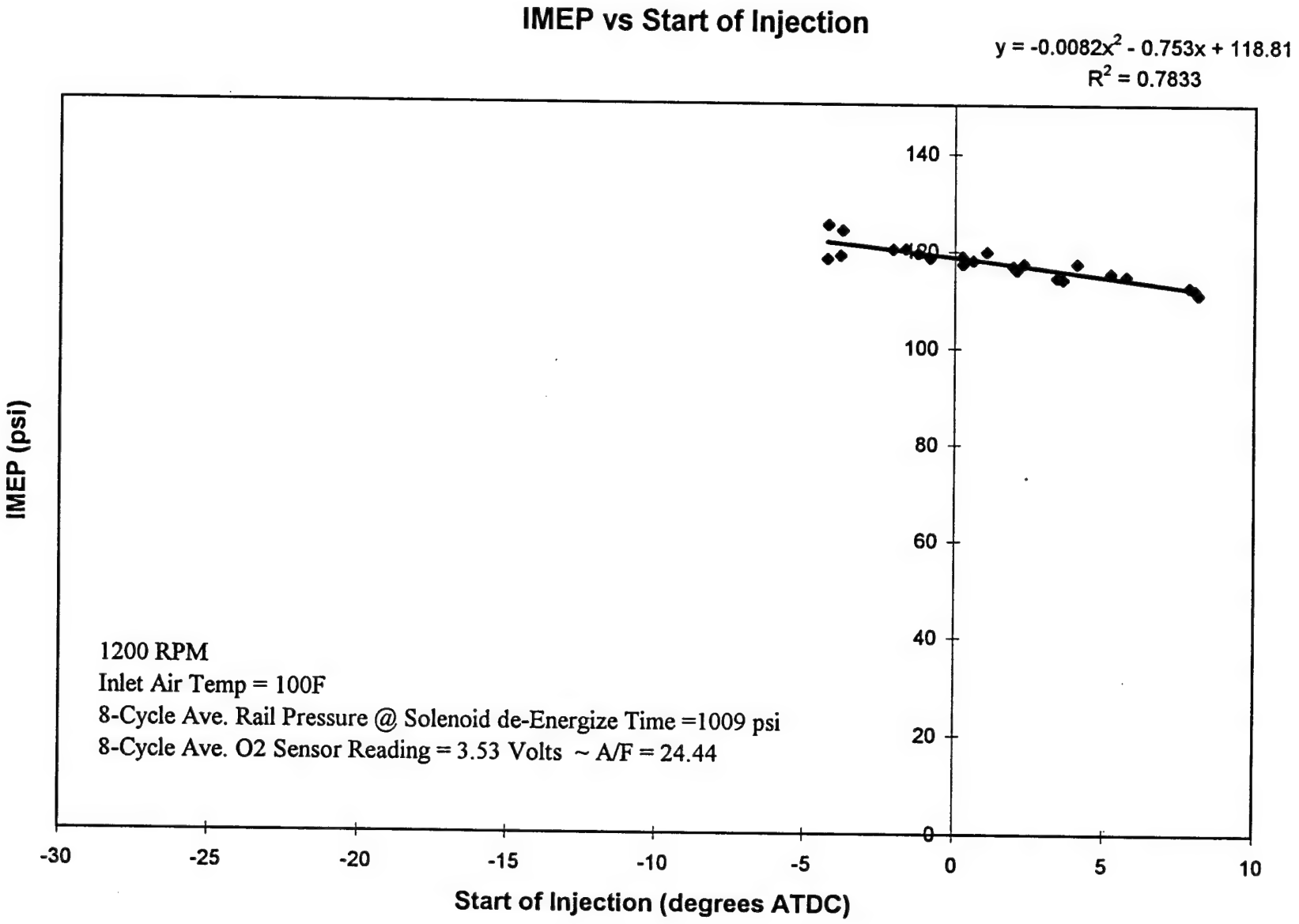
IMEP vs Start of Injection
y = -0.0082x² - 0.753x + 118.81
R² = 0.7833
IMEP (psi)
140
120
100
80
60
40
20
0
-30
-25
-20
-15
-10
-5
0
5
10
Start of Injection (degrees ATDC)
1200 RPM
Inlet Air Temp = 100F
8-Cycle Ave. Rail Pressure @ Solenoid de-Energize Time =1009 psi
8-Cycle Ave. O2 Sensor Reading = 3.53 Volts ~ A/F = 24.44

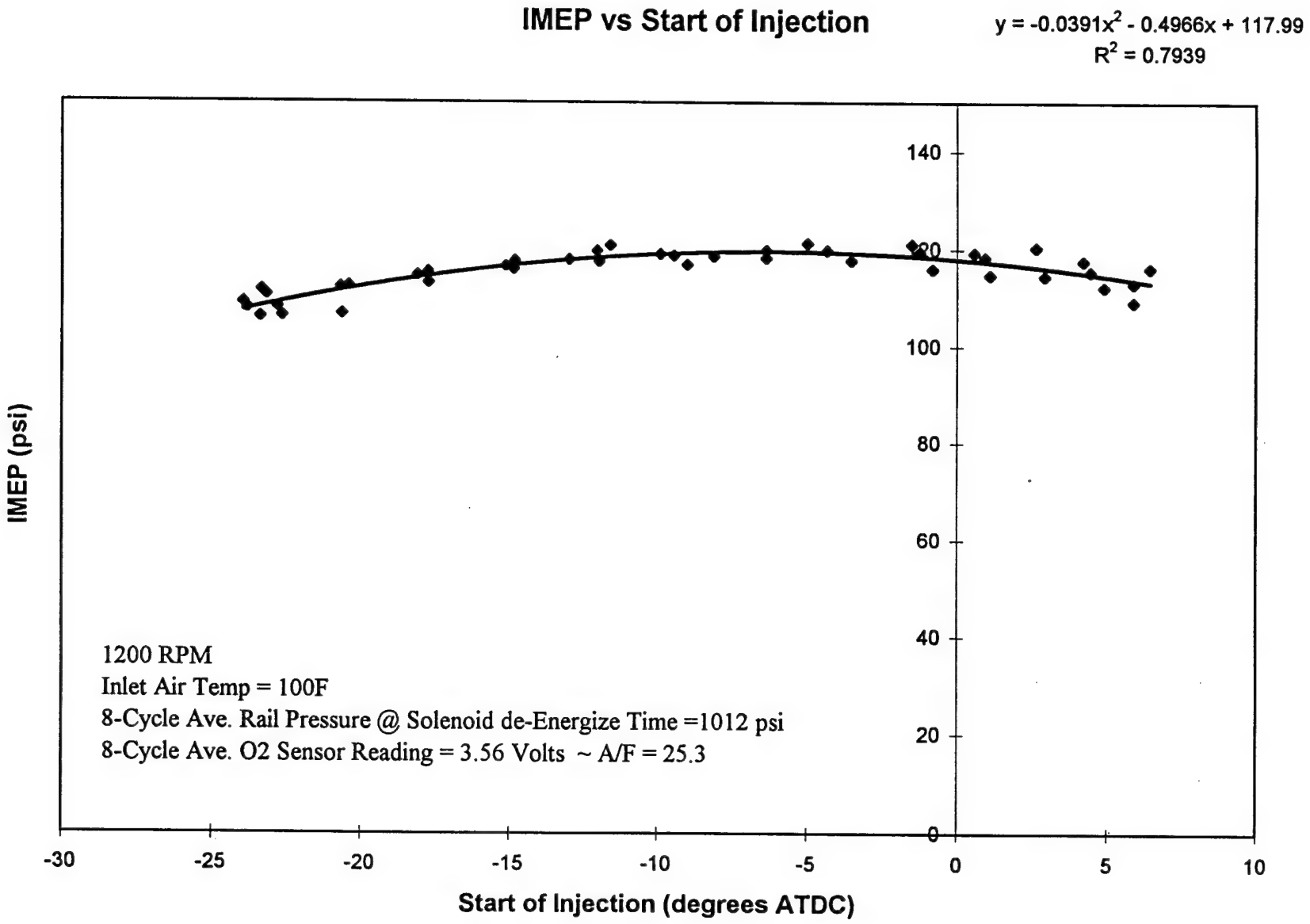
IMEP vs Start of Injection
y = -0.0391x² - 0.4966x + 117.99
R² = 0.7939
IMEP (psi)
140
120
100
80
60
40
20
0
-30
-25
-20
-15
-10
-5
0
5
10
Start of Injection (degrees ATDC)
1200 RPM
Inlet Air Temp = 100F
8-Cycle Ave. Rail Pressure @ Solenoid de-Energize Time =1012 psi
8-Cycle Ave. O2 Sensor Reading = 3.56 Volts ~ A/F = 25.3

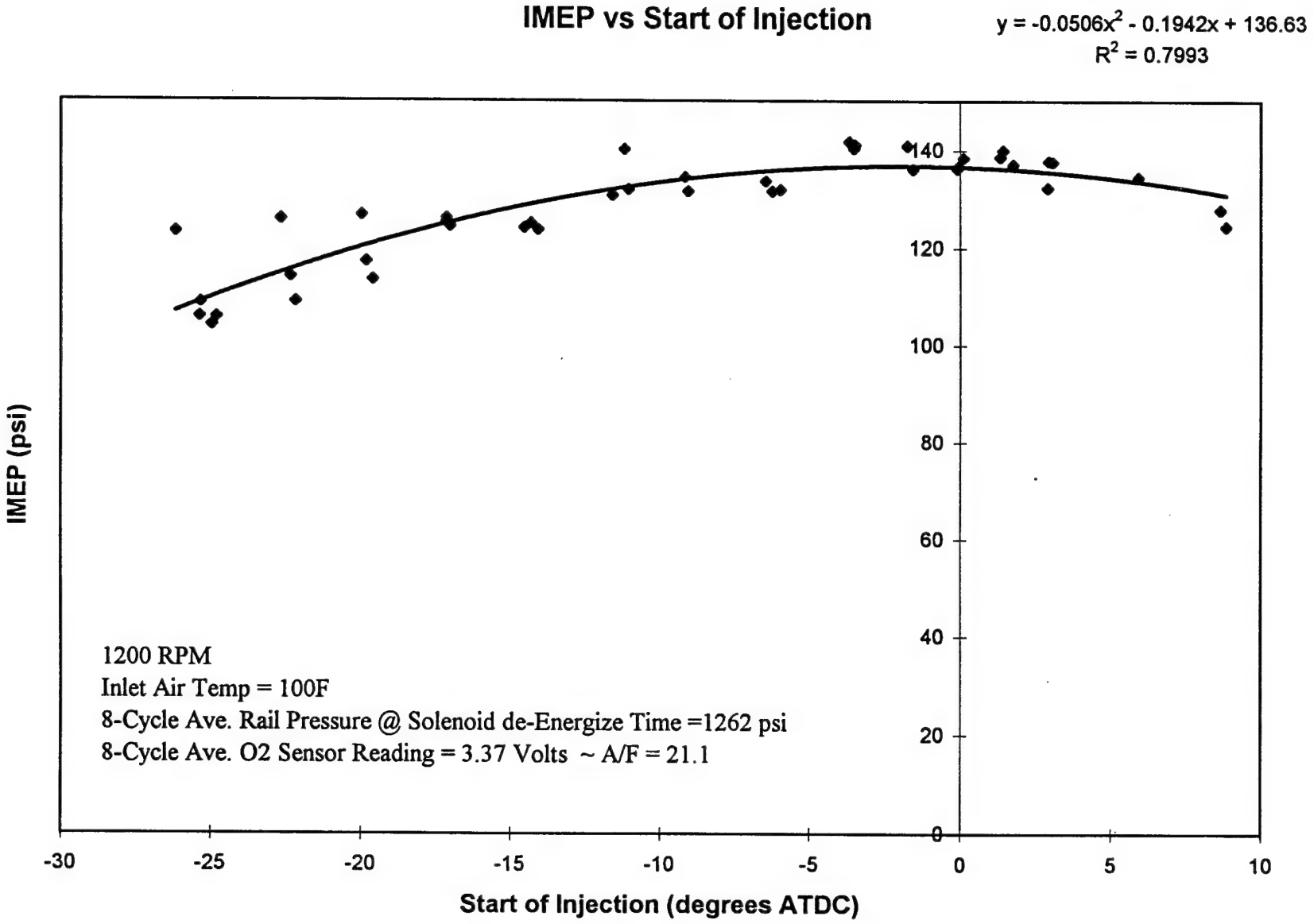
IMEP vs Start of Injection
y = -0.0506x² - 0.1942x + 136.63
R² = 0.7993
IMEP (psi)
140
120
100
80
60
40
20
0
-30
-25
-20
-15
-10
-5
0
5
10
Start of Injection (degrees ATDC)
1200 RPM
Inlet Air Temp = 100F
8-Cycle Ave. Rail Pressure @ Solenoid de-Energize Time =1262 psi
8-Cycle Ave. O2 Sensor Reading = 3.37 Volts ~ A/F = 21.1

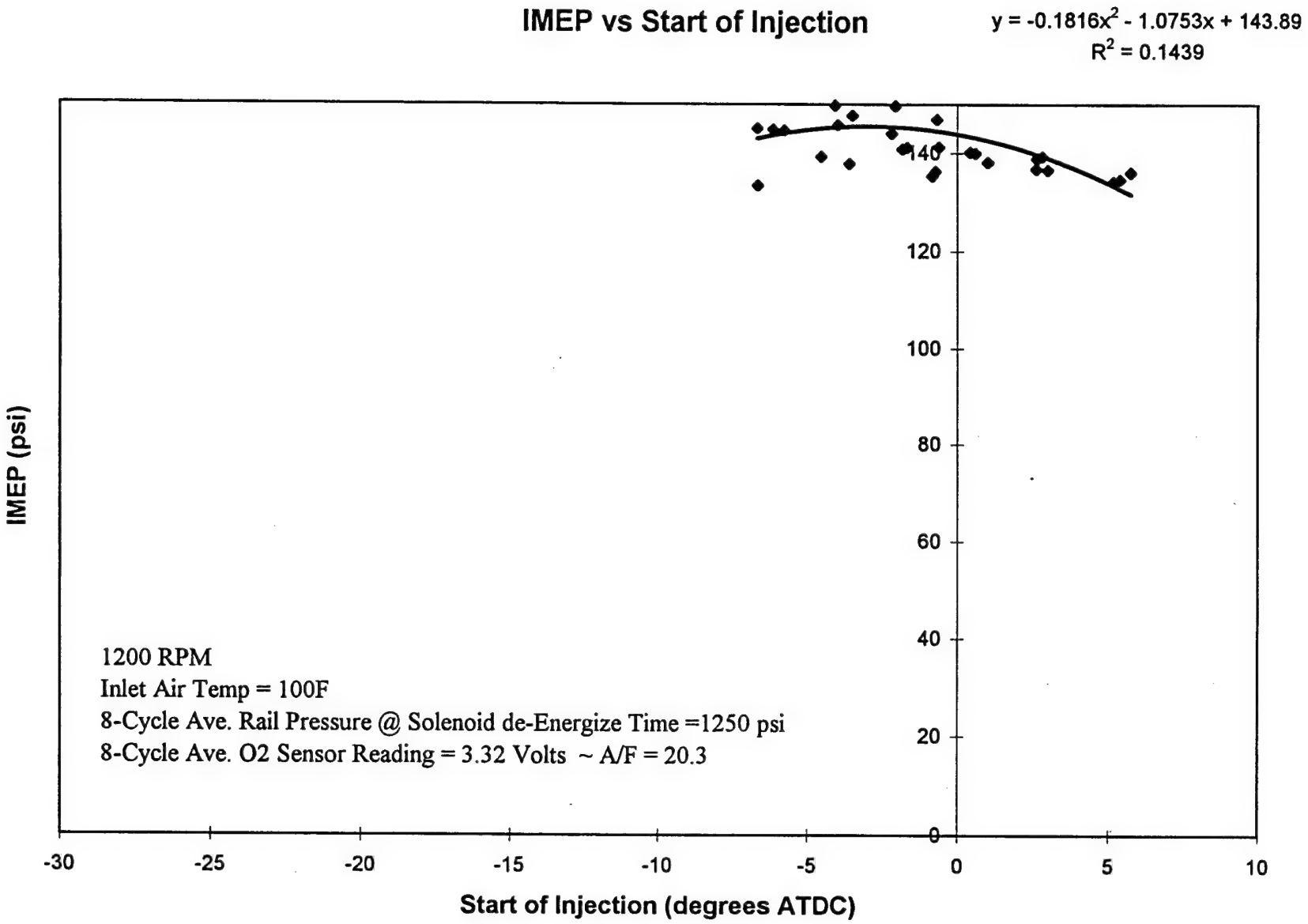
IMEP vs Start of Injection
y = -0.1816x2 - 1.0753x + 143.89
R2 = 0.1439
IMEP (psi)
140
120
100
80
60
40
20
0
-30
-25
-20
-15
-10
-5
0
5
10
Start of Injection (degrees ATDC)
1200 RPM
Inlet Air Temp = 100F
8-Cycle Ave. Rail Pressure @ Solenoid de-Energize Time =1250 psi
8-Cycle Ave. O2 Sensor Reading = 3.32 Volts ~ A/F = 20.3

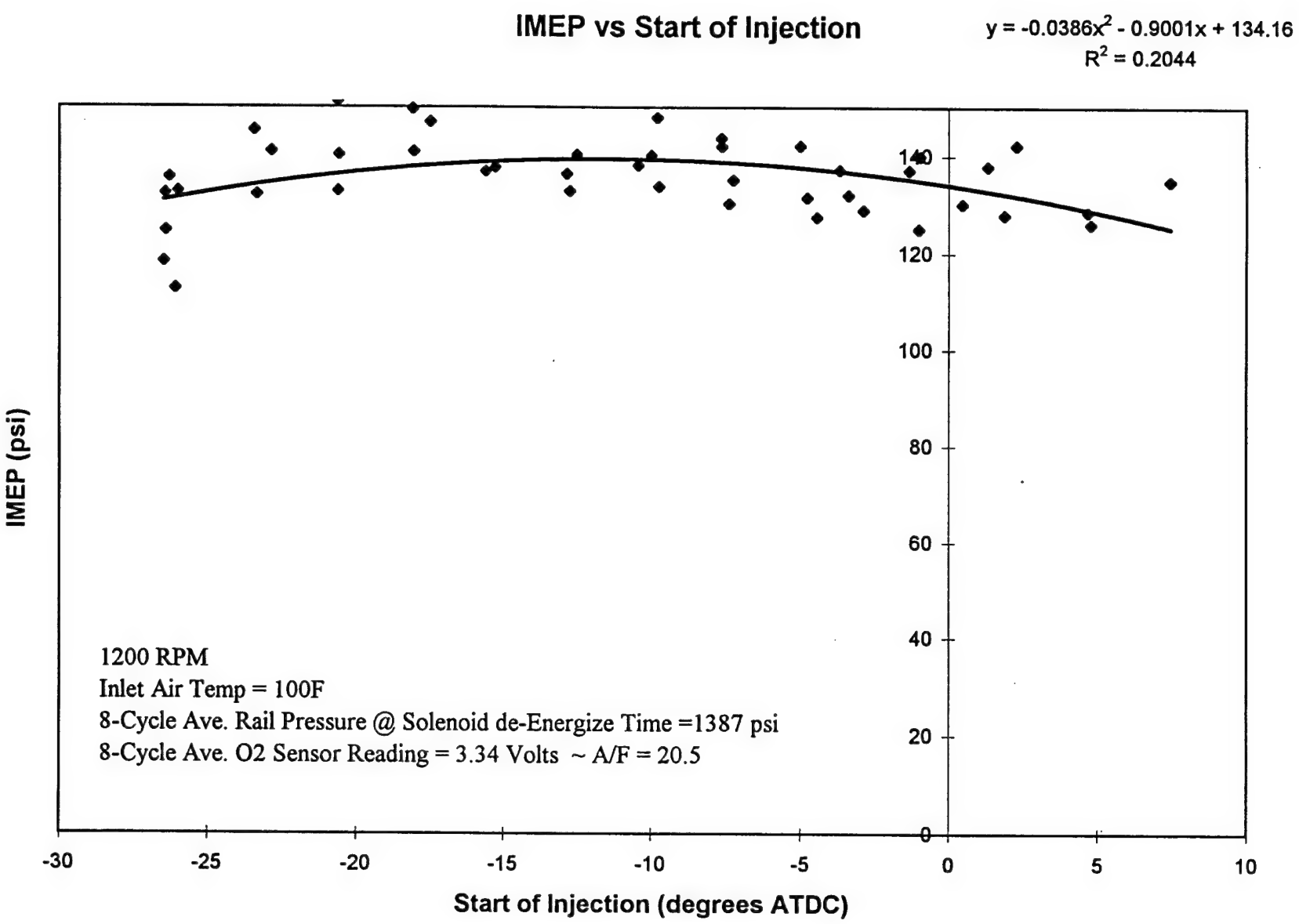
IMEP vs Start of Injection
y = -0.0386x2 - 0.9001x + 134.16
R2 = 0.2044
IMEP (psi)
140
120
100
80
60
40
20
0
-30
-25
-20
-15
-10
-5
0
5
10
Start of Injection (degrees ATDC)
1200 RPM
Inlet Air Temp = 100F
8-Cycle Ave. Rail Pressure @ Solenoid de-Energize Time =1387 psi
8-Cycle Ave. O2 Sensor Reading = 3.34 Volts ~ A/F = 20.5

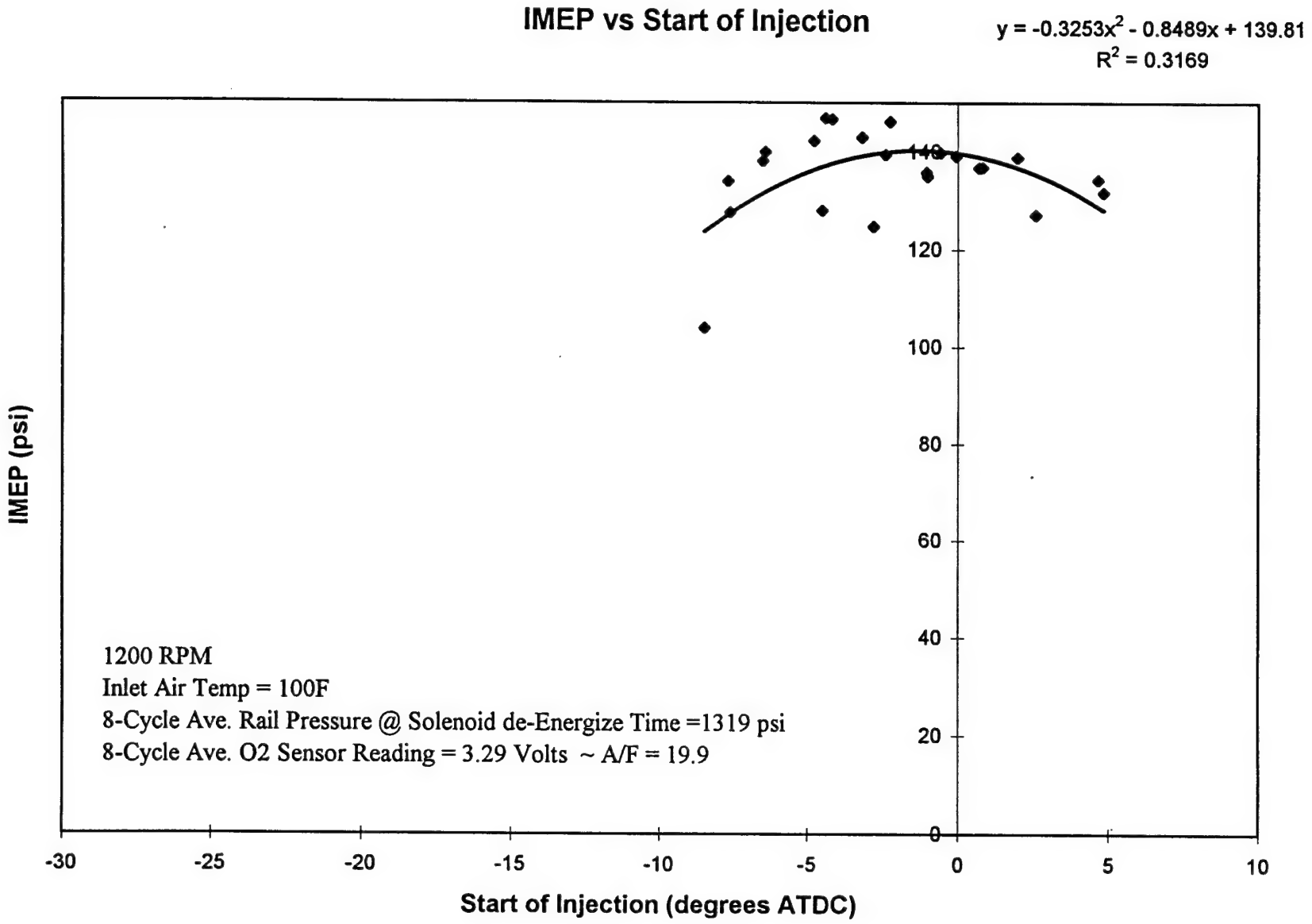
IMEP vs Start of Injection
y = -0.3253x² - 0.8489x + 139.81
R² = 0.3169
IMEP (psi)
140
120
100
80
60
40
20
0
-30
-25
-20
-15
-10
-5
0
5
10
Start of Injection (degrees ATDC)
1200 RPM
Inlet Air Temp = 100F
8-Cycle Ave. Rail Pressure @ Solenoid de-Energize Time =1319 psi
8-Cycle Ave. O2 Sensor Reading = 3.29 Volts ~ A/F = 19.9

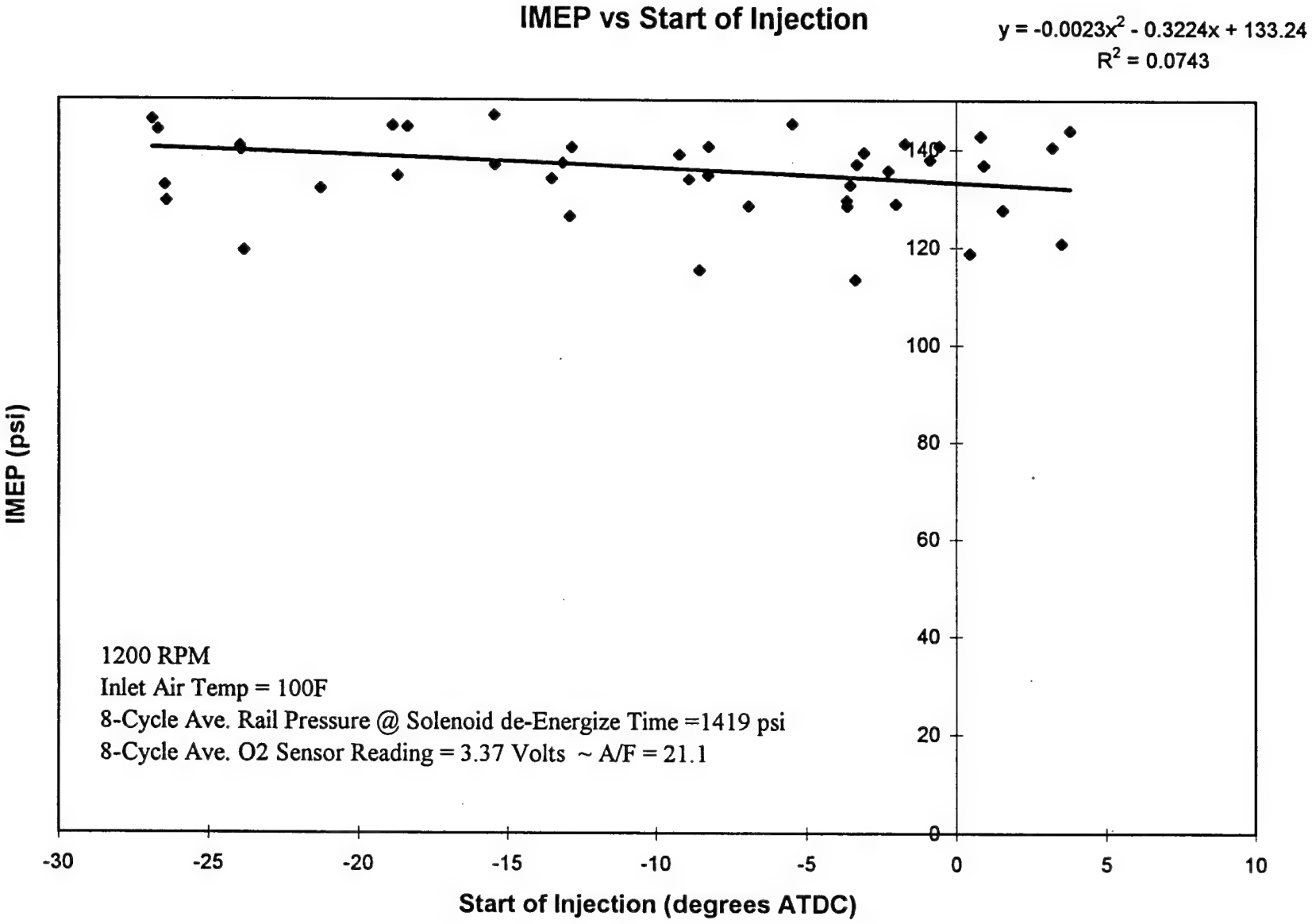
IMEP vs Start of Injection
y = -0.0023x2 - 0.3224x + 133.24
R2 = 0.0743
IMEP (psi)
140
120
100
80
60
40
20
0
-30
-25
-20
-15
-10
-5
0
5
10
Start of Injection (degrees ATDC)
1200 RPM
Inlet Air Temp = 100F
8-Cycle Ave. Rail Pressure @ Solenoid de-Energize Time =1419 psi
8-Cycle Ave. O2 Sensor Reading = 3.37 Volts ~ A/F = 21.1

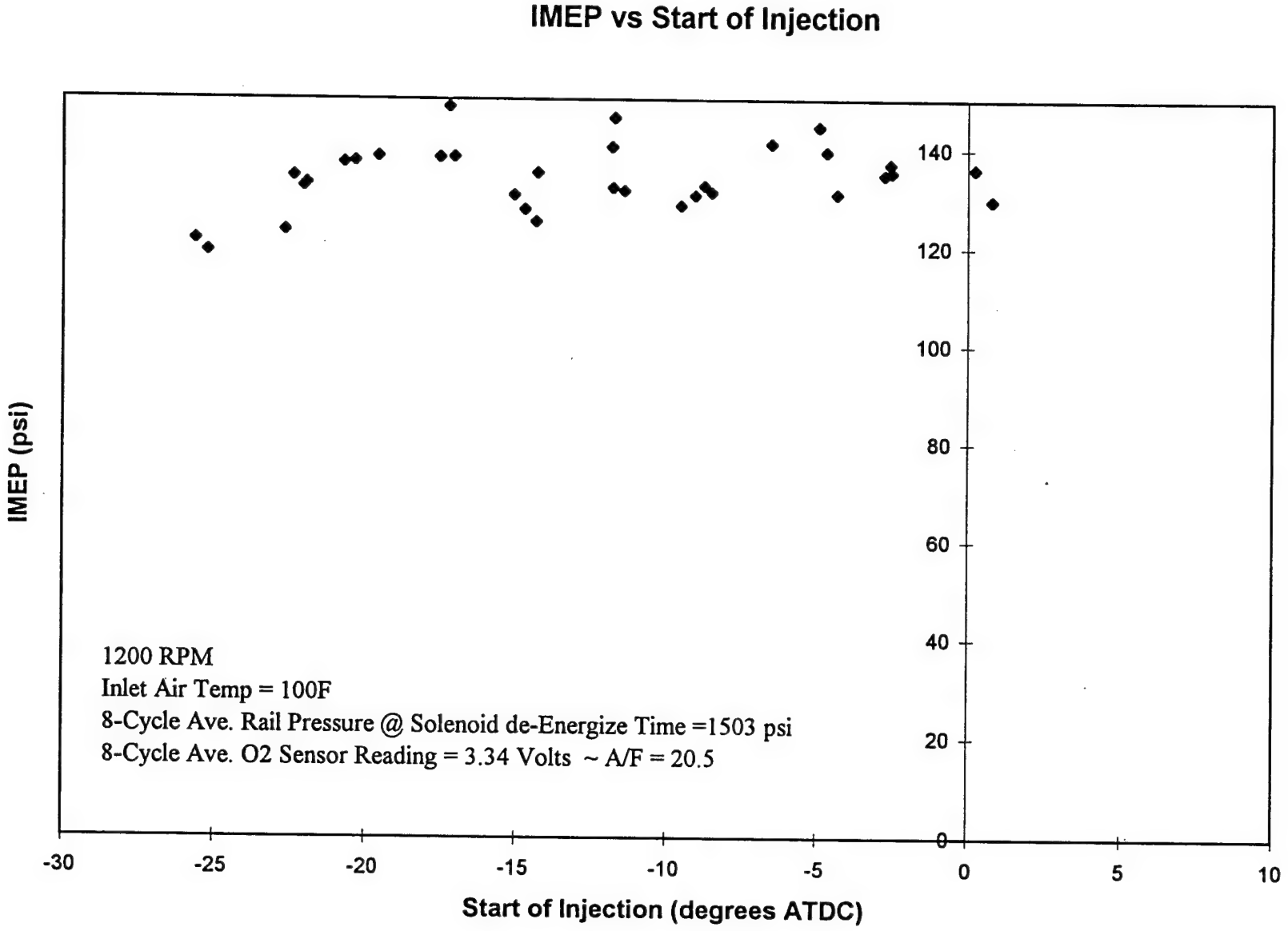
IMEP vs Start of Injection
IMEP (psi)
140
120
100
80
60
40
20
0
-30
-25
-20
-15
-10
-5
0
5
10
Start of Injection (degrees ATDC)
1200 RPM
Inlet Air Temp = 100F
8-Cycle Ave. Rail Pressure @ Solenoid de-Energize Time =1503 psi
8-Cycle Ave. O2 Sensor Reading = 3.34 Volts ~ A/F = 20.5

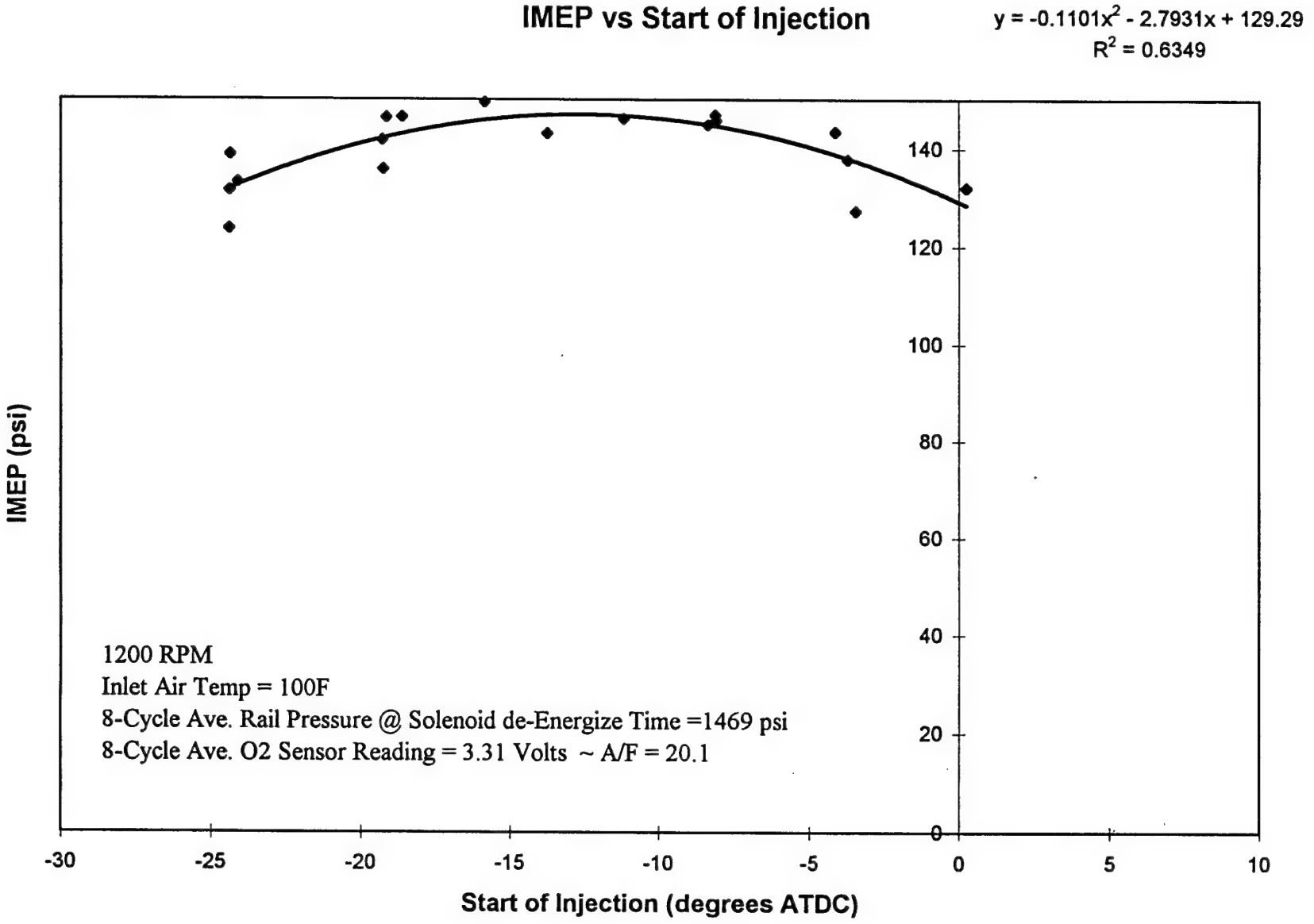
IMEP vs Start of Injection
y = -0.1101x² - 2.7931x + 129.29
R² = 0.6349
IMEP (psi)
140
120
100
80
60
40
20
0
-30
-25
-20
-15
-10
-5
0
5
10
Start of Injection (degrees ATDC)
1200 RPM
Inlet Air Temp = 100F
8-Cycle Ave. Rail Pressure @ Solenoid de-Energize Time =1469 psi
8-Cycle Ave. O2 Sensor Reading = 3.31 Volts ~ A/F = 20.1

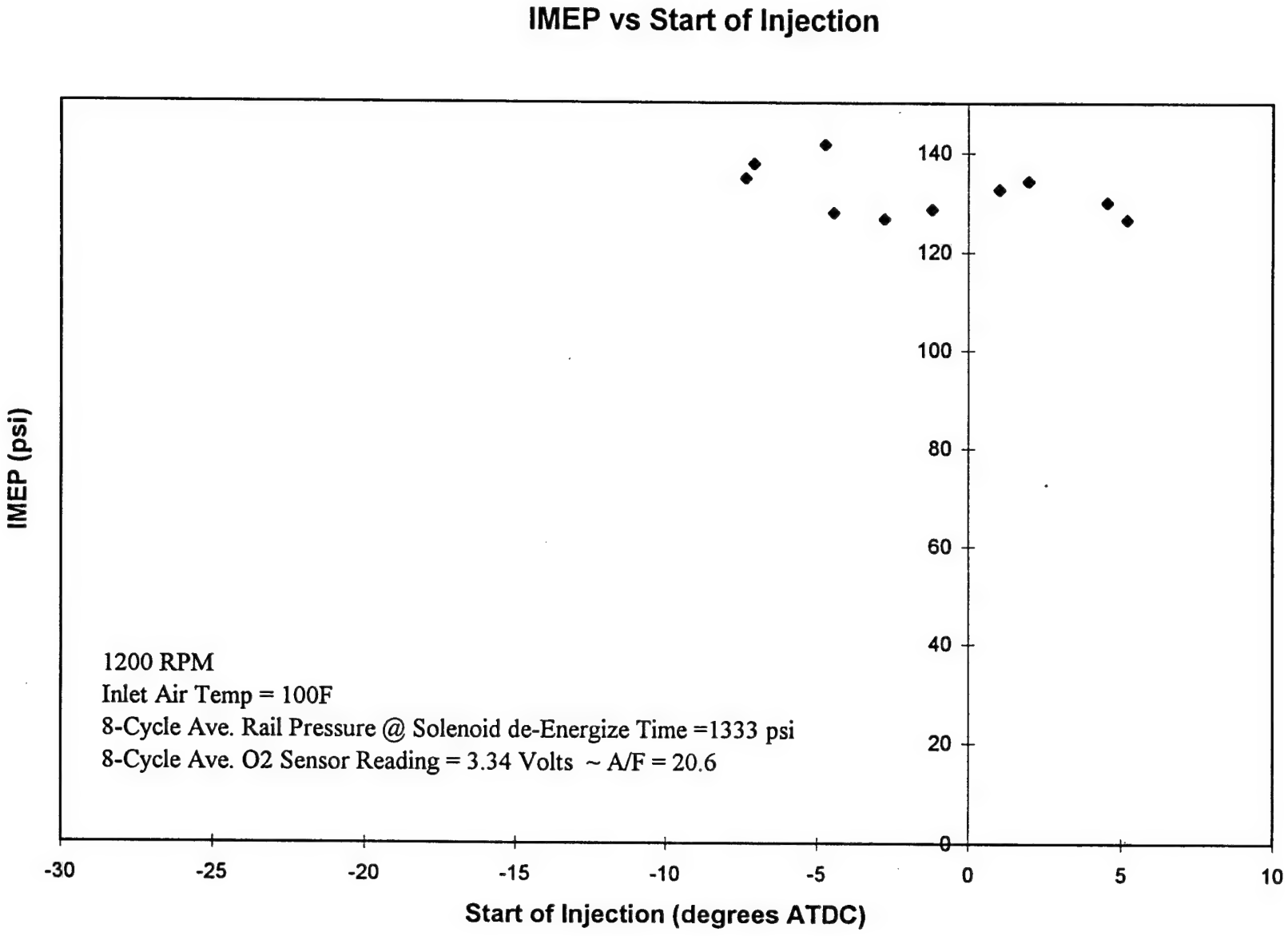
IMEP vs Start of Injection
IMEP (psi)
140
120
100
80
60
40
20
0
-30
-25
-20
-15
-10
-5
0
5
10
Start of Injection (degrees ATDC)
1200 RPM
Inlet Air Temp = 100F
8-Cycle Ave. Rail Pressure @ Solenoid de-Energize Time =1333 psi
8-Cycle Ave. O2 Sensor Reading = 3.34 Volts ~ A/F = 20.6

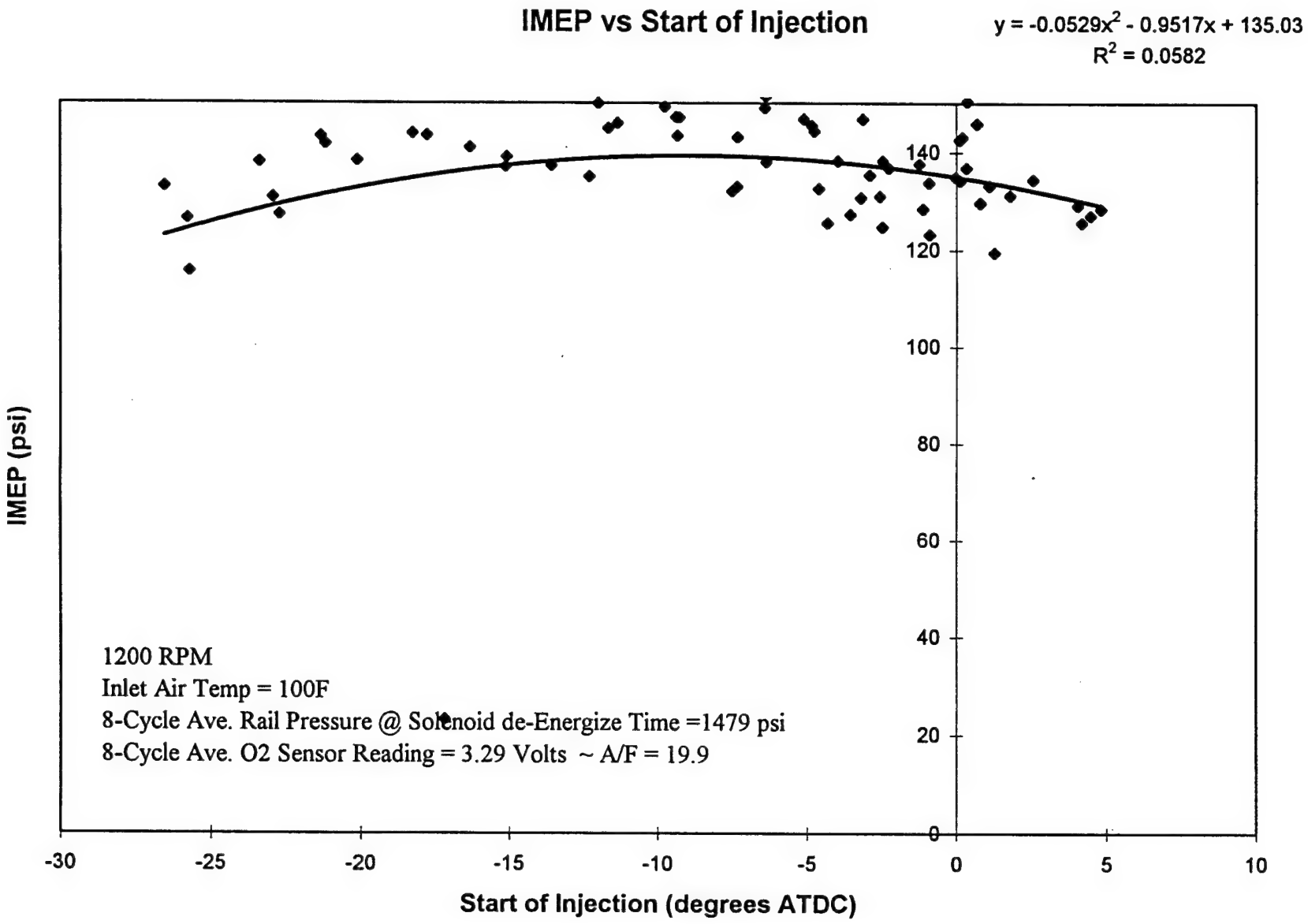
IMEP vs Start of Injection
y = -0.0529x2 - 0.9517x + 135.03
R2 = 0.0582
IMEP (psi)
140
120
100
80
60
40
20
0
-30
-25
-20
-15
-10
-5
0
5
10
Start of Injection (degrees ATDC)
1200 RPM
Inlet Air Temp = 100F
8-Cycle Ave. Rail Pressure @ Solenoid de-Energize Time =1479 psi
8-Cycle Ave. O2 Sensor Reading = 3.29 Volts ~ A/F = 19.9

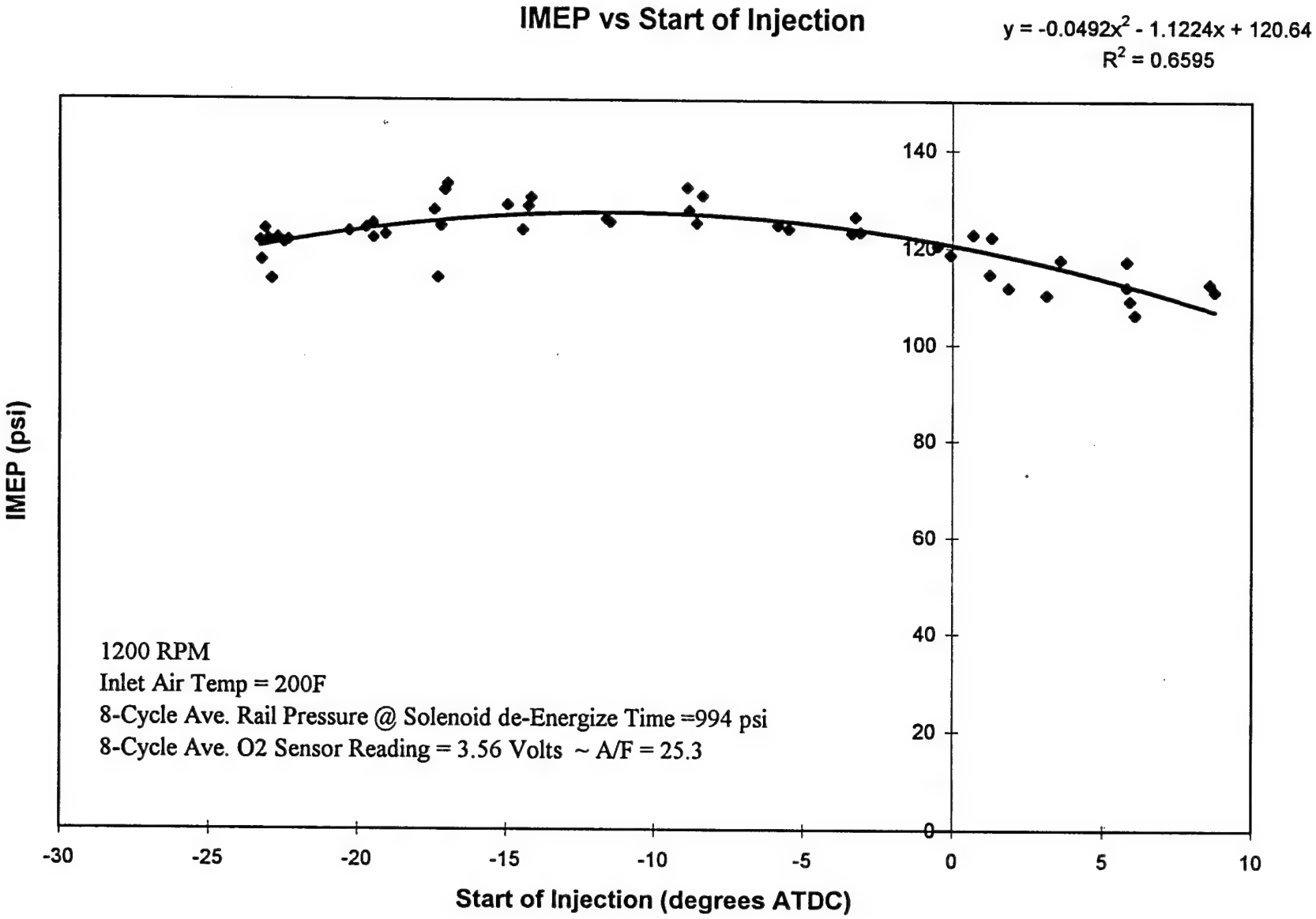
IMEP vs Start of Injection
y = -0.0492x² - 1.1224x + 120.64
R² = 0.6595
IMEP (psi)
140
120
100
80
60
40
20
0
-30
-25
-20
-15
-10
-5
0
5
10
Start of Injection (degrees ATDC)
1200 RPM
Inlet Air Temp = 200F
8-Cycle Ave. Rail Pressure @ Solenoid de-Energize Time =994 psi
8-Cycle Ave. O2 Sensor Reading = 3.56 Volts ~ A/F = 25.3

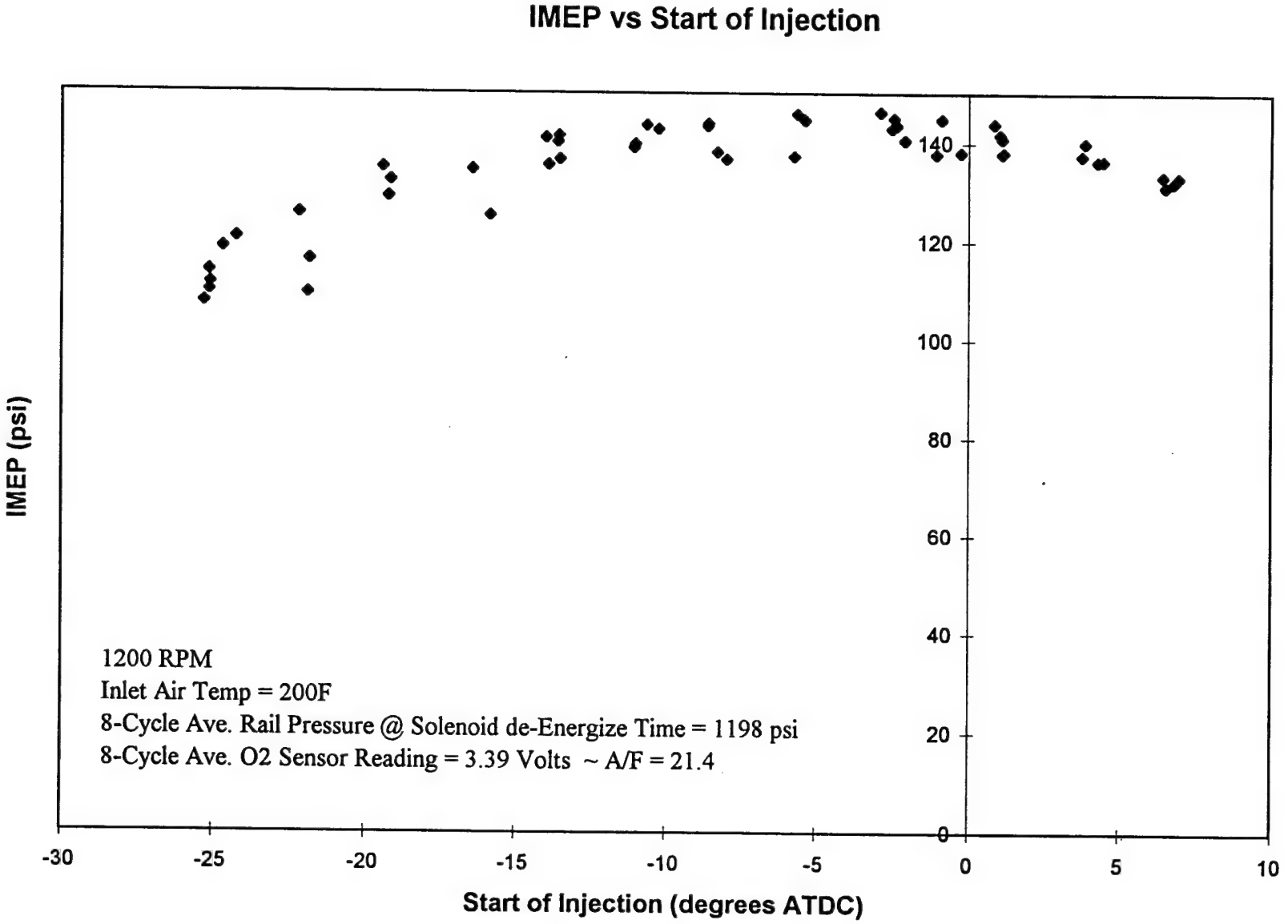
IMEP vs Start of Injection
IMEP (psi)
0
20
40
60
80
100
120
140
-30
-25
-20
-15
-10
-5
0
5
10
Start of Injection (degrees ATDC)
1200 RPM
Inlet Air Temp = 200F
8-Cycle Ave. Rail Pressure @ Solenoid de-Energize Time = 1198 psi
8-Cycle Ave. O2 Sensor Reading = 3.39 Volts ~ A/F = 21.4

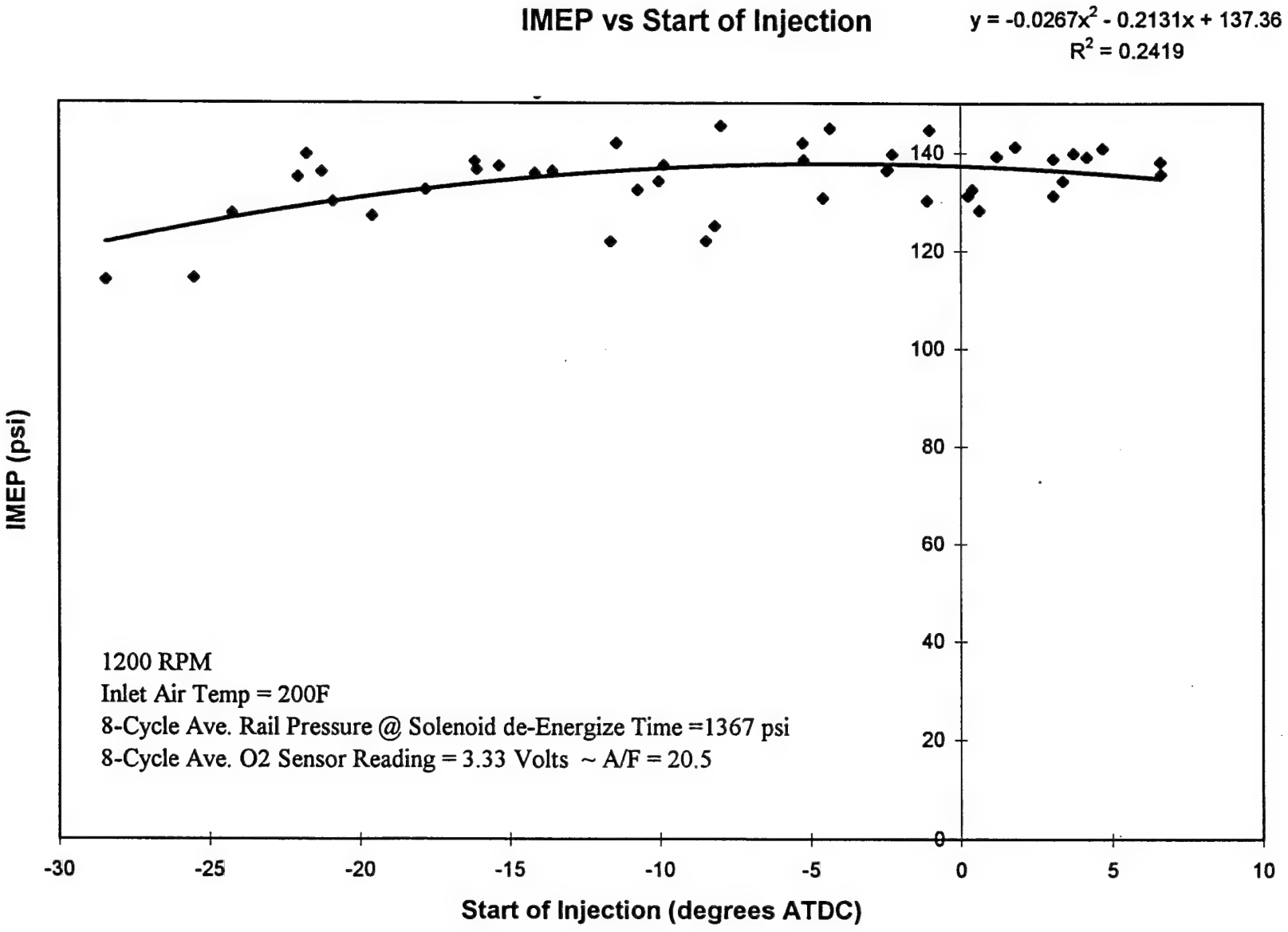
IMEP vs Start of Injection
y = -0.0267x² - 0.2131x + 137.36
R² = 0.2419
IMEP (psi)
140
120
100
80
60
40
20
0
-30
-25
-20
-15
-10
-5
0
5
10
Start of Injection (degrees ATDC)
1200 RPM
Inlet Air Temp = 200F
8-Cycle Ave. Rail Pressure @ Solenoid de-Energize Time =1367 psi
8-Cycle Ave. O2 Sensor Reading = 3.33 Volts ~ A/F = 20.5

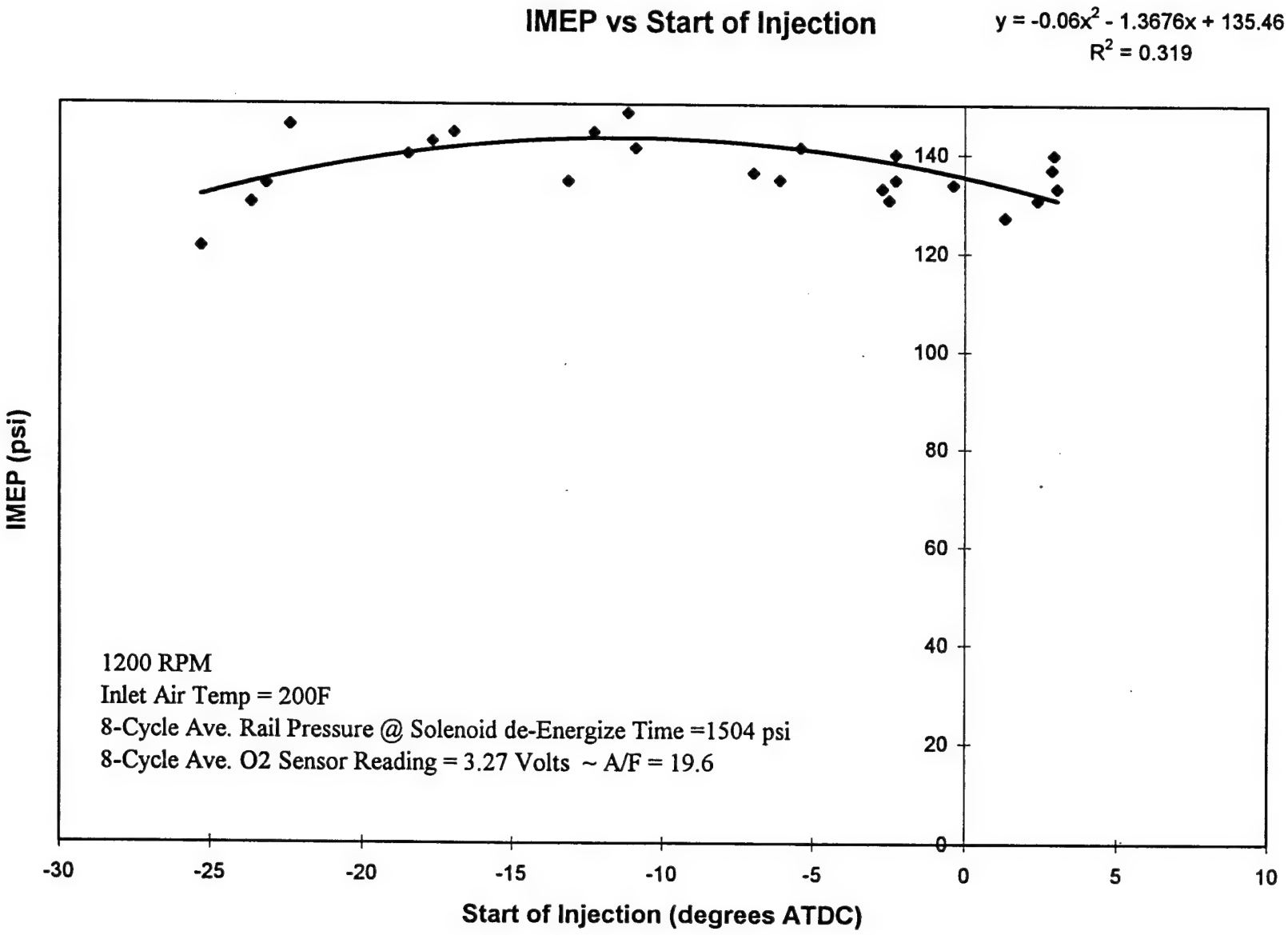
IMEP vs Start of Injection
y = -0.06x² - 1.3676x + 135.46
R² = 0.319
IMEP (psi)
140
120
100
80
60
40
20
0
-30
-25
-20
-15
-10
-5
0
5
10
Start of Injection (degrees ATDC)
1200 RPM
Inlet Air Temp = 200F
8-Cycle Ave. Rail Pressure @ Solenoid de-Energize Time =1504 psi
8-Cycle Ave. O2 Sensor Reading = 3.27 Volts ~ A/F = 19.6

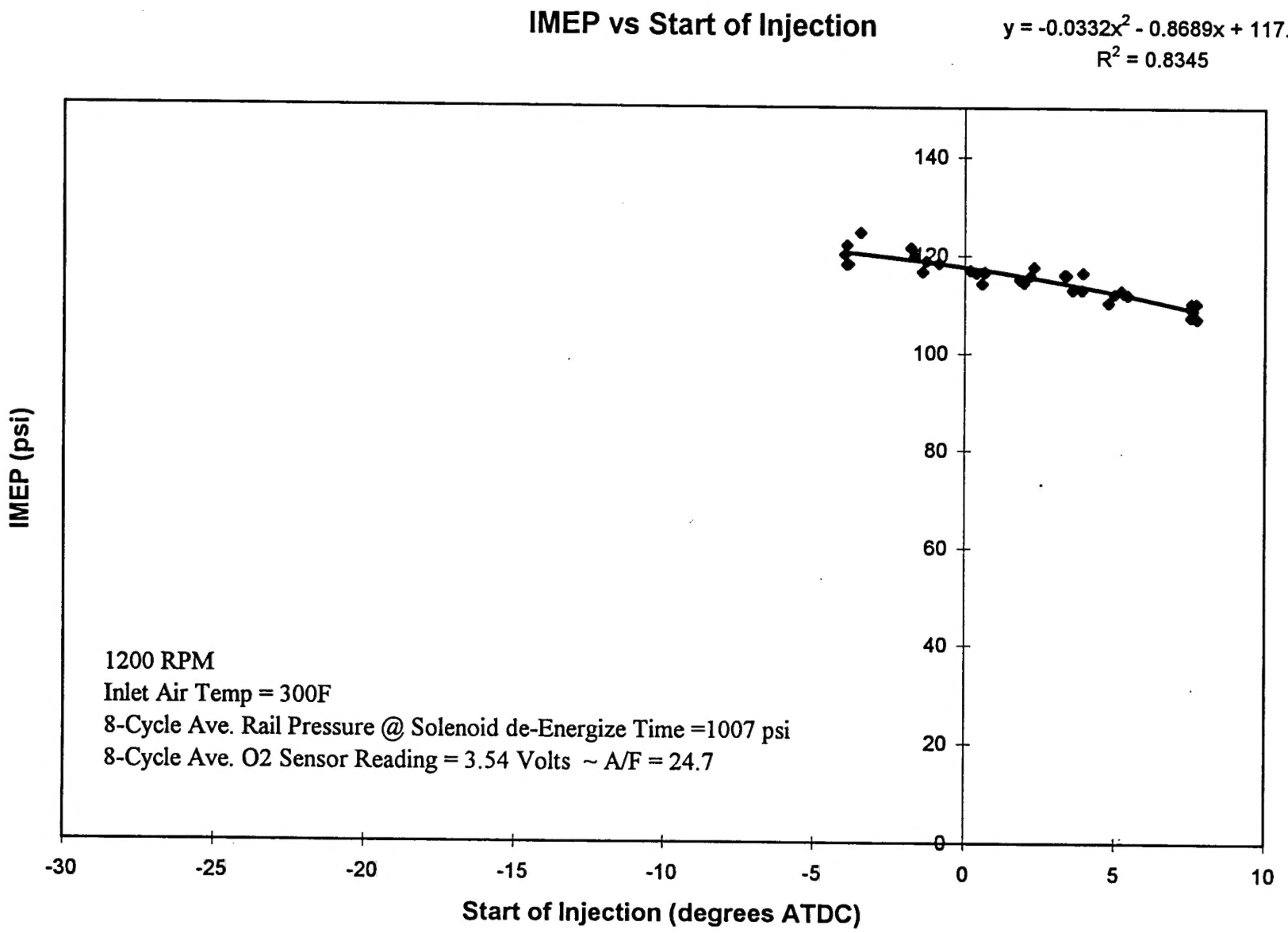
IMEP vs Start of Injection
y = -0.0332x² - 0.8689x + 117.7
R² = 0.8345
IMEP (psi)
140
120
100
80
60
40
20
0
-30
-25
-20
-15
-10
-5
0
5
10
Start of Injection (degrees ATDC)
1200 RPM
Inlet Air Temp = 300F
8-Cycle Ave. Rail Pressure @ Solenoid de-Energize Time =1007 psi
8-Cycle Ave. O2 Sensor Reading = 3.54 Volts ~ A/F = 24.7

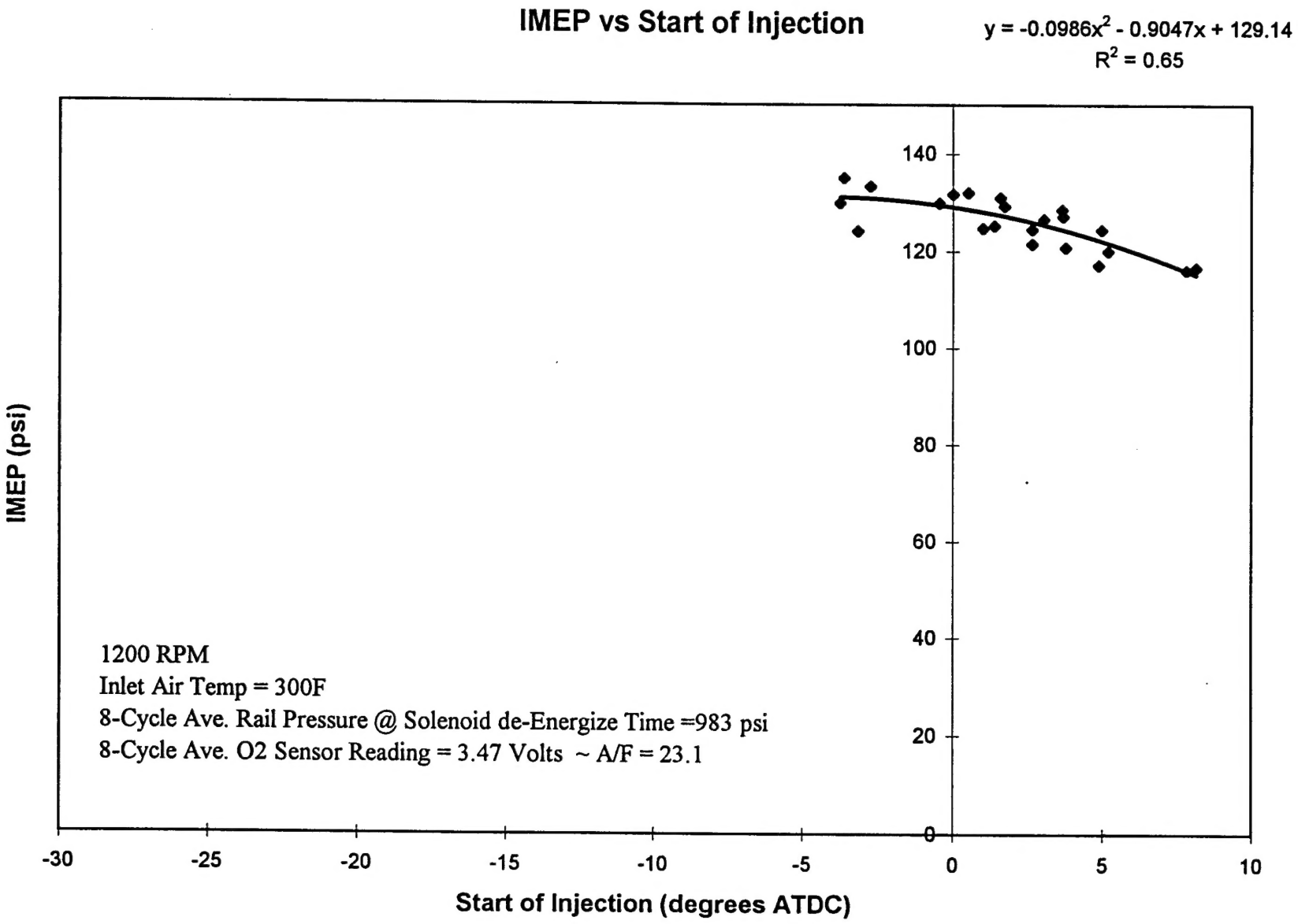
IMEP vs Start of Injection
y = -0.0986x² - 0.9047x + 129.14
R² = 0.65
IMEP (psi)
140
120
100
80
60
40
20
0
-30
-25
-20
-15
-10
-5
0
5
10
Start of Injection (degrees ATDC)
1200 RPM
Inlet Air Temp = 300F
8-Cycle Ave. Rail Pressure @ Solenoid de-Energize Time =983 psi
8-Cycle Ave. O2 Sensor Reading = 3.47 Volts ~ A/F = 23.1

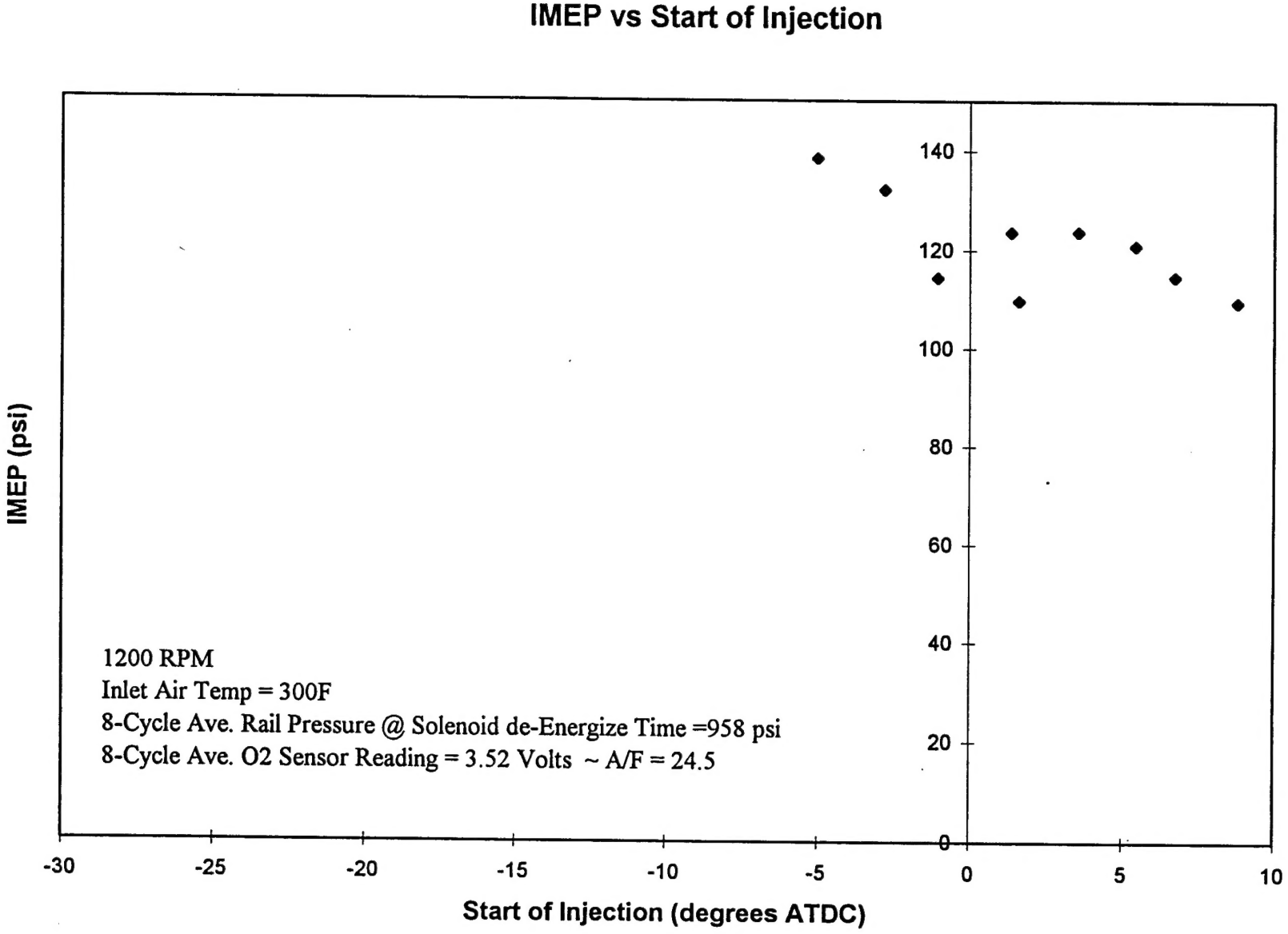
IMEP vs Start of Injection
IMEP (psi)
140
120
100
80
60
40
20
0
-30
-25
-20
-15
-10
-5
0
5
10
Start of Injection (degrees ATDC)
1200 RPM
Inlet Air Temp = 300F
8-Cycle Ave. Rail Pressure @ Solenoid de-Energize Time =958 psi
8-Cycle Ave. O2 Sensor Reading = 3.52 Volts ~ A/F = 24.5

SF 298 MASTER COPY , KEEP, THIS COPY FOR REPRODUCTION PURPOSES

REPORT DOCUMENTATION PAGE

Form Approved
OMB NO. 0704-0188

1. AGENCY USE ONLY *(Leave blank)*	2. REPORT DATE	3. REPORT TYPE AND DATES COVERED
	March 16, 1999	Final 9/30/97-2/28/99

4. TITLE AND SUBTITLE

Study of Very High-pressure Fuel-Injection for High-BMEP DI-Diesel Engine

5. FUNDING NUMBERS

DAAH04-96-1-0459

6. AUTHOR(S)

K. T. Rhee

7. PERFORMING ORGANIZATION NAMES(S) AND ADDRESS(ES)

Rutgers, The State University of New Jersey
College of Engineering
Mechanical and Aerospace Engineering
Piscataway, NJ 08854

8. PERFORMING ORGANIZATION REPORT NUMBER

9. SPONSORING / MONITORING AGENCY NAME(S) AND ADDRESS(ES)

U.S. Army Research Office
P.O. Box 12211
Research Triangle Park, NC 27709-2211

10. SPONSORING / MONITORING AGENCY REPORT NUMBER

ARO 36386.1-EG

11. SUPPLEMENTARY NOTES

The views, opinions and/or findings contained in this report are those of the author(s) and should not be construed as an official Department of the Army position, policy or decision, unless so designated by other documentation.

12a. DISTRIBUTION / AVAILABILITY STATEMENT

Approved for public release; distribution unlimited.

12 b. DISTRIBUTION CODE

13. ABSTRACT *(Maximum 200 words)*

In order to help design a high-power-density (HPD) low-heat-rejection (LHR) high-injection-fuel (HIP) direct-injection compression-ignition engine (DI-CI), two main methods were employed: (1) engine performance analysis; and (2) in-cylinder imaging. In the performance analysis, a Cummins 903 engine was used.

The range of air/fuel ratio studied was from 18-1 to over 35-1, the injection pressure investigated was as high as 30,625 psi (210 Mpa) under varied intake air temperature over 150°C.

In the in-cylinder imaging, a separate optical single-cylinder Cummins 903 engine was used. A high-speed four-color IR digital imaging systemwas greatly improved during this contract period. New spectrometric methods were developed to simultaneously determine the distributions of temperature, water vapor and soot concentrations. In addition, a new data analysis and presentation method has been developed.

The performance analysis results are reported in two parts: a preliminary report as included in Appendix-I and an additional set of results (Appendix-III). Some of the in-cylinder imaging results, which are now being captured by the improved SIS after incorporating with new electronic packages (designed and fabricated in our laboratory), are included with discussions.

14. SUBJECT TERMS

High BMEP engine, Low Heat Rejection, Diesel Combustion, Spectral IR images, Engine Response to High-pressure fuel injection.

15. NUMBER IF PAGES

67

16. PRICE CODE

17. SECURITY CLASSIFICATION OR REPORT	18. SECURITY CLASSIFICATION OF THIS PAGE	19. SECURITY CLASSIFICATION OF ABSTRACT	20. LIMITATION OF ABSTRACT
UNCLASSIFIED	UNCLASSIFIED	UNCLASSIFIED	UL